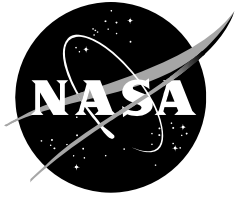


NASA/CP—2010–217041



Abstracts of the Annual Meeting of Planetary Geologic Mappers, Flagstaff, AZ, 2010

Edited by:

Leslie F. Bleamaster III
Planetary Science Institute, Tucson, AZ

Kenneth L. Tanaka
U.S. Geological Survey, Flagstaff, AZ

Michael S. Kelley
NASA Headquarters, Washington, DC

June 2010

NASA STI Program ... in Profile

Since its founding, NASA has been dedicated to the advancement of aeronautics and space science. The NASA scientific and technical information (STI) program plays a key part in helping NASA maintain this important role.

The NASA STI program operates under the auspices of the Agency Chief Information Officer. It collects, organizes, provides for archiving, and disseminates NASA's STI. The NASA STI program provides access to the NASA Aeronautics and Space Database and its public interface, the NASA Technical Report Server, thus providing one of the largest collections of aeronautical and space science STI in the world. Results are published in both non-NASA channels and by NASA in the NASA STI Report Series, which includes the following report types:

- **TECHNICAL PUBLICATION.** Reports of completed research or a major significant phase of research that present the results of NASA Programs and include extensive data or theoretical analysis. Includes compilations of significant scientific and technical data and information deemed to be of continuing reference value. NASA counterpart of peer-reviewed formal professional papers but has less stringent limitations on manuscript length and extent of graphic presentations.
- **TECHNICAL MEMORANDUM.** Scientific and technical findings that are preliminary or of specialized interest, e.g., quick release reports, working papers, and bibliographies that contain minimal annotation. Does not contain extensive analysis.
- **CONTRACTOR REPORT.** Scientific and technical findings by NASA-sponsored contractors and grantees.

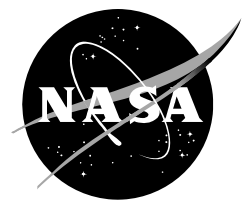
- **CONFERENCE PUBLICATION.** Collected papers from scientific and technical conferences, symposia, seminars, or other meetings sponsored or co-sponsored by NASA.
- **SPECIAL PUBLICATION.** Scientific, technical, or historical information from NASA programs, projects, and missions, often concerned with subjects having substantial public interest.
- **TECHNICAL TRANSLATION.** English-language translations of foreign scientific and technical material pertinent to NASA's mission.

Specialized services also include organizing and publishing research results, distributing specialized research announcements and feeds, providing help desk and personal search support, and enabling data exchange services.

For more information about the NASA STI program, see the following:

- Access the NASA STI program home page at <http://www.sti.nasa.gov>
- E-mail your question via the Internet to help@sti.nasa.gov
- Fax your question to the NASA STI Help Desk at 443-757-5803
- Phone the NASA STI Help Desk at 443-757-5802
- Write to:
NASA STI Help Desk
NASA Center for AeroSpace Information
7115 Standard Drive
Hanover, MD 21076-1320

NASA/CP—2010–217041



Abstracts of the Annual Meeting of Planetary Geologic Mappers, Flagstaff, AZ, 2010

Edited by:

Leslie F. Bleamaster III
Planetary Science Institute, Tucson, AZ

Kenneth L. Tanaka
U.S. Geological Survey, Flagstaff, AZ

Michael S. Kelley
NASA Headquarters, Washington, DC

Annual Meeting of Planetary Geologic Mappers
Flagstaff, AZ
June 21-23, 2010

National Aeronautics and
Space Administration

NASA Headquarters
Washington, DC 20546

June 2010

Acknowledgments

This publication is supported by a grant from the NASA Planetary Geology and Geophysics Program.

Available from:

NASA Center for AeroSpace Information
7115 Standard Drive
Hanover, MD 21076-1320
443-757-5802

This report is also available in electronic form at
<http://astrogeology.usgs.gov/Projects/PlanetaryMapping/>

Report of the Annual Mappers' Meeting
U.S. Geological Survey
Astrogeology Science Center
Flagstaff, Arizona
June 21-23, 2010

The Annual Meeting of Planetary Geologic Mappers, started in 1989, has become a unique opportunity for the planetary geologic mapping community to gather in a relatively relaxed atmosphere to exchange ideas, discuss mapping strategies and methodologies, and remain informed of technological advances directly related to creating and producing geologic maps of bodies throughout the Solar System. The meeting also serves as the primary venue for Planetary Geology and Geophysics (PG&G) funded Principal Investigators, and associated teams, to present the progress and highlight significant findings of their mapping projects.

This volume is the compilation of abstracts submitted by meeting attendees, abstracts submitted in absentia, and additional materials appropriate for distribution to the planetary mapping community; in all, 29 abstracts were accepted this year (16 Mars, 7 Venus, 3 Lunar, 1 Io, 1 Mercury, and 1 technical).

The 2010 meeting was convened by Les Bleamaster (Planetary Science Institute (PSI) and Trinity University), Ken Tanaka (U.S. Geological Survey (USGS)), and Michael Kelley (NASA Headquarters) and was hosted by the U.S. Geological Survey in Flagstaff, Arizona. Nearly 40 participants attended this year's meeting and associated Geographic Information Systems (GIS) workshop.

The 2010 meeting began on Monday, June 21st with a lecture style GIS workshop; PowerPoint presentation and tutorials from this workshop are available on the PIGWAD website (<http://webgis.wr.usgs.gov/pigwad/tutorials/planetarygis/index.html>). The GIS workshops are becoming an increasingly important part of the mappers' meeting as the PG&G supported mapping community transitions to 100% GIS submission of map products beginning in 2011 and publication by 2013. The workshop, organized and run by Trent Hare, Jim Skinner, Corey Fortezzo, and Richard Nava (all of the USGS, Flagstaff), provided review and instruction on i) geodatabase design, organization, and management, ii) polyline and polygon creation and editing, iii) querying and spatial analysis, iv) introduction to a newly developed crater helper tool, and v) final map preparation, annotation, and cartography, as well as providing a sneak peek at ArcGIS 10.0. The PG&G program is committed to producing the best geologic mapping products using the best available technologies and training, thus GIS workshops will continue to accompany the mappers' meeting for years to come (certainly when the meeting is convened in Flagstaff).

Oral presentations and poster discussions of geologic mapping projects took place on Tuesday, June 22nd and Wednesday, June 23rd. Ken Tanaka welcomed everyone to the USGS and provided a brief overview of mapping coordination activities including the introduction of new mapping starts funded by PG&G this year, discussion of recent international involvement and cooperation, and some minor revisions to the planetary geologic mapping handbook (the new 2010 version is included as an appendix in this abstract volume). The planetary geologic mapping handbook (Tanaka et al., 2010; edited and approved by GEMS) provides guidance for new and seasoned mappers by outlining

programmatic details for map preparation and submission in attempts to continue to streamline and standardize our geologic mapping products, which in the long run will facilitate their use by others in the planetary science community both domestically and abroad. Michael Kelley (PG&G Discipline Scientist) followed with a PG&G program update and explanation of some of the recent delays from headquarters.

Tuesday's science presentations were devoted to Mars and provided a real eye-opening experience to the wide array of complex datasets available for geologic mapping studies. Dramatic increases in the spatial, spectral, and temporal resolutions of Mars data have become real issues for which innovative approaches are beginning to be implemented. Jim Skinner kicked off with a semi-technical presentation regarding the incorporation of newly acquired high-resolution datasets as well as the implementation of GIS technologies that he employed during map preparation in the northern polar region. Peter Mouginis-Mark (Univ. of Hawaii) then took us on a close up tour of Tooting crater where mapping at scales as high as 1:10,000 reveals complex relations between impact melt and volatile-rich sediments. Scott Mest (PSI and NASA Goddard Space Flight Center) followed with results from Reull Vallis and newly named* Waikato Vallis in southern Hesperia Planum (*information regarding planetary nomenclature and naming features can be found at <http://planetarynames.wr.usgs.gov/>). Kevin Williams (Buffalo State College), and Ross Irwin (PSI) continued with further discussions of basin formation and fluvial processes in Margaritifer Terra along Himera, Samara, and Loire Valles, and the Uzboi-Ladon-Morava outflow system, respectively. David Williams (Arizona State University) presented a new project (funded through the Mars Data Analysis Program) looking at volcanic styles at Olympus Mons and the Tharsis Montes. Next, the group took a long break for lunch, posters and the semi-annual GEMS (Geologic Mapping Subcommittee) meeting.

Les Bleamaster provided a quick summary of work in Nili Fossae and Mawrth Vallis. Jim Zimbelman (Smithsonian Institution) provided an update on his work with the Medusae Fossae Formation and David Crown (PSI) discussed results of mapping and mineralogic investigations to the northwest of Hellas Planitia. James Dohm (University of Arizona) introduced his new Argyre basin project. Jim Skinner presented results from his mapping in the southern Utopia Planitia and Libya Montes regions and Tracy Gregg (University of Buffalo) reported on her continued mapping of Tyrrhena Patera and Hesperia Planum. Brian Hynek (University of Colorado) reported on his soon to be submitted 1:2M-scale map of Meridiani and Ken Tanaka wrapped up the Mars presentations with the Scandia region in the northern hemisphere and the 1:20M-scale global map of Mars.

Wednesday began with another technical presentation, this time by Stephan van Gasselt (Freie University, Berlin) highlighting the importance and advantages of integrating geodatabase design into mapping projects. We then turned our attention to objects other than Mars. David Williams returned to provide an update on the global Io map currently in review. Trevelyn Lough (University of Buffalo) reported on preliminary work on Aristarchus plateau within LQ-10 and Scott Mest presented work from South Pole-Aiken basin in LQ-30. Debra Buczkowski (Johns Hopkins University Applied Physics Lab) introduced her new project on Caloris basin, Mercury using MESSENGER fly-by data. Mapping presentations finished up with Venus. Eileen McGowan (University of Massachusetts) discussed the vast plains of V-18 and Les Bleamaster presented current

progress in Devana Chasma (V-29) and efforts in the Beta-Atla-Themis region.

Group discussion centered on the use of Geographic Information Systems for mapping and how to get older work ready for submission prior to the Jan. 2011 deadline for GIS submission. Ken Tanaka and others at the USGS are willing to provide basic assistance for mappers who find themselves in this situation. The USGS personnel are also open to hosting visitors in Flagstaff for one-on-one tutorial sessions. Granted, time and monetary limitations exist, so one's best option is to contact USGS personnel sooner rather than later (contact information can be found in the Planetary Geologic Mapping Handbook). It was noted that two GIS maps (one Venus and one Mars) will soon be published and will be available as templates for future submissions. Also, look for new crater mapping and counting tools for GIS, a new cross-section tool, and standardized map symbols and unit naming conventions.

The next meeting likely will be convened between June 19 and 25 at a venue to be announced at a later date.

CONTENTS (in alphabetical order by author)

Mercury

Detailed Analysis of the Intra-ejecta Dark Plains of Caloris Basin, Mercury. <i>D.L. Buczkowski and K.S. Seelos</i>	1
------------------------------------------------------------------------------------------------------------------------------	---

Venus

The Formation and Evolution of Tessera and Insights into the Beginning of Recorded History on Venus: Geology of the Fortuna Tessera Quadrangle (V-2). <i>J.W. Head and M.A. Ivanov</i>	3
-------------------------------------------------------------------------------------------------------------------------------------------------------------------------------------------------	---

Geologic Map of the Snegurochka Planitia Quadrangle (V-1): Implications for the Volcanic History of the North Polar Region of Venus. <i>D.M. Hurwitz and J.W. Head</i>	5
---------------------------------------------------------------------------------------------------------------------------------------------------------------------------------	---

Geological Map of the Fredegonde (V-57) Quadrangle, Venus: Status Report. <i>M.A. Ivanov and J.W. Head</i>	7
---------------------------------------------------------------------------------------------------------------------	---

Geologic Mapping of V-19. <i>P. Martin, E.R. Stofan and J.E. Guest</i>	9
---------------------------------------------------------------------------------	---

Geology of the Lachesis Tessera Quadrangle (V-18), Venus. <i>E.M. McGowan and G.G. McGill</i>	11
--------------------------------------------------------------------------------------------------------	----

Comparison of Mapping Tessera Terrain in the Phoebe Regio (V-41) and Tellus Tessera (V-10) Quadrangles. <i>D.A. Senske</i>	13
-------------------------------------------------------------------------------------------------------------------------------------	----

Geologic Mapping of the Devana Chasma (V-29) Quadrangle, Venus. <i>E.R. Tandberg and L.F. Bleamaster, III</i>	14
------------------------------------------------------------------------------------------------------------------------	----

Moon

Geologic Mapping of the Aristarchus Plateau Region on the Moon. <i>T.A. Lough, T.K.P. Gregg, and R. Aileen Yingst</i>	16
--------------------------------------------------------------------------------------------------------------------------------	----

Geologic Mapping of the Lunar South Pole Quadrangle (LQ-30). <i>S.C. Mest, D.C. Berman, and N.E. Petro</i>	18
---------------------------------------------------------------------------------------------------------------------	----

The Pilot Lunar Geologic Mapping Project: Summary Results and Recommendations from the Copernicus Quadrangle. <i>J.A. Skinner, L.R. Gaddis, and J.J. Hagerty</i>	20
---------------------------------------------------------------------------------------------------------------------------------------------------------------------------	----

Mars

Geologic Mapping of the Nili Fossae Region of Mars: MTM Quadrangles 20287, 20282, 25287, 25282, 30287, and 30282. <i>L.F. Bleamaster III, and D.A. Crown</i>	22
Geologic Mapping of the Mawrth Vallis Region, Mars: MTM Quadrangles 25022, 25017, 25012, 20022, 20017, and 20012. <i>F.C. Chuang and L.F. Bleamaster III</i>	24
Evidence for an Ancient Buried Landscape on the NW Rim of Hellas Basin, Mars. <i>D.A. Crown, L.F. Bleamaster III, S.C. Mest, J.F. Mustard, and M. Vincendon</i>	26
New Geologic Map of the Argyre Region of Mars: Deciphering the Geologic History Through Mars Global Surveyor, Mars Odyssey, and Mars Express Data Sets. <i>J.M. Dohm, M. Banks, and D. Buczkowski</i>	28
Geologic Mapping in the Hesperia Planum Region of Mars. <i>T.K.P. Gregg and D.A. Crown</i>	30
Geologic Mapping of the Meridiani Region of Mars. <i>B.M. Hynek and G. Di Achille</i>	32
Geologic Mapping in Southern Margaritifer Terra. <i>R.P. Irwin III and J.A. Grant</i>	34
Geology of -30247, -35247 and -40247 Quadrangles, Southern Hesperia Planum, Mars. <i>S.C. Mest and D.A. Crown</i>	36
The Interaction of Impact Melt, Impact-Derived Sediment, and Volatiles at Crater Tooting, Mars. <i>P. Mouginis-Mark and J. Boyce</i>	38
Geologic Map of the Olympia Cavi Region of Mars (MTM 85200): A Summary of Tactical Approaches. <i>J.A. Skinner, Jr. and K. Herkenhoff</i>	40
Geology of the Terra Cimmeria-Utopia Planitia Highland Lowland Transitional Zone: Final Technical Approach and Scientific Results. <i>J.A. Skinner, Jr. and K.L. Tanaka</i>	42
Geology of Libya Montes and the Interbasin Plains of Northern Tyrrhena Terra, Mars: First Year Results and Second Year Work Plan. <i>J.A. Skinner, Jr., A.D. Rogers, and K.D. Seelos</i>	44

Mars Global Geologic Mapping Progress and Suggested Geographic-Based Hierarchical Systems for Unit Grouping and Naming.

*K.L. Tanaka, J.M. Dohm, R. Irwin, E.J. Kolb, J.A. Skinner, Jr., and T.M. Hare..*46

Progress in the Scandia Region Geologic Map of Mars.

*K.L. Tanaka, J.A.P. Rodriguez, C.M. Fortezzo, R.K. Hayward, and J.A. Skinner, Jr.....*48

Geomorphic Mapping of MTMs -20022 and -20017.

*K.K. Williams.....*50

Geologic Mapping of the Medusae Fossae Formation, Mars, and the Northern Lowland Plains, Venus.

*J.R. Zimbelman.....*52

Io

Volcanism on Io: Results from Global Geologic Mapping.

*D.A. Williams, L.P. Keszthelyi, D.A. Crown, P.E. Geissler, P.M. Schenk, Jessica Yff, and W.L. Jaeger.....*54

Other

Employing Geodatabases for Planetary Mapping Conduct – Requirements, Concepts and Solutions.

*S. van Gasselt and A. Nass.....*56

Appendix

Planetary Geologic Mapping Handbook - 2010

DETAILED ANALYSIS OF THE INTRA-EJECTA DARK PLAINS OF CALORIS BASIN, MERCURY.

D.L. Buczowski and K.S. Seelos, Johns Hopkins University Applied Physics Laboratory, Laurel, MD 20723, Debra.Buczowski@jhuapl.edu.

Introduction: The Caloris basin on Mercury (Fig. 1) is floored by light-toned plains and surrounded by an annulus of dark-toned material interpreted to be ejecta blocks and smooth, dark, ridged plains. Strangely, preliminary crater-counts indicate that these intra-ejecta dark plains are younger than the light-toned plains within the Caloris basin. This would imply a second, younger plains emplacement event, possibly involving lower albedo material volcanics, which resurfaced the original ejecta deposit. On the other hand, the dark plains may be pre-Caloris light plains covered by a thin layer of dark ejecta. Another alternative to the hypothesis of young, dark volcanism is the possibility that previous crater-counts have not thoroughly distinguished between superposed craters (fresh) and partly-buried craters (old) and therefore have not accurately determined the ages of the Caloris units.

This abstract outlines the tasks associated with a new mapping project of the Caloris basin, intended to improve our knowledge of the geology and geologic history of the basin, and thus facilitate an understanding of the thermal evolution of this region of Mercury.

Task 1: Classify craters based on geomorphology and infilling: The established crater classification scheme – used in the Tolstoj and Shakespeare quadrangles [1,2] and formalized in 1981 [3] – was based on degree of crater degradation, in which fresh craters were labeled C_5 and the most degraded craters were identified as C_1 . We will design a classification scheme for Mercurian craters that includes both degradation state and level and type of infilling. We will incorporate a classifier that notes the level of infilling in a crater, from mostly buried (we presumably would not be able to observe a completely buried crater in visible imagery) to completely unfilled, after the observations by [4]. We will also distinguish between craters infilled with 1) lava, 2) impact melt and 3) ejecta, based on our interpretation of the MDIS images.

The difference between craters filled with lava and craters filled with impact melt may not always be easy to determine. The amount of impact melt associated with a crater is proportional to the impact velocity squared. Since the impact velocity on Mercury is ~ 40 km/s there should be far more impact melt associated with craters on Mercury than on the Moon or Mars, where impact velocities are ~ 20 km/s and ~ 15 km/s respectively [5]. Also, the greater gravity of Mercury could tend to accentuate the amount of melt present. A flat-floored crater with melt in the rim is most likely a crater filled with impact melt. A crater with a breached rim, or flow lobes stretching over the rim, is more likely to be a crater filled with lava. We expect that the identification between the two types of fill will not always be obvious and opinions from all team members will be debated for the more ambiguous craters.

We will identify all primary craters on the Caloris floor and within the dark annulus surrounding the basin in the MESSENGER MDIS data. We will identify craters in either a previously released mosaic or a mosaic that we have cre-

ated ourselves using ENVI, and then use the individual MDIS images to measure and analyze the geomorphic features. Each crater will be assigned a classification, following the scheme developed in the first part of the task.

Secondary craters usually have morphologies distinct from primary craters and they tend to occur in either clusters or chains. Observed Caloris secondaries will be classified as Van Eyck formation, after the geomorphic mapping in the Tolstoj [1] and Shakespeare [2] quadrangles.

No crater classification scheme can be rigorously or consistently applied until all of Mercury is imaged at a variety of lighting angles [6]. This will not be truly possible until MESSENGER goes into orbit on March 18, 2011. Right now we only have access to images of Mercurian craters at multiple lighting angles in quadrant A. To account for the non-ideal range of solar incidence angles in the released MDIS images we will utilize image processing techniques, such as high-pass filtering, to enhance edge detection and thus encourage crater identification. However, we will also revisit our crater classifications as new data are released.

Task 2: Create a high-resolution map of the intra-ejecta dark plains: We will use the new high resolution (200-300 m/p) imaging data from the MDIS instrument to create a new geomorphic map of the dark annulus around the Caloris basin. We will start in the region where MESSENGER data overlaps Mariner 10 images (quadrant A in Figure 1). By comparing the Caloris group formations mapped in the Tolstoj [1] and Shakespeare [2] quadrangles to the overlapping MDIS images, we will determine the distinctive geomorphology of each of these units and use this as diagnostic criteria for identifying these units in regions never before mapped. We will then utilize the developed diagnostic criteria to map quadrants B, C and D. Caloris group formations will be mapped where identified and any new units will be defined and mapped as necessary. Specifically, we will delineate hummocks and smooth plains within the Odin formation and map them separately. We will look for unequivocal evidence of volcanic activity within the dark annulus and the Odin Formation, such as vents and flow lobes. The location of any filled craters observed in Task 1 will be especially noted.

Task 3: Perform crater counts of the intra-ejecta dark plains, the ejecta, and the Caloris floor light plains: Craters identified in Task 1 will be compared to the geomorphic units mapped in Task 2. The diameters of craters superposed on each individual surface unit will be measured and counted separately. The area covered by each geomorphic unit will then be determined.

Crater counts will be normalized to a common area of one million square kilometers. We will determine the crater size-frequency distribution (SFD) of each geomorphic unit by plotting crater diameter against the normalized cumulative crater count on a log-log graph. Younger surfaces have SFDs that plot to the left and below older surfaces and so the relative ages of multiple units can be determined. Statistical uncertainties and plotting techniques will follow the form

outlined by the Crater Analysis Techniques Working Group [7]. Given the resolution of the images, we expect to be able to compile reliable statistics down to crater diameters of 1-2 km.

We will analyze the crater density of the Caloris floor plains unit, the Odin Formation ejecta and the Odin Formation intra-ejecta dark plains. We will do a second count of craters on the Caloris floor that includes all observed craters, including those that are filled, to attempt to get a minimum age for the underlying dark basement. Crater counting on any additional geologic units will depend upon results of the geomorphic mapping.

Task 4: Refine the stratigraphy of Caloris basin units: Presently, mapping relationships indicate that the stratigraphy of the Caloris basin is as illustrated in Figure 1b. However, this stratigraphic cross-section does not take into account the nature of the Odin Formation intra-ejecta dark plains. If these plains are in fact a lava flow younger than the Odin ejecta and distinct from the smooth plains (ps), then this needs to be reflected in both the cross-section and a stra-

tigraphic column. Similarly, the cross-section should more clearly reflect the stratigraphy of the Caloris units if the Odin Formation is comprised of multiple facies (hummocks and plains) of excavated dark basement material. If the intra-ejecta dark plains are ps material embaying the ejecta, this too should be somehow reflected in any stratigraphic analysis of the basin.

The new crater counts in Task 3 will help determine the timing relations between the units identified in Task 2. We can then refine the stratigraphy of the Caloris basin units.

References: [1] Schaber and McCauley (1980) USGS Map I-1199. [2] Guest and Greeley (1983) USGS Map I-1408. [3] McCauley et al. (1981) *Icarus* 47, 184-202. [4] Murchie et al. (2008) *Science* 321, 73-76. [5] Cintala and Grieve (1998) *Meteorit. Planet. Sci.* 33, 889-912. [6] Spudis and Guest (1988) in *Mercury*, eds. Vilas, Chapman and Matthews, 118-164. [7] Crater Analysis Techniques Working Group (1979) *Icarus* 37, 467-474.

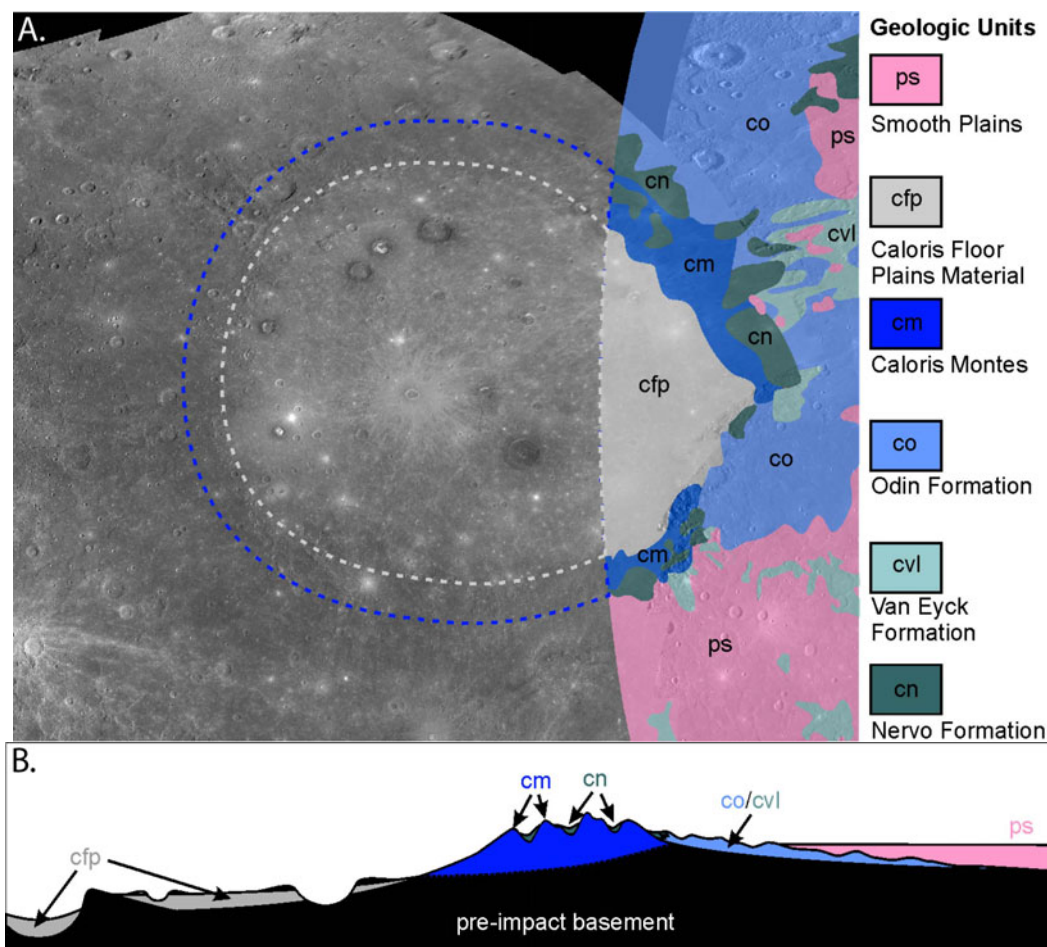


Figure 1. A) Mosaic of Mariner 10 (colorized, right side) and MESSENGER (left) high-resolution narrow angle camera data for the Caloris basin. Overlain on the Mariner 10 data are sketch geologic units after Schaber and McCauley [1980] and Guest and Greeley [1983] (crater and ejecta-related materials not included). Dashed lines illustrate the approximate extension of the Caloris Floor Plains Material unit (grey) and the Caloris Montes basin rim unit (blue). B) Schematic geologic cross-section from the Caloris basin center (left edge) and outward. Odin (co) and Van Eyck (cvl) Formations are combined for simplicity.

THE FORMATION AND EVOLUTION OF TESSERA AND INSIGHTS INTO THE BEGINNING OF RECORDED HISTORY ON VENUS: GEOLOGY OF THE FORTUNA TESSERA QUADRANGLE (V-2).

J. W. Head¹ and M. A. Ivanov^{1,2}. Providence, RI 02912 USA (james_head@brown.edu), ²Vernadsky Institute, Russian Academy of Sciences, Moscow, Russia (mikhail_ivanov@brown.edu).

Introduction: Today, and throughout its recorded history, Venus can be classified as a "one-plate planet." The observable geological record of the planet comprises only the last 1/4 or less of its overall geologic history. As shown by many authors, it started with intensive deformation in broad regions to form tessera [1-6] during the Fortunian period of history [7]. The period of tessera formation quickly changed to numerous zonal deformational belts of ridges and grooves that were followed by emplacement of vast volcanic plains (shield plains, regional plains) [7,8]. During the final epoch of the geologic history of Venus, large but isolated centers of volcanism formed extensive fields of lavas, with tectonics concentrated within fewer very prominent rift zones [8,9]. The observable changes in intensity and character of volcanism and tectonics suggest progressive changes from thin lithosphere early in the geologic history to thick lithosphere during later epochs [6,10]. We have little idea of the character of the first 3/4 of Venus' history. So, what does the earliest period of recorded history tell us about the transition from the Pre-Fortunian to the Fortunian period and what insight does this give us into this earlier period?

Major problems to address: About 60% of the area of the Fortuna Tessera quadrangle (V-2) forms one of the largest tessera regions on Venus [11-12] as well as surrounding deformational belts and broad plains units. Relationships of intratessera structural domains with the surrounding tectonic and volcanic features can be investigated in detail. This provides the basis to establish major sequences of events that operated near the visible beginning of the geologic history of Venus. Arranging of the events into a stratigraphic order is key to addressing a number of important questions in the geology of Venus. What is the nature of the transition from the currently observed geological record to that of the first ca. 75% of the history of Venus? What were the dominant geological processes operating at the transition? How do they compare to those operating in the ensuing history? What do these features and processes tell us about the nature of the transition from earlier history to later history? Was this transition a peak of activity or a more gradual transition? What do the features and processes tell us about the nature of Venus in the first 3/4ths of its history?

The strategy: The area of the V-2 quadrangle represents one of the most fundamental areas showing the earliest recorded stratigraphic record, Fortuna Tessera (the type area for the Fortunian Period). A main goal of our mapping within this quadrangle is to analyze the tessera unit in detail to understand its morphologic na-

ture, the topographic configuration, structural patterns/subtypes, boundaries, and stratigraphic relations of tessera with the surrounding units/terrains. Is there any evidence for "pre-tessera" terrain? What can we learn about the sequence and internal structure of Fortuna (syntaxis, ribbons, troughs, etc. [13,14])? How do these characteristics of Fortuna relate to other tesserae on Venus and what are the key differences [5]? The synthesis of these observations will provide insight into both the processes of tessera formation and contrasts between pre- and post-Fortuna history of Venus.

Results of preliminary mapping: During preliminary mapping of the V-2 quadrangle we have defined ten material units (including two units related to impact craters) and two structural units and placed them in a stratigraphic sequence using embayment and cross-cutting relationships. From older to younger, these units are as follows. Tessera material (t) represents one of the most tectonically deformed types of terrain [12,15,16]. Both the material and tectonic structures play a key role in the definition of the unit. Tessera occupies the majority of the quadrangle (~50%, Fig. 2) and occurs in two major regions: Fortuna and Laima Tesserae. Type locality: 63.4°N, 19.5°E. Densely lineated plains material (pdl) heavily dissected by numerous densely packed narrow (<100s of m), short (10s of km), parallel and subparallel lineaments (fractures). Type locality: 52.4°N, 9.7°E. Mountain belts (mb) represent a structural unit that surrounds Lakshmi Planum and forms the highest mountain ranges on Venus [15,17-21]. Densely packed ridges that are 5-15 km wide and tens to a few hundreds of kilometers long characterize all mountain belts. Within the quadrangle, only the eastern portion of Maxwell Montes is represented. Type locality: 65.5°N, 0.9°E. Ridged plains material (pr) These are characterized by the morphology of lava plains and are deformed by broad (5-10 km) and long (10s of km) linear and curvilinear ridges. In places, the ridges are concentrated into prominent belts. Type locality: 53.2°N, 27.8°E. Groove belts (gb) represent a structural unit, which consists of dense swarms of linear and curvilinear subparallel lineaments (fractures or graben). Occurrences of the unit have a distinct belt-like shape. Between the structures within the belts, small fragments of preexisting units are seen in places. These fragments are usually too small to be mapped at the scale of the mapping (1:5M). Type locality: 56.4°N, 25.3°E.

Shield plains material (psh) is characterized by abundant small (<10 km) shield and cone-like features that are interpreted as volcanic edifices [22-25]. In places, the shields form clusters of structures. In contrast to the

above units, the material of shield plains occurs at lower elevations and is mildly deformed by tectonic structures (wrinkle ridges and sparse fractures/graben). Type locality: 61.4°N, 33.9°E. Material of the lower unit of regional plains (rp₁) is characterized by a morphologically smooth surface with a homogeneous and relatively low radar backscatter. The surface of the unit is mildly deformed by wrinkle ridges. The lower unit of regional plains occurs within low-lying areas and embays the heavily tectonized units and shield plains material. Type locality: 51.5°N, 25.6°E. Material of the upper unit of regional plains (rp₂) has a morphologically smooth surface that is moderately deformed by wrinkle ridges that belong to the same family of structures that deform unit rp₁. The unit (in contrast to the unit rp₁) shows higher radar albedo and often forms flow-like occurrences that are superposed on the surface of the lower unit of regional plains. Type locality: 52.9°N, 7.2°E.

Smooth plains material (ps) has a morphologically smooth, usually dark and featureless surface, which is tectonically undisturbed. The unit makes small equidimensional and elongated patches a few tens of km across. Type locality: 54.8°N, 2.4°E. Lobate plains material (pl) is characterized by a morphologically smooth surface with an albedo pattern consisting of numerous bright and dark flow-like features. The material of lobate plains is tectonically undisturbed and fields are associated with several medium-sized (a few hundreds of km across) volcanic centers near the northern and southern edges of the quadrangle. Type locality: 50.5°N, 22.0°E.

Impact crater materials, undivided (c) includes materials of the central peak, floor, walls, rim, and continuous ejecta. Type locality: 59.7°N, 26.8°E (crater Goeppert-Mayer). Impact crater outflow material (cf), type locality: 61.6°N, 36.2°E (outflow from the crater Baker).

Evolutionary trends: Consistent relationships of cross-cutting and embayment among the mapped units/structures suggest progressive decline of the amount of tectonic deformation from heavily tectonized units such as tesserae, densely lineated plains, ridged plains, and deformational belts through mildly deformed plains units (psh, rp₁, rp₂) to tectonically undeformed smooth and lobate plains. The elevated regions within the quadrangle correspond to the occurrences of the older and heavily tectonized units and mildly tectonized plains occur in topographic lows. This correlation suggests that the regional topographic patterns within the quadrangle were established during the earlier stages of the geologic history and that the processes of crustal thickening/thinning mostly operated at this time.

Clear morphological differences between the broad and mildly deformed plains units as well as their consistent age relationships suggest that there were significant changes in the volcanic style from shield plains (distributed small sources) through regional plains (volcanic

flooding) to lobate plains (several major volcanic centers).

Tentative conclusions: 1. Tessera represents a distinctive beginning of recorded history with focused deformation that shows a fundamental difference from later processes. 2. This early period (Fortunian) was characterized by "intense" regional (continental-scale) deformation that implies very large-scale lateral movement measured in hundreds of kilometers and associated lateral deformation and crustal thickening processes. 3. Later periods were characterized by less intense distributed deformation (wrinkle ridges) and localized deformation (ridge belts, fracture belts, rift zones). 4. The patterns in Fortuna Tessera show that pre-Fortunian crust was deforming at scales that imply a thin lithosphere, variations in crustal thickness, large-scale lateral movement, crustal underthrusting and imbrication, and possible subduction. 5. The Fortunian Period took place over a short period of time, as indicated by the small number of superposed craters. This implies either: 1) that the deformation was a peak, or 2) that if the deformation was simply transitional the transition occurred very rapidly and the rates of earlier processes were very high. 6. The nature of Fortunian/Pre-Fortunian geodynamics: The regional patterns of deformation and tessera preservation require that the following things were occurring at this time: Local downwelling and upwelling, regional plate boundary-like deformation, Archean-like ductile deformation: Delamination and sub-lithospheric spreading and subduction.

References: [1] Solomon S. et al. (1992) *JGR*, 97, 13199. [2] Basilevsky, A. and J. Head (1995a) *EMP* 66, 285. [3] Basilevsky, A. and J. Head (1995b) *PSS* 43, 1523. [4] Ivanov, M. and J. Head (1996) *JGR* 101, 14861. [5] Hansen, V. and J. Willis (1996) *Icarus* 123, 296. [6] Brown, C. and R. Grimm (1999) *Icarus* 139, 40. [7] Basilevsky, A. and J. Head (1998) *JGR* 103, 8531. [8] Ivanov, M. and J. Head (2001) *JGR* 106, 17515. [9] Basilevsky, A. and J. Head (2000) *JGR* 105, 24583. [10] Phillips R. and V. Hansen (1998) *Science* 279, 1492. [11] Sukhanov, A. et al. (1989) Geomorphologic/geological map of part of the Northern hemisphere of Venus, scale 1:15M, USGS Map I-2059. [12] Sukhanov, A. (1992) *In: Venus Geology, Geochemistry, and Geophysics*, V. Barsukov et al., eds. 82. [13] Grosfils, E. and J. Head (1990) *LPSC XXI* 439. [14] Ghent, R. and V. Hansen (1999) *Icarus* 139, 116. [15] Barsukov, V. et al. (1986) *JGR*, 91, D399. [16] Bindshadler, D. and J. Head (1991) *JGR* 96, 5889. [17] Pettengill, G. et al. (1980) *JGR* 85, 8261. [18] Masursky, H., et al. (1980) *JGR* 85, 8232. [19] Head, J. (1990) *Geology* 18, 99. [20] Pronin, A. (1992) *In: Venus Geology Geochemistry, and Geophysics*, V.L. Barsukov et al., eds. 68. [21] Ivanov, M. and J. Head (2008) *PSS* 56 1949. [22] Aubele, J. and E. Slyuta (1990) *EMP* 50/51, 493. [23] Head, J.W. et al. (1992) *JGR* 97, 13153. [24] Guest, J. et al. (1992) *JGR* 97, 15949. [25] Ivanov, M. and J. Head (2004) *JGR* 109, doi:10.1029/2004JE002252.

GEOLOGIC MAP OF THE SNEGUROCHKA PLANITIA QUADRANGLE (V-1): IMPLICATIONS FOR THE VOLCANIC HISTORY OF THE NORTH POLAR REGION OF VENUS. D. M. Hurwitz and J. W. Head, Department of Geological Sciences, Brown University, Providence RI 02912, debra_hurwitz@brown.edu.

Introduction: Geologic mapping of Snegurochka Planitia (V-1) reveals a complex stratigraphy of tectonic and volcanic features that can provide insight into the geologic history of Venus and Archean Earth [1,2], including 1) episodes of both localized crustal uplift and mantle downwelling, 2) shifts from local to regional volcanic activity, and 3) a shift back to local volcanic activity. We present our interpretations of the volcanic history of the region surrounding the north pole of Venus and explore how analysis of new data support our interpretations.

Mapping Methods: We have used full-resolution (75 m/pixel) images where available to produce a detailed map in ArcGIS and a correlation chart of mapped units (Figures 1-3) in conjunction with the USGS planetary mapping effort [3]. Twelve material units and two structural units have been identified and mapped and are found to be similar to those identified in previous studies [e.g., 4,5]. The material units include (from older to younger) tessera material (*t*), densely lineated plains material (*pld*), belts of ridged material (*rb*), deformed and ridged plains material, both radar dark and radar bright (*pdd*, *pbd*), shield plains material (*psh*), smooth radar dark plains material (*pds*), smooth radar bright plains material (*pbs*), belts of fractured material (*fb*), lobate plains material surrounding large edifices >100 km in diameter (*lp*), small edifice features (*ed*, ~20-100 km in diameter), and crater materials (*c*). Structural units identified are wrinkle ridges (*wr*) and lineaments (*lin*) that deform the material units.

Mapped Units: The tessera terrain is consistently the oldest material in the region and is characterized by high elevation, extensively deformed radar bright material that is embayed by younger plains units. The fractures that define this unit are generally characterized by at least two intersecting orientations of deformation (subunit *t1*), though localized exceptions to this trend have the radar bright, deformed morphology but lack the clear intersecting deformation patterns (subunit *t2*). In contrast, *pld* material, while also generally characterized by a rough surface texture, has a single primary orientation of fractures. If these *pld* plains are observed to be confined to a single belt of material, they have been identified as *rb*. These three types of deformed plains are all typically embayed by surrounding plains units.

The next suite of material units identified includes the regional plains material units. The oldest plains units include *pdd* and *pbd*, material that is characterized by dense, small scale fractures and ridges. These units are commonly embayed by *ps*, material with a high concentration of small volcanic shields that range in size from 1-20 km in diameter. In turn, *psh* plains are embayed by the *pbs* and *pds* units, deposits that have generally not been heavily deformed by tectonic processes. Smooth *pbs* plains are commonly spatially related to small shield clusters, though there are examples of *pbs* that lack evidence of nearby shield volcanism.

The youngest material units in Snegurochka Planitia are *fb*, *lp*, and *ed*. Units of *fb* are characterized by local belts of fractured material, indicating episodes of localized uplift possibly related to initial stages of volcanism. Deposits of *lp* material, mostly surrounding Renpet Mons (+76° 235°E) and Sarasvati Mons (+76° 354°E), are characterized by lobate-

tipped flows surrounding smaller edifice structures. Gash-like fractures (*lin*) and jagged wrinkle ridges (*wr*) are mapped as individual structures and are superposed on material units.

New Insights: Analysis of mapped features have indicated that the V-1 region experienced significant tectonic uplift in the formation of tessera units such as Itzpapalotl Tessera as well as early episodes of mantle downwelling in the formation of ridge belt material (*rb*). These older tectonic features were subsequently modified by a series of volcanic events. The first variety of volcanic activity involved small-scale, local volcanic eruptions that resulted in the formation of small shield volcanoes (*psh*), the second variety involved a regional expression of the proposed planet-wide resurfacing event that resulted in the formation of the plains (*pds*, *pbs*, [2,6-9]), and the third variety involved a transition back to more localized volcanic activity that resulted in the formation of large shield volcanoes (*lp*, *ed*) and fracture belts (*fb*).

These observations suggest that localized regions of extensional deformation of the surface may be induced by mantle upwelling and may indicate the locations of stalled or actively ascending volcanic plumes. Recent work using ESA Venus Express VIRTIS emissivity data targeted Idunn Mons, Hathor and Innini Montes, and Mielikki Mons, three of nine identified 'hot spot' volcanoes on the surface of Venus. The elevated emissivity signatures found in association with the stratigraphically youngest portions of these volcanoes have been proposed to indicate that volcanism in some locations of Venus may have occurred as recently as within the past 250,000 – 2.5 million years [10]. In addition, analyses of gravity and topography anomalies on Venus indicate local density anomalies beneath Idunn, Hathor, and Innini Montes [11]. While similar analyses have not yet been completed for the north polar region of Venus, these observations support our interpretation that the youngest volcanism on the surface of Venus is concentrated in large shield volcanoes.

Many questions still remain as to how volcanism shifted from localized, small shield forming activity to broad, plains forming activity and back to localized, large shield and fracture belt forming activity. For example, did plate tectonics once exist on Venus, and did the termination of this process lead to a catastrophic resurfacing event? Further analysis of mapped stratigraphic relationships in conjunction with Venus Express data can enhance our understanding of these processes. Understanding the mechanics behind the evolution of volcanism on Venus is vital for understanding the geologic history of Venus and for identifying possible analogs behind the volcanic history of Venus to apply to our understanding of the volcanic history and/or future of Earth.

References: [1] J. Head et al., *EPSC* (abs.) 2008 [2] M. Ivanov et al., *LPSC* abs. #1391, 2008 [3] K. Tanaka, *USGS Open File Report 94-438*, 1994 [4] A. Basilevsky & J. Head *Plan. Space Sci.*, 48, 75, 2000 [5] M. Ivanov & Head J. W. *JGR*, 106, 17,515, 2001 [6] A. Basilevsky and J. Head *Plan. Space Sci.*, 43(12), 1523-1553, 1995 [7] R. J. Phillips et al., *JGR*, 97, 1992 [8] N. Namiki and S. Solomon, *Science*, 265, 929-933, 1994 [9] I. Romeo and D. L. Turcotte, *Icarus*, 203(1), 13-19, 2009 [10] S. E. Smrekar et al., *Science*, 328(5978), 605-608, 2010 [11] B. Steinberger et al., *Icarus*, 207(2), 564-577, 2010.

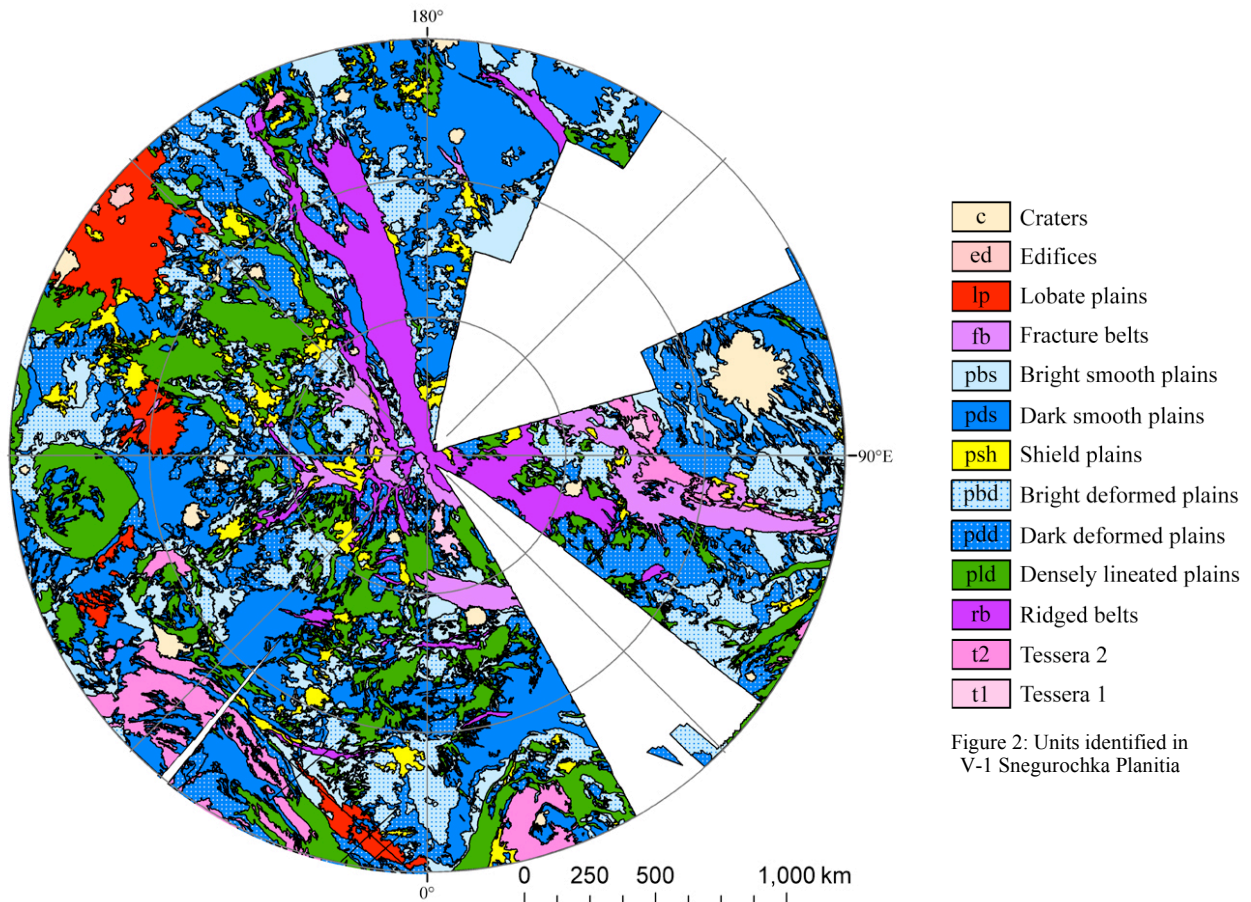


Figure 1: Geologic map of the V-1 Snegurochka Planitia quadrangle.
Map status: Submitted, revisions in progress

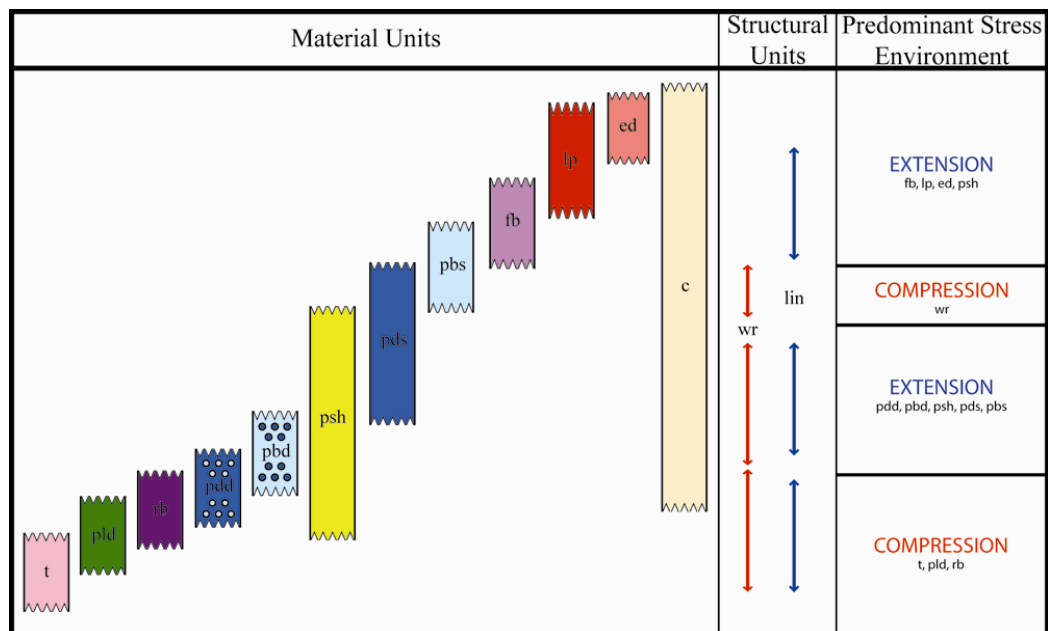


Figure 3: Correlation of mapped units for V-1 Snegurochka Planitia.

Introduction: The Fredegonde quadrangle (V-57; 50-75°S, 60-120°E, Fig. 1) corresponds to the northeastern edge of Lada Terra and covers a broad area of the topographic province of midlands (0-2 km above MPR [1,2]). This province is most abundant on Venus and displays a wide variety of units and structures [3-11]. The sequence of events that formed the characteristic features of the midlands is crucially important in understanding of the timing and modes of evolution of this topographic province.

Topographically, the Fredegonde quadrangle is within a transition zone between the elevated portion of Lada Terra to the west (Quetzalpetlatl-Boala Coronae rise, ~3.5 km) and the lowland of Aino Planitia to the north and northeast (~0.5 km). This transition is one of the key features of the V-57 quadrangle. In this respect the quadrangle resembles the region of V-4 quadrangle [12] that shows transition between the midlands and the lowlands of Atalanta Planitia. One of the main goals of our mapping within the V-57 quadrangle is comparison of this region with the other transitional topographic zones such as quadrangles V-4 and V-3 [13].

The most prominent features in the V-57 quadrangle are linear deformational zones of grooves and large coronae. The zones characterize the central and NW portions of the map area and represent broad (up to 100s of km wide) ridges that are 100s of m high. Morphologically and topographically, these zones are almost identical to the groove belt/corona complexes at the western edge of Atalanta Planitia [12]. Within the Fredegonde area, however, the zones are oriented at high angles to the general trend of elongated Aino Planitia, whereas within the V-4 quadrangle they are parallel to the edge of Atalanta Planitia. Relatively small (100s of km across, 100s of m deep) equidimensional basins occur between the corona-groove-chains in the area of V-57 quadrangle. These basins are similar to those that populate the area of the V-3 quadrangle [13]. Broad regional plains cover the surface of the basins in both regions. In contrast to Fredegonde, the area of the V-3 quadrangle displays a greater diversity of units and features [13].

Here we describe units that make up the surface within the V-57 quadrangle and present a summary of our geological map that shows the areal distribution of the major groups of units.

Material and structural units and their relationships: During our mapping we have defined the following material units that can be divided into four groups on the basis of embayment and cross-

cutting relationships. *I. The first group* consists of heavily tectonized units. (1) Densely lineated plains (pdl) with a surface that is heavily dissected by subparallel narrow and dense lineaments a few hundred meters wide and several kilometers long. Usually the lineaments completely obscure the morphology of the underlying materials. In some occurrences, however, remnants of the older lava plains are visible between the lineaments. The unit pdl is interpreted as volcanic plains, heavily deformed by extensional and/or shear structures. Type locality: 59.0°S, 85.2°E. (2) Ridged plains (pr): displays a morphology of smooth lava plains that are deformed by broad (5-10 km) and long (10s of km) linear and curvilinear ridges with rounded and slightly undulating hinges. The ridges appear to be symmetrical in cross section and sometimes form prominent belts (Oshumare Dorsa). Type locality: 57.1°S, 78.1°E. (3) Groove belts (gb) form a structural unit that consists of swarms of linear and curvilinear, long (many 10s of km), and radar bright lineaments. They are usually wide enough to show the morphology of fractures. Within the V-57 quadrangle, groove belts form the most prominent structural and topographic zones hundreds of km long and many tens of km wide that are often associated with coronae. Rims of most coronae in the map area consist of arcuate swarms of grooves. Type locality: 58.8°S, 91.6°E.

II. The second group includes three material units. (1) Shield plains (psh): are characterized by the presence of numerous small (<10 km) shield-like features that are interpreted as volcanic edifices [14-16]. Materials of shield plains (shields and intershield plains) embay all units from the first group. Shield plains represents the oldest unit that displays no pervasive tectonic structures and is mildly deformed by wrinkle ridges Type locality: 59.4°S, 76.2°E. (2) Regional plains (lower unit, rp₁): are morphologically smooth and usually have a homogeneous albedo pattern that can be locally mottled. The radar backscatter of the surface is relatively low. Numerous low, narrow, and sinuous wrinkle ridges deform the surface of the lower unit of regional plains. This unit makes up ~50% of the map area (the most abundant unit) and preferentially occurs on the floor of the low-lying basins. Type locality: 52.7°S, 107.9°E. (3) Regional plains (upper unit, rp₂): have a morphologically smooth surface that is moderately deformed by wrinkle ridges of the same family that cut the unit rp₁. Both units of regional plains embay shield plains and the units of the first group. The key

difference between the upper and lower units of regional plains is their radar albedo. In contrast to the uniform and relatively low albedo of rp_1 , the upper member of the plains is noticeably brighter and sometimes displays flow-like features. The unit rp_2 covers ~10-15% of the map area and forms equidimensional or slightly elongated occurrences from tens of kilometers to several hundred kilometers across. Type locality: 61.0°S, 74.6°E.

III. The third group includes three units that postdate units from the previous groups. There is no good evidence to establish relative ages among the units from this group (1) Shield clusters (sc): are morphologically similar to shield plains (psh) [17] but tectonically undeformed. Type locality: 69.7°S, 86.7°E. (2) Smooth plains (ps): have morphologically smooth, tectonically undisturbed, and featureless surfaces, which are usually dark. The unit occurs as small equidimensional and elongated patches several tens of km across. Type locality: 71.6°S, 92.5°E. (3) Lobate plains (pl): have a morphologically smooth and undeformed surface. The characteristic feature of the unit is its albedo pattern that consists of numerous bright and dark flow-like features that can be several tens of km long. Occurrences of the unit form equidimensional fields many tens of km across that are associated with Dunne-Musun and Ambar-ona Coronae. Type locality: 62.0°S, 91.6°E.

IV. The fourth group includes materials related to impact craters and consists of: (1) impact crater materials, undivided (central peak, floor, walls, rim, and continuous ejecta, c), type locality 56.2°S, 98.9°E, and (2) impact crater outflow material (cf), type locality 57.0°S, 101.7°E.

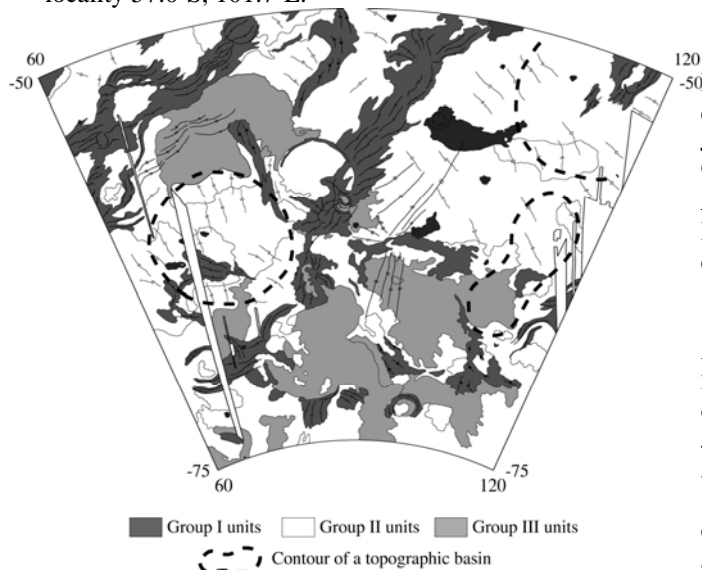


Fig. 1. Preliminary geological map of the V-57 quadrangle.

Summary: Preliminary results of the mapping of the V-57 quadrangle suggest the following sequence of major episodes in the geologic history of this region. Tectonic deformation prevailed over volcanism at the beginning of history recorded in surface geological units. Tectonic structures overprinted volcanic materials and were related to formation of the deformational belts, the most prominent of which are the corona-groove chains. Main topographic features of the region (broad linear ridges and equidimensional basins) formed during this period.

During the middle stages of evolution, regional volcanism was more important and resulted in formation of vast plains units such as psh, rp_1 and rp_2 . Tectonics played a secondary role and led to the formation of pervasive but small structures of wrinkle ridges. There is little evidence suggesting continued development of major topographic features during the middle stages of the geologic history of the region. The flow direction of lobate plains (from the broad ridges toward the floor of the basins) suggests that the overall topographic configuration of the midlands within the map area was established prior to emplacement of the youngest volcanic plains. The main structures of coronae predate shield plains and regional plains but the youngest lobate plains are typically associated with some coronae. This means that these coronae evolved during the majority of the discernible geologic record of the region. The other coronae that demonstrate only tectonic elements probably died out in the early stages of the geologic history.

References: [1] Masursky, H., et al., *JGR*, 85, 8232, 1980; [2] Pettengill, G.H., et al., *JGR*, 85, 8261, 1980; [3] Barsukov, V.L. et al., *JGR*, 91, D399, 1986; [4] Solomon, S.C. et al., *JGR*, 97, 13199, 1992; [5] Head, J.W. et al., *JGR*, 97, 13153, 1992; [6] Guest, J.E. et al., *JGR*, 97, 15949, 1992; [7] Stofan, E.R. et al., *JGR*, 97, 13347, 1992; [8] Roberts, K.M. et al., *JGR*, 97, 15991, 1992; [9] Basilevsky, A.T. et al., in: *Venus II* S.W. Bougher et al. eds., UAP, 1047, 1997; [10] Hansen, V.L. et al., in: *Venus II* S.W. Bougher et al. eds., UAP, 797, 1997; [11] Smrekar, S.E. et al., in: *Venus II* S.W. Bougher et al. eds., UAP, 845, 1997; [12] Ivanov, M.A. and J.W. Head, Geologic map of the Atalanta Planitia (V-4) quadrangle, *USGS Map* 2792, 2004; [13] Ivanov, M.A. and J.W. Head, Geologic map of the Meskhent Tessera (V-3) quadrangle, *USGS Map* 3018, 2008; [14] Aubele, J.C. and E.N. Slyuta, *EMP*, 50/51, 493, 1990; [15] Addington, E.A., *Icarus*, 149, 16, 2001; [16] Ivanov, M.A. and J.W. Head, *JGR*, 109, doi:10.1029/2004JE002252, 2004; [17] Ivanov, M.A. and J.W. Head, Geologic map of the Mylitta Fluctus (V-61) quadrangle, *USGS Map* 2920, 2006.

GEOLOGIC MAPPING OF V-19. P. Martin¹, E.R. Stofan^{2, 3} and J.E. Guest³, ¹Durham University, Dept. of Earth Sciences, Science Laboratories, South Road, Durham, DH1 3LE, UK, (paula.martin@durham.ac.uk), ²Proxemy Research, 20528 Farcroft Lane, Laytonsville, MD 20882 USA (ellen@proxemy.com), ³Department of Earth Sciences, University College London, Gower Street, London, WC1E 6BT, UK.

Introduction: A geologic map of the Sedna Planitia (V-19) quadrangle is being completed at 1:5,000,000 scale as part of the NASA Planetary Geologic Mapping Program, and will be submitted for review by September 2010.

Overview: The Sedna Planitia quadrangle (V-19) extends from 25°N - 50°N latitude, 330° - 0° longitude. The quadrangle contains the northernmost portion of western Eistla Regio and the Sedna Planitia lowlands. Sedna Planitia consists of low-lying plains units, with numerous small volcanic edifices including shields, domes and cones. The quadrangle also contains several tholi, the large flow-field Neago Fluctūs, the Manzan-Gurme Tesserae, and Zorile Dorsa and Karra-mähte Fossae which run NW-SE through the southwestern part of the quadrangle. There are six coronae in the quadrangle (Table 1), the largest of which is Nissaba (300 km x 220 km), and there are fourteen impact craters (Table 2).

Table 1. Coronae of V-19.

Name	Lat.	Long.	Max Width	Type
Ba'het	48.4	0.1	300 x 145	Concentric
Tutelina	29.0	348.0	180	Concentric
Purandhi	26.1	343.5	170	Concentric
Mesca	27.0	342.6	190	Type II
Nissaba	25.5	355.5	300 x 220	Concentric
Idem-Kuva	25.0	358.0	280	Concentric

Table 2. Impact Craters of V-19.

Name	Lat.	Long.	Diameter (km)
Ariadne	43.9	0.0	20.8
Veta	42.6	349.5	6.4
Jeanne	40.1	331.5	19.5
Unnamed	37.6	350.1	2.1
Zuhrah	34.7	357.0	6.6
Vassi	34.4	346.5	8.8
Al-Taymuriyya	32.9	336.2	21
Nutsa	27.5	341.8	4.2
Barton	27.4	337.5	50
Lachappelle	26.7	336.7	35.3
Roxanna	26.5	334.6	9.2
Kumba	26.3	332.7	11.4
Bakisat	26.0	356.8	7.4
Lilian	25.6	336.0	13.5

Six types of materials have been mapped in the V-19 quadrangle: tessera, plains, volcanic edifice and flow, corona, crater, and surficial materials. All types of material units occur throughout the quadrangle, with the exception of tessera materials, which crop out only in the eastern part of the mapped region.

Highly deformed materials that have been mapped as tessera (unit t) range in size from < 50 km to several hundreds of kilometers across, and include the Manzan-Gurme Tesserae which are made up of several indi-

vidual outcrops distributed along the eastern edge of this quadrangle.

Seven plains materials units have been mapped in V-19 (from oldest to youngest): Sedna deformed plains material (unit pdS), Sedna patchy plains material (unit ppS), Sedna composite-flow plains material (unit pcS), Sedna homogeneous plains material (unit phS), Sedna uniform plains material (unit puS), Sedna mottled plains material (unit pmS) and Sedna lobate plains material (unit plS). These seven units range from relatively localized, limited extent units (e.g. unit pdS) to more regional plains units (e.g. unit phS). Each of the mapped plains units are composed of groups of many smaller plains units of varying age. These smaller plains units have been grouped into a mappable unit because of their similarity in appearance and stratigraphic position relative to other plains units. The regional-scale plains unit (unit phS) dominates the northeastern half of the map. The dominance of this regional-scale plains unit is similar to other mapped quadrangles on Venus [1, 2]. The remaining plains units, units pcS, pdS, ppS, puS, pmS and plS, tend to crop out as isolated patches of materials.

The V-19 quadrangle contains a variety of mappable volcanic landforms including two shield volcanoes (Evaki Tholus and Toci Tholus) and the southern portion of a large flow field (Neago Fluctūs). A total of sixteen units associated with volcanoes have been mapped in this quadrangle, with multiple units mapped at Sif Mons, Sachs Patera and Neago Fluctūs. An oddly textured, radar-bright flow is also mapped in the Sedna plains, which appears to have originated from a several hundred kilometer long fissure. The six coronae within V-19 have a total of eighteen associated flow units. Several edifice fields are also mapped, in which the small volcanic edifices both predate and postdate the other units. Impact crater materials are also mapped.

The geologic history of the V-19 quadrangle is dominated by multiple episodes of plains formation and wrinkle ridge formation interspersed in time and space with edifice- and corona-related volcanism. The formation of Eistla Regio to the southwest of this quadrangle postdates most of the mapped plains units, causing them to be deformed by wrinkle ridges and overlaid by corona and volcano flow units.

Conclusions: V-19 is comparable with our previously mapped quadrangles, V-39, V-46, V-28 and V-53 [3, 4, 5 and 6]. V-19, V-39 and V-46 have a similar number of mapped plains units, whereas V-28 and V-53 have a greater number. V-19, V-28 and V-53 are similar to one another in that all three quadrangles have very horizontal stratigraphic columns, as limited contact between units prevents clear age determinations. This does not mean that all units within each quadrangle formed at the same time. Rather, the stratigraphic columns reflect the limited nature of our stratigraphic knowledge in these quadrangles, allowing for numerous possible geologic histories. This uncertainty is illustrated by the use of hachured columns for each unit. Resurfacing in these quadrangles is on the scale of 100s of square kilometers, consistent with the fact that they lie in the most volcanic region of Venus.

References: [1] Bender, K. C. et al., 2000, Geologic map of the Carson Quadrangle (V-43), Venus. [2] McGill, G. E., 2000, Geologic map of the Sappho Patera Quadrangle (V-20), Venus. [3] Brian, A. W. et al., 2005, Geologic Map of the Taussig Quadrangle (V-39), Venus. [4] Stofan, E. R. and Guest, J. E., 2003, Geologic Map of the Aino Planitia Quadrangle (V-46), Venus. [5] Stofan, E. R. et al., 2009, Geologic Map of the Hecate Chasma Quadrangle (V-28), Venus. [6] Stofan, E. R. and Brian, A. W., 2009, Geologic Map of the Themis Regio Quadrangle (V-53), Venus.

Introduction: The Lachesis Tessera Quadrangle (V-18) lies between 25° and 50° north, 300° and 330° east. Most of the quadrangle consists of “regional plains” (1) of Sedna and Guinevere Planitiae. A first draft of the geology has been completed, and the tentative number of mapped units by terrain type is: tesserae – 2; plains – 4; ridge belts – 1; fracture belts – 1 (plus embayed fragments of possible additional belts); coronae – 5; central volcanoes – 2; shield flows – 2; paterae – 1; impact craters – 13; undifferentiated flows – 1; bright materials – 1.

Material units: By far the areally most extensive materials are regional plains. These are mapped as two units, based on radar backscatter (“radar brightness”). The brighter unit appears to be younger than the darker unit. This inference is based on the common presence within the lighter unit of circular or nearly circular inliers of material with radar backscatter characteristic of the darker unit. The circular inliers are most likely low shield volcanoes, which are commonly present on the darker unit, that were only partially covered by the brighter unit. Clear cut examples of wrinkle ridges and fractures superposed on the darker unit but truncated by the brighter unit have not been found to date. These relationships indicate that the brighter unit is superposed on the darker unit, but that the difference in age between them is very small. Because they are so widespread, the regional plains are a convenient relative age time “marker.” The number of impact craters superposed on these plains is too small to measure age differences (2), and thus we cannot estimate how much time elapsed between the emplacement of the darker and brighter regional plains units. More local plains units are defined by significantly lower radar backscatter or by a texture that is mottled at scores to hundreds of kilometers scale. A plains-like unit with a homogenous, bright diffuse backscatter is present as scattered exposures in the eastern part of the quadrangle. These exposures have been mapped as “bright material,” but it is not clear at present if this is a valid unit or if it is part of the brighter regional plains unit.

Tessera terrain is primarily found along the western border of the quadrangle, where Lachesis Tessera refers to the southern exposures, and Zirka Tessera refers to northern exposures. A second tessera unit has been mapped with the symbol “t?” This unit appears to be deformed by the requisite 2 sets of closely spaced structures, but it is so extensively flooded by regional plains materials that the structural fabric is partially

obscured. Tessera terrain is present in the adjacent V-17 quadrangle, where both Lachesis Tessera and Zirka Tessera are areally more extensive than in V-18.

Features: Ridge and fracture belts are both present, but not as extensive as is the case in, for example, the Pandrosos Dorsa (3) and Lavinia Planitia (4) quadrangles. As is commonly the case, it is difficult to determine if the materials of these belts are older or younger than regional plains. A recent study using radar properties (5) demonstrated that at least most ridge belts appear to be older than regional plains. The materials of fracture belts probably are also older than regional plains, but the fractures themselves can be both older and younger than regional plains (e.g., 3).

Four named coronae are present, but only Zemire Corona has significant associated flows. An interesting nearly linear structure extends from the fracture belt Breksta Linea in the western part of the quadrangle east-southeastward through Zemire Corona to Pasu-Ava Corona. The tectonic significance of this composite structure is unclear at present. Jaszai Patera is located at 32.0° north, 305.0° east, and is approximately 70 km in diameter. There is an unnamed feature just north-northeast of Jaszai Patera. An unnamed feature located in the southeastern part of the quadrangle appears to be a corona that is obscured by a gore.

Volcanic materials and landforms are abundant in the Lachesis Tessera quadrangle. In particular, small domes and shields are abundant and widespread. In places, small shields are not only exceptionally abundant, but they are associated with mappable materials, and thus help define a “shield flows” unit. Isolated flows are common, and where these are areally large enough they have been mapped as undifferentiated flows. Other volcanic features include two relatively large shield volcanoes, both with complete calderas and with flows extensive enough to map. A number of pancake domes occur in the Lachesis Tessera quadrangle. Various mechanisms for forming flat-topped domes such as these have been proposed, but none is really satisfactory. This quadrangle is not likely to provide breakthrough evidence for the genetic processes responsible for pancake domes.

The 13 impact craters in the Lachesis Tessera quadrangle range in diameter from 2.4 to 40 km. Four of these are actually doublets. Five of the craters have associated radar-dark halos or parabolas. Only 2 of the 13 craters are significantly degraded. All 13 craters are superposed on either regional plains or on flows that are, in turn, superposed on regional plains.

The fragmented record of tessera and some deformation belts suggests that flooding by regional plains materials has had a significant effect on the distribution of materials older than the regional plains. This, in turn, indicates that regional plains must be relatively thin in the Lachesis Tessera quadrangle, or else the tessera and deformation belts exhibit less relief than generally is the case.

References: [1] McGill, G.E., V-20 quadrangle, 2000; [2] Campbell, B.A., JGR 104, 21,951, 1999; [3] Rosenberg, E., and McGill, G.E., V-5 quadrangle, 2001; [4] Ivanov, M.A., and Head, J.W., III, V-55 quadrangle, 2001; [5] McGill, G.E., and Campbell, B.A., JGR 111, E12006, doi:10.1029/2006JE002705, 2006.

COMPARISON OF MAPPING TESSERA TERRAIN IN THE PHOEBE REGIO (V-41) AND TELLUS TESSERA (V-10) QUADRANGLES. D. A. Senske, Jet Propulsion Laboratory/California Institute of Technology, Pasadena, CA 91109.

Introduction: Tessera terrain was first described from data collected by the Venera 15/16 spacecraft [1]. These high standing crustal plateaus are characterized by enhanced radar-scale roughness (*i.e.* at the 12-cm Magellan radar wavelength), low radar reflectivity and multiple episodes of deformation. Outcrops range from local exposures (100s of km across) to continent sized (*e.g.* Aphrodite Terra). To understand the tectonic history of these relatively old terrains, detailed geologic and stratigraphic relations have been assessed by a number of investigators [2,3,4]. Tessera is typically mapped as a global-scale unit although significant variations in both geologic setting and character are observed. This leads to the suggestion that the rock material making up these terrains may vary across the planet. As such, we are carrying out geologic mapping of both the Phoebe Regio (V-41) and Tellus Tessera (V-10) quadrangles to ascertain their geologic history and make comparisons between these distinct upland plateaus.

Phoebe Regio: Located to the south of Beta Regio, Phoebe Regio rises to an elevation of 1.5- to 2.5-km above the surrounding plains. Although the core part of Phoebe exhibits evidence of deformation due to compression (*e.g.* near 15°S, 282°), the dominant tectonic style is characterized by intersecting and radiating sets of fractures and grabens [5,6]. The margins of Phoebe are embayed by the surrounding plains producing significant outliers and kipukas. At the scale of the Magellan data, it is not possible to distinguish layering within the high standing rock outcrops. In some locations the tessera appears to form a gradational contact with the surrounding plains. The eastern and southern margins of the elevated terrain are bound by major rift valleys (Devana Chasma and Pinga Chasma respectively). Normal faulting associated with these rifts is widely distributed and represents some of the most recent activity in this area. The extensional environment is interpreted to have facilitated widespread volcanic activity resulting in the emplacement of large edifices such as Yunya-mana Mons and a significant number of lava flow fields.

Tellus Tessera: Located to the north of Aphrodite Terra, Tellus reaches an elevation of 2.0- to 3.0-km above the adjacent plains. The geology of this part of the planet is quite complex and is generally characterized by large-scale (10s to 100s of km wide) ridges and valleys crosscut by smaller scale graben forming what has been termed ribbon terrain [7]. Geologic mapping has revealed the presence of compressional

zones along the eastern and western margins of the upland. In addition, the presence of belts of ridges in the interior of this highland suggests a significant episode of collisional activity has taken place that incorporates individual blocks of tessera. The northern part of this upland is extensively embayed by plains materials suggesting tectonic activity has given way to a predominately volcanic environment. This is also distinguished by the relatively high concentration of coronae along the northern part of Tellus. In the vicinity of Eliot Patera there is evidence for possible layering within outcrops [8]. Although of limited extent, this may suggest the presence of stacked volcanics, providing support to the assertion for variability in crustal materials within Tellus [8].

Tessera Geologic Comparisons: From the standpoint of geologic setting and morphology, there are significant differences between Phoebe Regio and Tellus Tessera. The former is dominated by an extensional environment and the latter by compression and later extension. Phoebe lacks evidence of outcrop layers (at the limit of the resolution of the data). Gradational contacts between the tessera material and the surrounding plains may indicate that parts of Phoebe may be older regional plains that have been deformed. Tellus shows evidence of limited layering within rock units and it may be made up of smaller occurrences of tessera assembled into a larger unit through collision and compression.

Regional and global-scale mapping of Venus typically classifies tessera as a single unit type. Detailed study provides insight into the geologic and morphologic variability between different occurrences of this terrain. A goal of future Venus exploration will be to understand how rock compositions vary across the planet. Additional mapping along with surface property and geophysical analysis is needed to determine sites to investigate from orbiters and landers.

References: [1] Barsukov, V. L., et al. (1986) *JGR*, 91, D378-D398. [2] Bindschadler, D. L. and Head, J. W. (1991) *JGR*, 96, 5889-5907. [3] Gilmore, M. S. et al. (1998) *JGR*, 103, 16813-16840. [4] Hansen, V. L. et al. (2000) *JGR*, 105, 4135-4152. [5] Bindschadler, D. L. et al. (1992) *JGR*, 97, 13495-13532. [6] Hansen, V. L. and Willis, J. J. (1996) *Icarus*, 123, 296-312. [7] Hansen, V. L. and Willis, J. J. (1998) *Icarus*, 132, 321-343. [8] Senske, D. A. and Plaut, J. J. (2009) *LPSC XL*, Abstract # 1707.

Introduction: The Devana Chasma quadrangle (V-29; 0-25°N/270-300°E) is situated over the north-eastern apex of the Beta-Atla-Themis (BAT) province and includes the southern half of Beta Regio, the northern and transitional segments of the Devana Chasma complex, the northern reaches of Phoebe Regio, Hyndla Regio, and Nedolya Tesserae, and several smaller volcano-tectonic centers and impact craters.

Methodology & Data Sets: Aiming to discover the types of processes that have shaped the Venusian surface, geologic mapping began with the identification of major structural and morphologic features (lava flow boundaries, shield fields and edifices, radial and concentric deformation zones) and follows with the formal delineation of geologic map units. Temporal constraints are determined by embayment and cross-cutting relations as well as crater morphology and crater halo modification and degradation [1].

All data used were acquired during NASA's Magellan mission (operational 1989-1994) and includes: Synthetic Aperture Radar (SAR; basemap provided by the United States Geological Survey at 75 meter/pixel), altimetry and reflectance (~10 x 10 km footprint), and emissivity (~20 x 20 km footprint). Mapping is facilitated with the use of a georeferenced digital synthetic stereo (red-blue anaglyph, which merges SAR and altimetry together). ESRI ArcGIS software is used along with a WACOM Cinitiq 21 inch interactive monitor and digitizing pen; important geological features are digitized and attributed in the ArcGIS geodatabase as a location feature (point), linear feature (line), or geocontact (polyline features that will be converted into polygon features at a later time). While the published map scale will be 1:5M, linework is constructed at a scale larger than the published scale. Location features and linear features are mapped at a scale of 1:300,000; geocontacts are mapped at a scale of 1:500,000. Excess linework (i.e., very closely spaced lineament sets) may be edited prior to printed map publication but will be preserved in digital archives. The accuracy of the linework is controlled using streaming (500 map units) and snapping tolerances (set to 250 map units). Upon the completion of mapping, the geodatabase within ArcGIS will allow for efficient data analysis.

Preliminary mapping: Devana Chasma. The most prominent feature, and hence namesake of the V-

29 quadrangle, is Devana Chasma - a narrow (~150 km) 1000 km long, segmented topographic trough (1-3 km deep with respect to the surrounding terrain), which accommodates 3 to 9 kilometers of extension [2]. Devana Chasma is one of three radiating arms of tectonic lineaments that trends south from Beta Regio and marks a physiographic divide between the relatively young Beta-Atla-Themis province to the west and the older highlands and plains to the east according to Average Surface Model Age (ASMA) [3,4]. Near the center of the map area (8°N, 286°E), Devana Chasma's northern lineament suite decreases in lineament density and changes trend to the southeast where it meets the southern section of Devana Chasma, which trends north and veers to the northwest. Preliminary mapping has delineated major structural trends (mostly large normal faults, which agree with previous investigators [5-8]), but has yet to reveal significant temporal constraints between the northern and southern segments. Identification and delineation of nearby volcanic units and assessment of their relative timing may help constrain the timing of Devana Chasma lineaments, which deform the local and regional flows.

Tessera. Geologic contacts are drawn in order to define individual geologic units. In the case of tessera, geologic contacts mark regions of highly deformed material characterized by intersecting structures. In the Devana Chasma quadrangle, tesserae are typically high standing regions with a polygonal, mosaic-like surface, and are located predominantly to the east of Devana Chasma. Tessera units are easily recognized in the SAR by their distinct polygonal surface and bright radar properties but altimetry is also useful in defining their boundaries. Two major tessera units are defined in V-29 (Nedolya Tesserae and Hyndla Regio); each is part of much larger tessera provinces outside of the V-29 cartographic boundaries. In addition to the two large tessera units, several smaller outliers, or kipuka, of tessera are found throughout the V-29 quadrangle; some kipuka clearly represent lateral extensions of tesserae underneath embaying flows, whereas other kipuka cannot be tied to larger expanses of tesserae.

Within the Nedolya and Hyndla tessera units, localized low-lying areas exhibit a dark radar characteristic of intra-tessera plains. We hypothesize two possi-

ble scenarios for this dark material. The first possibility is that the material is produced by shields within the tessera. The second is that dark plains material flowed through the troughs seen in the tessera and in-filled the low-lying areas. Both of these possibilities require that the dark material be younger than the bright material. Although timing is clear, identifying pathways for these materials to the plains is difficult given the present topographic resolution.

Volcanic Features. Contacts have been drawn to define the major volcanic edifices found in the V-29 quadrangle including Beta Regio and the smaller Tuulikki Mons (diameter of approximately 1000 kilometers). The contact around Beta Regio is well defined in places by lobate lava flows that superimpose the surrounding plains units. However, the bright radar characteristic of Devana and Žverine Chasmata southwest of Beta Regio (due to higher density of structural lineaments) interferes with individual flow boundaries making the contact difficult to follow; the contact here is inferred. The contact to the southeast of Beta is defined by a transition from mottled terrain with fractures, which radiate outward from Beta, to homogeneous plains with polygonal lineaments. Shield clusters roughly follow this boundary and may indicate a transition in the types of volcanic processes at work. The contact around Tuulikki Mons is largely defined by flow aprons that superpose the plains and/or interfingered with flows from other volcanic centers. Flow arrow symbology has been used to indicate where flow margins are clearly visible and can be traced to their source(s).

A variety of small volcanic edifices (< 20 km in diameter) are present in V-29, including: densely populated shield fields, pancake domes, edifices with scalloped margins and flat-topped relief, edifices with steep margins and concentric flat-topped relief and a cratered center, and edifices where radar backscatter suggests a more conical shape. It is unclear whether there is a relationship between the types of volcanic edifices present and the difference in terrain between the eastern and western regions of the V-29 quadrangle. However, it is clear that there is a difference in the concentration of small volcanic edifices between these two regions. The concentration to the west of Devana Chasma is ~ 1.4 volcanoes/ 10^6 km² whereas the concentration to the east is ~ 0.73 volcanoes/ 10^6 km². Beta Regio and the rift itself have small, localized, densely clustered shield fields but the overall concentration

and distribution is difficult to determine because of the lack of radar contrast in these “bright” terrains.

Craters. There are 19 impact craters in the V-29 quadrangle that range in size from 2.8 km to 102.2 km in diameter [9]. The ejecta from craters is identified by its bright radar characteristics; however, many craters also exhibit more diffuse ejecta with darker radar properties that radiate farther from the center of the crater than the bright ejecta and have been assigned to a second ejecta unit. Lava flows, which may have formed during the time of impact, are also seen and mapped as crater flow material (i.e., Rosa Bonheur and Boivin craters).

Conclusion: Distinct morphologic differences are observed between the western and eastern portions of the map region. The terrain to the east of Devana is dominated by thousands of square kilometers of tessera (see above), whereas the west contains Tuulikki Mons, a higher concentration of small shield edifices and shield-type plains, and only a few isolated kipuka of tessera. Local ebayment relations between the large tessera regions and plains, including the intra-tessera plains, suggests that tessera are locally the oldest units within the V-29 quadrangle. Tesserae are laterally extensive to the east, and their high-standing nature facilitates their preservation whereas the lower-lying plains to the west are more susceptible to resurfacing by intermediate and small scale volcanism (e.g., Tuulikki Mons, and shields). The geographic distribution of our preliminary geologic units corresponds to the age relations delineated by the ASMA studies [3, 4].

References: [1] Basilevsky, A.T. et al. (2003) *Geophys. Res. Lett.* 30, doi:10.1029/2003GL017504. [2] Keifer, W.S and Swafford, L.C. (2006) *J. Struct. Geo.*, 28, p. 2144-2155. [3] Phillips, R.J. and Izenberg, N.R. (1995) *Geophys. Res. Lett.*, 22, p. 1517-1520. [4] Hansen, V.L. and Young, D.A. (2007) Geological Society of America Special Paper 419, p. 255-273. [5] Stofan et al. (1989) *GSA Bull.* 101, p. 143-156. [6] Solomon et al. (1992) *J. Geophys. Res.*, 97, p.13,199-13,255. [7] Foster and Nimmo (1996) *EPSL* 143, p. 183-195. [8] Connors and Suppe (2001) *J. Geophys. Res.*, 106, p. 3237-3260. [9] Herrick, R.R. et al. (1997) in *Venus II*, p.1015-1046.

GEOLOGIC MAPPING OF THE ARISTARCHUS PLATEAU REGION ON THE MOON. T.A. Lough¹, T.K.P. Gregg¹, and R. Aileen Yingst²; ¹411 Cooke Hall, Geology Dept., University at Buffalo, Buffalo, NY 14260 (talough@buffalo.edu), ²2420 Nicolet Dr., Natural and Applied Sciences, University of Wisconsin-Green Bay, WI 54311.

Introduction: Aristarchus plateau (~25°N, 40°W) is a volcanologically diverse region containing sinuous rilles, volcanic depressions, mare material of various ages—including a candidate for the youngest mare unit on the lunar surface—pyroclastic deposits, and material of possible highland origin [1-5]. Here, we present preliminary mapping of a 13° x 10° area around Aristarchus plateau [6]. Interpretations of the region's volcanic evolution have implications for the global history of lunar volcanism, the crustal and mantle development of the Moon, and may ultimately help support successful lunar exploration [7].

Background: The map area contains: mountainous highland terrain; primary and secondary impact craters; the highest concentration of sinuous rilles on the Moon (probably lava channels and/or collapsed lava tubes); volcanic depressions and hills [1]; lava flows ranging in age from possibly as young as 1.2 Ga to >3.4 Ga [2]; and a blanket of dark mantling material interpreted to be pyroclastic deposits [e.g., 3-5]. Kiefer [8] found positive gravitational anomalies on the eastern and southern margins of the pla-

teau that may correlate with a magma intrusion. Radon detection around the region suggests it is still degassing [8, 10].

Researchers created several geologic maps of the Aristarchus region using Apollo-era data [e.g., 11-13] as well as compositional maps from ground-based radar and orbital remote sensing data [e.g., 14-16]. The map presented here combines new observations with previous mapping results to more accurately assess volcanic timing and emplacement mechanisms.

Methods: The USGS provided orthorectified digital basemaps of the Lunar Orbiter (LO) and Clementine data sets and a geodatabase containing the features used to map the Copernicus quadrangle [17]. The basemap is mosaicked Lunar Orbiter IV and V images because: 1) they are the highest resolution comprehensive dataset available (~1 - ~150 m/pixel); and 2) low sun angles highlight morphologic and topographic features. We also consulted iron and titanium ratio maps [18] as well as high-resolution Apollo and LO images.

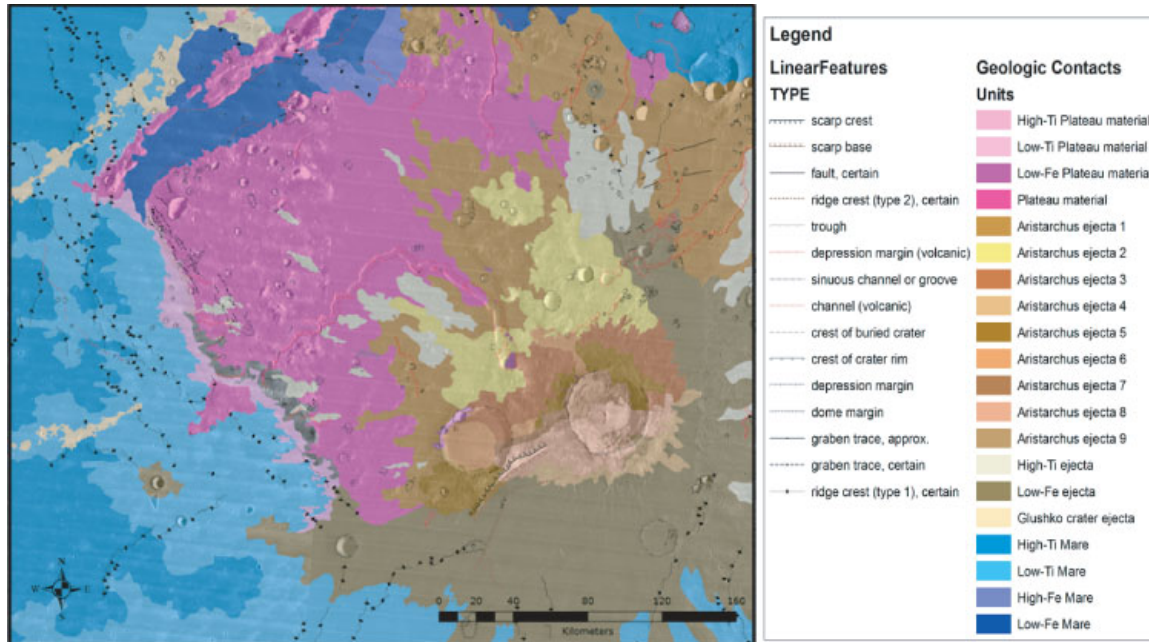


Figure 1. Preliminary geologic map of the Aristarchus plateau region superimposed on a Mercator projection of the Lunar Orbiter mosaicked basemap. Mare units are in shades of blue, plateau units are in shades of pink, and ejecta units are in shades of brown. Upper left is 30°N, 58°W; lower right is 20°N, 45°W.

Units: They are defined based on their spectral and morphological characteristics. We have identified three unit types: Mare material, Plateau material, and Ejecta material. Four mare units surround Aristarchus plateau, filling topographically low areas. The four plateau units range from relatively low Fe content and high albedo to high Ti and low albedo. Two plateau units sandwich the plateau's margin. The "inside" unit has relatively high Ti content whereas the "outside" unit has relatively low Ti content. Twelve ejecta units comprise Aristarchus crater ejecta as well as ejecta from smaller local impacts, and ejecta rays from Glushko crater. The ejecta units are based on target-material composition, albedo, and deposit texture. Two Aristarchus crater ejecta units share spectral characteristics with smaller impact craters and are interpreted to be one or more excavated subsurface layers continuous across the region.

Structures: We have identified the following features within the Aristarchus plateau map area.

Sinuuous rilles are concentrated in the northeastern corner and typically radiate away from the plateau. Secondary orientation trends align with local features such as impact crater rims and fractures [19]. Rilles range from <5 km to >310 km long. Only Schrödinger Valley contains a younger rille cutting the primary rille floor.

Hills. Two hills with spectral characteristics congruent with the surrounding unit are identified within the map area (23.3°N, 47.6.0°W and 20.3°N, 50.0°W). The first is in Aristarchus ejecta 1. It is ~3 km in diameter and within 1 km of the source crater for a sinuous rille. This feature may be highland material mantled by a fluid, low-viscosity, mafic lava or by a mafic regolith, or a volcanic construct. The second hill is within the Low-Fe ejecta unit. It is ~11 km in diameter with a ~3 km diameter irregular depression slightly southeast of the center of the hill.

Irregular Depressions are typically situated at rille heads. Irregular depressions are also present in a heavily fractured region adjacent and parallel to the northwest plateau margin.

Mare-type Wrinkle Ridges display complicated cross-cutting patterns, typically trending from the northwest to the southeast. Krieger crater crosscuts a wrinkle ridge with a northeast/southwest orientation. Wrinkle ridges within ~40 km of the plateau parallel the plateau margins.

Linear Features: Linear troughs cross-cut and parallel sinuous rilles in the northeast. These troughs are interpreted to be fractures, many of which appear to have provided a path for rille-forming lava. Linear to sub-linear troughs cover ~30 km of the southwest edge of the plateau and run parallel to its margin. These depressions modify craters (e.g., Raman crater)

and are the origin for several volcanic depressions and sinuous rilles.

Aristarchus Crater: (Figure 2). Channels within Aristarchus crater cut through all units and structural features. These channels locally feed relatively smooth flat-lying deposits on the crater rim, wall terraces, or floor, and are interpreted to be impact-melt channels and ponds.

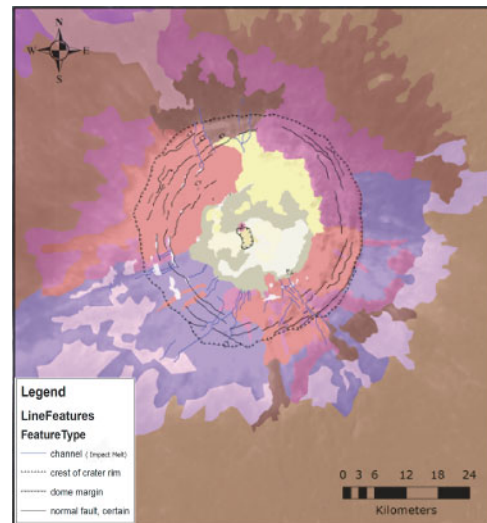


Figure 2 Units and features in the map are superimposed on a Mercator projection of the Lunar Orbiter mosaicked basemap. Ejecta units are shown in pink shades and floor units are shown in yellow shades.

References: [1] Wilhelms (1987) *The Geologic History of the Moon*, USGS Prof. Paper 1348. [2] Hiesinger et al. (2000) *JGR*, 105, 29,239-29,275. [3] Adams et al. (1974) *Proc. Lunar Plan. Conf.* 5, 1, 171-186. [4] Gaddis et al. (1985) *Icarus*, 61, 461-489. [5] Weitz et al. (1998) *JGR* 103, 22,725-22,759. [6] Yingst et al. (2009) LPSC abstract #1319 [7] NRC (2007) *The Scientific Context for Exploration of the Moon: Final Report*, <http://www.nap.edu/catalog/11954.html>, 120pp. [8] Kiefer (2009) LPSC # 1106. [9] Gorenstein and Bjorkholm (1973) *Science* 179, 792-794. [10] Lawson et al. (2005) *JGR*, 110, E09009, doi:10.1029/2005JE002433. [11] Moore (1965) *USGS Misc. Inv. Ser. Maps* I-465. [12] Moore (1967) *USGS Misc. Inv. Ser. Maps* I-527. [13] Zisk et al. (1977) *Moon*, 17, 59-99. [14] Lucey et al. (1986) *JGR*, 91, D344-D354. [15] McEwen et al. (1994) *Science* 266, 1858-1862. [16] Chevrel et al. (2009) *Icarus*, 199, 9-24. [17] Gaddis et al. (2006) LPSC abstract # 2135. [18] The LPI Clementine Mapping Project, <http://www.lpi.usra.edu/lunar/tools/clementine/>. [19] Lough and Gregg (2009) *GSA Annual Meeting*, abstract 276-10.

Introduction: In this study we use recent image, spectral and topographic data to map the geology of the lunar South Pole quadrangle (LQ-30) at 1:2.5M scale [1-7]. The overall objective of this research is to constrain the geologic evolution of LQ-30 (60°-90°S, 0°-±180°) with specific emphasis on evaluation of a) the regional effects of impact basin formation, and b) the spatial distribution of ejecta, in particular resulting from formation of the South Pole-Aitken (SPA) basin and other large basins. Key scientific objectives include: 1) Determining the geologic history of LQ-30 and examining the spatial and temporal variability of geologic processes within the map area. 2) Constraining the distribution of impact-generated materials, and determining the timing and effects of major basin-forming impacts on crustal structure and stratigraphy in the map area. And 3) assessing the distribution of potential resources (e.g., H, Fe, Th) and their relationships with surface materials.

Methodology: This project utilizes ArcGIS (v. 9.3) to compile image, topographic and spectral datasets to produce a geologic map of LQ-30. The study uses the Clementine UVVIS 750-nm mosaic (100 m/pixel) as its primary base to characterize geologic units from surface textures and albedo, identify contacts and structures, and map impact craters (D>1 km). Additional datasets are being used to complement the UVVIS base and include mosaics (Lunar Orbiter, Clementine NIR), images (LROC, Clementine UVVIS and HIRES, and Lunar Orbiter), Clementine color ratio data, and LOLA topography.

Regional Geology: LQ-30 exhibits ~16 km of relief. The near side consists predominantly of cratered highlands, is more heavily cratered and displays higher elevations than the far side. This difference is due to the overwhelming presence of SPA, which encompasses nearly all of the far side map area.

SPA is the largest (D=2600 km, ~18 km deep) and oldest (pre-Nectarian) impact basin identified on the Moon [8-10]. Models suggest that SPA formed by an oblique impact that excavated material from the upper crust [11,12] to the lower crust or upper mantle [13,14]. Galileo and Clementine multispectral data show enrichment in mafic materials [15-19] and LP-GRS data show enhancements in both Fe and Th [20-23] within the basin relative to the surrounding highlands. The materials exposed within SPA, such as in central peaks or in crater walls, could be used to estimate the composition of the lower crust/upper mantle.

Mapping Results: LQ-30 hosts all or part of 46 impact features greater than 100 km in diameter that would have significantly affected the structure of the crust and redistributed large amounts of material across

the surface [7]. Impact craters display morphologies ranging from simple to complex [7-9,24] and most contain floor deposits distinct from surrounding materials. Most of these deposits likely consist of impact melt; however, some deposits, especially on the floors of the larger craters and basins (e.g., Antoniadi), exhibit low albedo and smooth surfaces and may contain mare. Higher albedo deposits tend to contain a higher density of superposed impact craters.

Antoniadi Crater. Antoniadi crater (D=150 km; 69.5°S, 172°W) is unique for several reasons. First, Antoniadi is the only lunar crater that contains both a peak ring and a central peak, placing it morphologically between impact craters and multi-ring basins [8,9]. Second, it contains the lowest elevations on the Moon (-8.5 km), which may provide access to lower crustal/upper mantle materials via its central peak and peak ring. Its floor deposits consist of dark smooth material near the center of the crater, and brighter more rugged material between the peak ring and crater wall [7,25]. Recent mapping shows that the dark material embays the rugged material, as well as the peak ring and central peak. The rugged material likely includes impact melt. Superposition relationships indicate the dark material was emplaced after the rugged material and may consist of mare [7].

Crater size-frequency distributions for small craters (D<10 km) superposed on Antoniadi's ejecta blanket suggest an Upper Imbrian age, whereas craters greater than 10 km in diameter suggest a Lower Imbrian/Nectarian age [7,25]. It is important to note that Antoniadi's ejecta blanket also contains a significant number of secondary craters that are likely included in the counts and will affect age determination.

Schrödinger Basin. Schrödinger basin (76 °S, 134 °E) is one of the least modified lunar impact basins of its size, is believed to be Imbrian in age [6-8,26], and is likely one of the last major basin-forming impact events on the Moon, slightly older than the Orientale impact, which emplaced secondary craters on Schrödinger's floor [26]. The basin exhibits an outer ring (D=312 km) that defines its rim and an inner peak ring (D=160 km) represented by a discontinuous ring of mountains. LOLA topography shows the basin is ~8 km deep with elevations of ~2.5 km (max) along the western rim and -5.5 km (min) on the floor [6,7].

Arcuate to linear fractures are prominent on the basin floor and occur concentric and radial to the basin rim. Most fractures bisect plains-forming units, but some bisect the peak ring. These features are a few kilometers wide, and tens to a few hundred kilometers long and appear similar to other floor-fractured craters on the Moon and Mars [27].

Mapping has identified nine distinct units in the Schrödinger Assemblage organized into three groups - Basin Materials, the Plains Formation, and the Volcanic Formation [6,7].

Basin Materials: The oldest materials exposed in Schrödinger are *Schrödinger peak ring material* and *Schrödinger basin rim material* [6,7]. The peak ring material forms an incomplete ring of mountains around the center of Schrödinger. The basin rim material forms the topographic rim crest and interior wall of Schrödinger. These materials are interpreted to consist of pre-Schrödinger crustal materials uplifted following the impact event [6,7,12,28].

Plains Formation: The floor of Schrödinger is covered with plains-forming materials that display a variety of surface textures and albedos. *Schrödinger rugged plains material* is the oldest plains material on the basin floor. Most exposures are found outside of the peak ring and form heavily cratered and knobby plateaus and massifs of moderately high albedo [6]. *Schrödinger hummocky plains material* occupies much of the floor along the northern and western walls within Schrödinger, and in the south where the peak ring is the most discontinuous. Hummocky plains display moderately cratered, low albedo surfaces with gently rolling topography [6]. The rugged and hummocky plains materials are interpreted to consist of impact melt [6,7].

Schrödinger smooth plains material, found just inside the peak ring, embays the rugged plains, peak ring and basin wall materials. The smooth plains display moderate to high albedo and contain few craters [6]. *Schrödinger mottled plains material*, found primarily in the center of Schrödinger, displays a smooth surface that is lower in albedo and less cratered than the smooth plains. The smooth plains and mottled plains materials are interpreted to be volcanic (mare) in nature, possibly erupted via floor fractures [6,7].

Schrödinger knobby plains material forms two high-albedo deposits along the southern basin wall. These deposits exhibit lobate edges, and clusters of rounded and elongated knobs. Knobby plains material is interpreted to be (a) impact ejecta, (b) basin wall materials emplaced by landslides, and/or (c) more rugged exposures of the rugged plains [6,7].

Volcanic Formation: Volcanic materials are concentrated inside Schrödinger's peak ring. *Schrödinger dark plains material* displays a smooth, featureless, low albedo surface. Clementine UVVIS color ratio data show these deposits are more mafic relative to other Schrödinger plains [6]. Within one exposure, a long (10s of kilometers) sinuous rille emerges from the mottled plains and terminates within the dark plains. Dark plains material is interpreted to be composed of fluid basaltic lavas [5-7].

A small (D=5 km) well-preserved ovoidal cone is found in the eastern part of Schrödinger, just inside the peak ring. The cone displays ~500 m of relief above

the surrounding plains and is ~400 m deep from its floor to its rim [6]. The cone has been characterized as a "maar" crater [26] and a "dark-halo crater" (DHC) [29], and has been identified as the source of pyroclastic eruptions [26,29]. *Schrödinger dark material* forms a small deposit that surrounds and forms the flank of the DHC. This deposit exhibits a relatively smooth, lightly cratered surface with lower albedo than the surrounding plains [6]. Schrödinger dark material displays an unusually strong mafic band (950/750 nm versus 750 nm) in Clementine UVVIS data, but also displays similarities to lunar highland soils [29]. Based on the unit's relationship with the DHC and its spectral signature, Schrödinger dark material is interpreted to consist partly of mafic materials emplaced via pyroclastic eruptions originating from the DHC [6,7]. The deposit's spectral signature suggests contamination by feldspathic highland-type materials either by superposed crater materials and/or vertical mixing [29].

Mare Deposits. Mare deposits are found on the floors of some impact craters, but are also found on the floor of Australe basin along the eastern limb near the northern edge of the map area (~62°S, 90°E). These deposits are dark and smooth in appearance, but some are brighter and more rugged suggesting they are older and have been modified since their emplacement by (1) mantling by ejecta, (2) mixing by subsequent impacts, and/or (3) gardening and regolith development [7,8].

References: [1] Mest, S.C. (2007) LPSC XXXVIII, #1842. [2] Van Arsdaal, L.E. and S.C. Mest (2008) LPSC XXXIX, #1706. [3] Mest, S.C. and L.E. Van Arsdaal (2008) NLSI LSC, NASA ARC, #2089. [4] Mest, S.C. (2008) GSA Joint Annual Mtg., #324-3. [5] Mest, S.C. (2009) Ann. Mtg. of Planet. Geol. Mappers, San Antonio, TX. [6] Mest, S.C. (2010) in "Recent Advances in Lunar Stratigraphy," accepted for pub. [7] Mest, S.C. et al. (2010) LPSC XLI, #2363. [8] Wilhelms, D.E. et al. (1979) USGS MISM I-1162, 1:5M scale. [9] Wilhelms, D.E. (1987) *USGS Prof. Pap.* 1348. [10] Spudis, P.D. et al. (1994) *Science*, **266**, 1848-1851. [11] Schultz, P.H. (1997) LPSC, XXVII, #1259. [12] Schultz, P.H. (2007) LPSC, XXXVIII, #1839. [13] Melosh, H.J. (1989) *Impact Cratering*, 245 pp. [14] Cintala, M.J. and R.A.F. Grieve (1998) *Met. and Planet. Sci.*, **33**, 889-912. [15] Belton, M.J.S. et al. (1992) *Science*, **255**, 570-576. [16] Head, J.W. et al. (1993) *JGR*, **98**, 17,149-17,182. [17] Lucey, P.G. et al. (1998) *JGR*, **103**, 3701-3708. [18] Pieters, C.M. et al. (1997) *GRL*, **24**, 1903-1906. [19] Pieters, C.M. et al. (2001) *JGR*, **106**, 28,001-28,022. [20] Lawrence, D.J. et al. (1998) *Science*, **281**, 1484-1489. [21] Lawrence, D.J. et al. (2002) *New Views of the Moon*, Europe, 12-14. [22] Lawrence, D.J. et al. (2002) *JGR*, **107**, doi:10.1029/2001JE001530. [23] Jolliff, B.L. et al. (2000) *JGR*, **105**, 4197-4216. [24] Wood, C.A. and L. Andersson (1978) *Proc. Lunar Planet. Sci. Conf.*, 9th, 3669-3689. [25] Dominov, E. and S.C. Mest (2009) LPSC, XL, #1460. [26] Shoemaker, E.M. et al. (1994) *Science*, **266**, 1851-1854. [27] Schultz, P.H. (1976) *The Moon*, **15**, 241-273. [28] Spudis, P.D. (1993) *The Geology of Multi-ring Impact Basins: The Moon and Other Planets*. [29] Gaddis, L.R. et al. (2003) *Icarus*, **161**, 262-280.

THE PILOT LUNAR GEOLOGIC MAPPING PROJECT: SUMMARY RESULTS AND RECOMMENDATIONS FROM THE COPERNICUS QUADRANGLE. J. A. Skinner, Jr., L. R. Gaddis, and J. J. Hagerty, Astrogeology Science Center, U.S. Geological Survey, 2255 N. Gemini Drive, Flagstaff, AZ 86001 (jskinner@usgs.gov).

Introduction: The first systematic lunar geologic maps were completed at 1:1M scale for the lunar near side during the 1960s using telescopic and Lunar Orbiter (LO) photographs [1-3]. The program under which these maps were completed established precedents for map base, scale, projection, and boundaries in order to avoid widely discrepant products. A variety of geologic maps were subsequently produced for various purposes, including 1:5M scale global maps [4-9] and large scale maps of high ‘scientific interest’ (including the Apollo landing sites) [10]. Since that time, lunar science has benefitted from an abundance of surface information, including high resolution images and diverse compositional data sets, which have yielded a host of topical planetary investigations.

The existing suite of lunar geologic maps and topical studies provide exceptional context in which to unravel the geologic history of the Moon. However, there has been no systematic approach to lunar geologic mapping since the flight of post-Apollo scientific orbiters. Geologic maps provide a spatial and temporal framework wherein observations can be reliably benchmarked and compared. As such, a lack of a systematic mapping program means that modern (post-Apollo) data sets, their scientific ramifications, and the lunar scientists who investigate these data, are all marginalized in regard to geologic mapping. Marginalization weakens the overall understanding of the geologic evolution of the Moon and unnecessarily partitions lunar research.

To bridge these deficiencies, we began a pilot geologic mapping project in 2005 as a means to assess the interest, relevance, and technical methods required for a renewed lunar geologic mapping program [11]. Herein, we provide a summary of the pilot geologic mapping project, which focused on the geologic materials and stratigraphic relationships within the Copernicus quadrangle (0-30°N, 0-45°W).

Geologic Setting: The Copernicus region is dominated by high-albedo units of the young (~0.8 Ga) Copernicus crater. These units are superimposed on older basin rim and ejecta units of Imbrium basin (highlands of Montes Carpatius), as well as old or intermediate-aged highlands, mare, pyroclastic, and impact crater (e.g., Eratosthenes, diam. 58 km) units. Mapped geologic units within the quadrangle include the Lower Imbrian materials of Imbrium basin (Alpes and Fra Mauro Fms.), Upper Imbrian mare basalts, cones, dark-halo craters, and pyroclastic deposits (Mare Insularum, Sinus Aestuum, and SE Mare Im-

brium), Eratosthenian mare basalts (central Mare Imbrium) and crater materials, and young Copernican impact and related deposits. Previous geologic maps (at various scales), and numerous topical studies, have detailed the origin, distribution, and composition of geologic units within this region [e.g., 12-14].

Data and Methods: We processed, orthorectified, and coregistered data using image processing and geographic information system software. Geologic mapping layers included a LO-IV photomosaic (60 m/px; [e.g., 12]), Clementine 5-band ultraviolet and visible range mosaics (100 m/px, [13]), 6-band near infra-red data (500 m/px, [14]), derived maps of iron [15] and titanium, Clementine-derived topographic data [16], Earth-based 3.8 cm radar (3.1 km/px; [17]), and optical maturity (OMAT) [18]) data. We also used high (9 m/px) and very-high (1.3 m/px) resolution LO-IV frames of the Copernicus crater floor, wall, and central peak [12]. We did not define a particular data set as the dedicated geologic base map so that we could independently evaluate each in regard to unit delineation.

All digitization was completed in a geodatabase format to simplify data compilation, vector attribution, topological cleaning, interlayer analyses, and data sharing. Vector linework was digitally streamed between 1:500K (20% of the publication map scale) and 1:1.25M (50% of publication map scale) in order to assess sufficiency in detailing geologic contacts and features for both hard-copy and digital map publications. Linework was streamed directly into a GIS database in Mercator projection using a digital mapping tablet. The placement of vertices varied from 500 to 1250 meters (1 vertex per 1 mm at digitizing map scale). Attributes were assigned using attribute domains stored within the geodatabase, which was iteratively refined and updated over the course of the project. Geologic map symbols were derived from FGDC Digital Cartographic Standards for Geologic Map Symbolization and adapted where necessary to convey the geologic information unique to the quadrangle.

Results: The iterative and exploratory approach that we employed for the pilot mapping project provided scientific and technical observations that significantly expanded the results afforded by previous lunar mapping efforts. These include:

- Spectral data permit us to advance beyond “morphostratigraphic” mapping, allowing units to be divided by morphology and spectral characteristics.
- Stratigraphic relationship takes precedence over compositional or morphologic characteristic. For ex-

ample, we use "Ccr_a--Copernican-age, crater unit, rim sub-unit, member a" versus "Ccrh--Copernican-age, crater unit, rim sub-unit, hummocky member."

- Broad heterogeneity in optical maturity, reflectance, and morphology of Copernicus wall, floor, and ejecta units suggests that materials have diverse composition and, in some locations, were not intimately mixed during crater formation.
- Local 'KREEP-rich' rock unit is not present in Copernicus due to a lack of thorium enrichment.
- The northernmost ejecta of Imbrium basin may contain materials from excavated pre-Imbrium (Nectarian) basement rocks, based on rocks exhumed by Eratosthenes crater, which partly overlies highlands units of Imbrium basin rim deposits.
- Clementine-derived OMAT data allow for the stratigraphic re-evaluation of some small-diameter impact craters (including Aristillus, Autolycus, Taruntius, O'Day, Eudoxus, and Pytheas). However, the derivative nature of OMAT data does not allow them to supersede cross-cutting relationships and crater counts, where available, for stratigraphic subdivision.
- Ruled and dashed patterns are helpful in indicating unit subdivision based on color variations within a single geologic unit.
- Minor secondary scatters and chains are identified by a crater ray pattern, though overlapping rays of Copernicus, Kepler, and Aristarchus craters are not differentiated within the mapped ray patterns. We do not discriminate secondary rays, craters, or materials when they superpose primary rim materials of the parent impact.

Recommendations: The results of the pilot lunar geologic mapping project serve to outline the critical pathway for formalized and systematic lunar mapping. These results guide our recommendations on the strategic approach of a renewed lunar geologic mapping program.

- Renewed geologic mapping should follow a 1:2.5M scale mapping scheme that subdivides the lunar surface into 30 discrete quadrangles using three different and latitude-specific projections. The scheme sufficiently balances the areal coverage and scale of modern (post-Apollo) data sets with those previously used as base maps and we determined that it was appropriate for hard-copy and digital publication.
- Lunar mappers should employ a strategic approach that recognizes the uniqueness of the lunar surface relative to other planetary bodies and should consciously divide primary (base map) and supplemental (descriptive) data sets. The volume, type, resolution, and areal diversity of available data requires

preference and down-selection for timely completion.

- Compositional information is fundamental to a renewed geologic mapping program and critical to the delineation, description, and interpretation of geologic units. As a result, there is a need for multiple base maps for a particular mapping project. However, these should be carefully selected and justified in order to avoid narrowing the objective scope of the geologic map.
- Emphasis should be placed on the explicit delineation of multiple impact crater facies, contrary to recent geologic maps of other planetary bodies. The pervasive nature of surface impact as a predominant contributor to the evolution of the lunar crust is critical to placing compositional observations into appropriate context.
- Geologic maps should closely adhere to the guidelines provided in the recent Planetary Geologic Mapping Handbook [19], so that there is visual and contextual continuity between USGS published geologic map products.

Conclusions: Lunar geologic mapping is undergoing a renaissance similar to that experienced by Mars geologic mapping following the flight of Mars Global Surveyor. Lunar geologic map products are expected to hone closely to cartographic standards, which evolve over time as a result of increased types and scales of planetary observation. Moreover, the emergence of geospatial mapping and analytical environments has provided a need for the expedited evolution of lunar mapping strategies. The pilot lunar geologic mapping project has successfully raised awareness in regard to the need for a renewed geologic mapping program funded through NASA PGG. We note that geologic maps are expected (and suggested) at higher scales (smaller areas) based on recent and ongoing acquisition of high resolution LROC data.

References: [1] Schmitt et al. (1967), *USGS I-515*. [2] Wilhelms and McCauley (1971), *USGS I-703*. [3] Shoemaker and Hackman (1962), *Symp. 14 IAU*, 289. [4] Wilhelms and McCauley (1971), *USGS I-703*. [5] Lucchitta (1978), *USGS I-1062*. [6] Wilhelms et al. (1979), *USGS I-1162*. [7] Wilhelms and El-baz (1977), *USGS I-946*. [8] Scott et al. (1977), *USGS I-1034*. [9] Stuart-Alexander (1978), *USGS I-1047*. [10] Howard (1975), *USGS I-840*. [11] Skinner et al. (2006), *PGM 2006 abstract volume*. [12] Weller et al., *LPSC 37*. [13] Eliason et al. (1999), *PDS Vol. USA NASA PDS CL 4001 to 4078*. [14] Gaddis et al. (2006), *PDS archive*. [15] Lucey et al. (2000), *JGR* 105. [16] Archinal et al., *LPSC 37*. [17] Zisk et al. (1974), *The Moon*, 17-50. [18] Wilcox et al. (2005), *JGR* 110. [19] Tanaka et al. (2009) *Plan. Geo. Map. Handbook, PGM 2009 abstract volume*.

GEOLOGIC MAPPING OF THE NILI FOSSAE REGION OF MARS: MTM QUADRANGLES 20287, 20282, 25287, 25282, 30287, and 30282. Leslie F. Bleamaster III^{1,2}, and David A. Crown¹, Planetary Science Institute, ¹corporate address - 1700 E. Ft. Lowell Rd., Suite 106, Tucson, AZ 85719; ²mailing – Trinity University Geosciences, One Trinity Place #45, San Antonio, TX 78212, lbleamas@psi.edu.

Introduction: Geologic mapping studies at the 1:1M-scale are being used to assess geologic materials and processes that shape the highlands along the Arabia Terra dichotomy boundary. In particular, this mapping will provide a regional context and evaluate the distribution, stratigraphic position, and potential lateral continuity of compositionally distinct outcrops identified by spectral instruments currently in orbit (i.e., CRISM and OMEGA). Placing these landscapes, their material units, structural features, and unique compositional outcrops into spatial and temporal context with the remainder of the Arabia Terra dichotomy boundary may provide constraints on: 1) origin of the dichotomy boundary, 2) paleo-environments and climate conditions, and 3) various fluvial-nival modification processes related to past and present volatile distribution and their putative reservoirs (aquifers, lakes and oceans, surface and ground ice) and the influences of nearby volcanic and tectonic features on hydrologic processes, including hydrothermal alteration, across the region.

Data and Methods: Datasets include both Viking and THEMIS day IR basemaps, and 128 pixel/deg (~462 m/pixel) MOLA topographic data covering the entire mapping region. These basemaps and other data supplied by the U.S. Geological Survey are in a GIS-ready format. ESRI ArcGIS software in conjunction with a WACOM Cintiq 21 inch interactive display facilitates all mapping linework and geodatabase generation and storage. Because of the vast amount of Mars datasets available (and their highly variable resolutions), mapping proceeds directly on the THEMIS basemap; high-resolution data, when scale appropriate, is visualized using JMARS (Java Mission-planning and Analysis for Remote Sensing) and individual hot-linked images (e.g., HRSC, CTX, MOC). OMEGA and CRISM mineralogy maps generated by collaborator J. Mustard and colleagues will be used to assess and correlate geologic map units with widespread and isolated mineral outcrops including olivine,

pyroxene, hydrated silicate, phyllosilicates, and carbonate detections [1, 2].

Nili Fossae, located north of Syrtis Major volcano and west of Isidis basin, contains a series of curvilinear troughs oriented roughly concentric to the Isidis basin. The largest trough originates from Hesperian age volcanic flows, extends northward through Noachian etched and cratered units, and ends near the dichotomy boundary (Figure 1) [3, 4]. These structures most likely manifest as the surface expression of an outer ring fault related to the reasonably sized topographic and structural basin created by the Isidis impact into the underlying Noachian crust. Nili Fossae crosscuts materials that span the Noachian to late Hesperian and intersects with structural elements potentially related to original dichotomy formation, suggesting that Isidis has long been an influence on local geologic evolution.

Although masked in regions by volcanic flows from Syrtis Major, aeolian and fluvial deposition, and potential coastal deposits related to an ancient Martian ocean [5, 6], subsequent striping has revealed outcrops of significant geochemical importance. Like those observed in the Mawrth Vallis region (see Chuang and Bleamaster, this issue), several outcrops of phyllosilicate-bearing Noachian materials have been revealed by the MEX OMEGA instrument [7, 8]. Phyllosilicates in this location point to the ancient history of Mars when the stability of ground and/or surface water was present for significant periods of time, facilitating the widespread aqueous alteration observed [9].

Units: Geologic contacts, linear features (i.e., faults, ridges, and crater rims) and surface features (i.e., secondary crater chains) mapped thus far are provided in Figure 1. An initial set of geologic units will be built from the existing geologic contacts to be presented and displayed at the meeting. Most geologic units herein subdivide units originally defined by Greeley and Guest (Figure 1) [3] and more recently during northern plains mapping by Tanaka et al. [9] that skirts the area.

Sub-units are typically identified by the occurrence of an individual layer that caps isolated mesas and widespread plateau regions (MOLA topography is helpful in extrapolating some of these units, Figure 1). These cap materials are underlain by weaker materials, which are often preserved only as clusters of knobby terrain that remains after the resistant cap has been removed.

Additional geologic units including lineated valley fill (predominantly in the northwest corner), lineated and concentric crater fill (typical of northern craters), landslide and alluvial fan deposits (i.e., Jezero crater), dunes, and dust deposits are mapped when the scale is appropriate.

References: [1] Murchie et al., 2009: JGR v.114, doi:10.1029/2009JE003342. [2] Ehlmann et al., 2009: JGR v. 114, doi:10.1029/2009JE003339. [3] Greeley and Guest, 1987: US Geol. Surv. Misc. Invest. Ser. Map I-1802B. [4] Craddock, 1994: LPSC XXV, pp. 291-292. [5] Parker, 1989: Icarus, v. 82, p. 111-145. [6] Webb, V.E., 2004: JGR doi:10.1029/2003JE002205. [7] Poulet et al., 2005: Nature, v. 438, doi:10.1038/nature04274. [8] Mustard et al., 2005: Science, v. 307, p. 1594-1597. [9] Mustard and Ehlmann, 2009: NE Syrtis landing site abstract marsoweb.nas.nasa.gov/landingsites/index.html [10] Tanaka et al., 2009: US Geol. Surv. Sci. In. Map 2888.

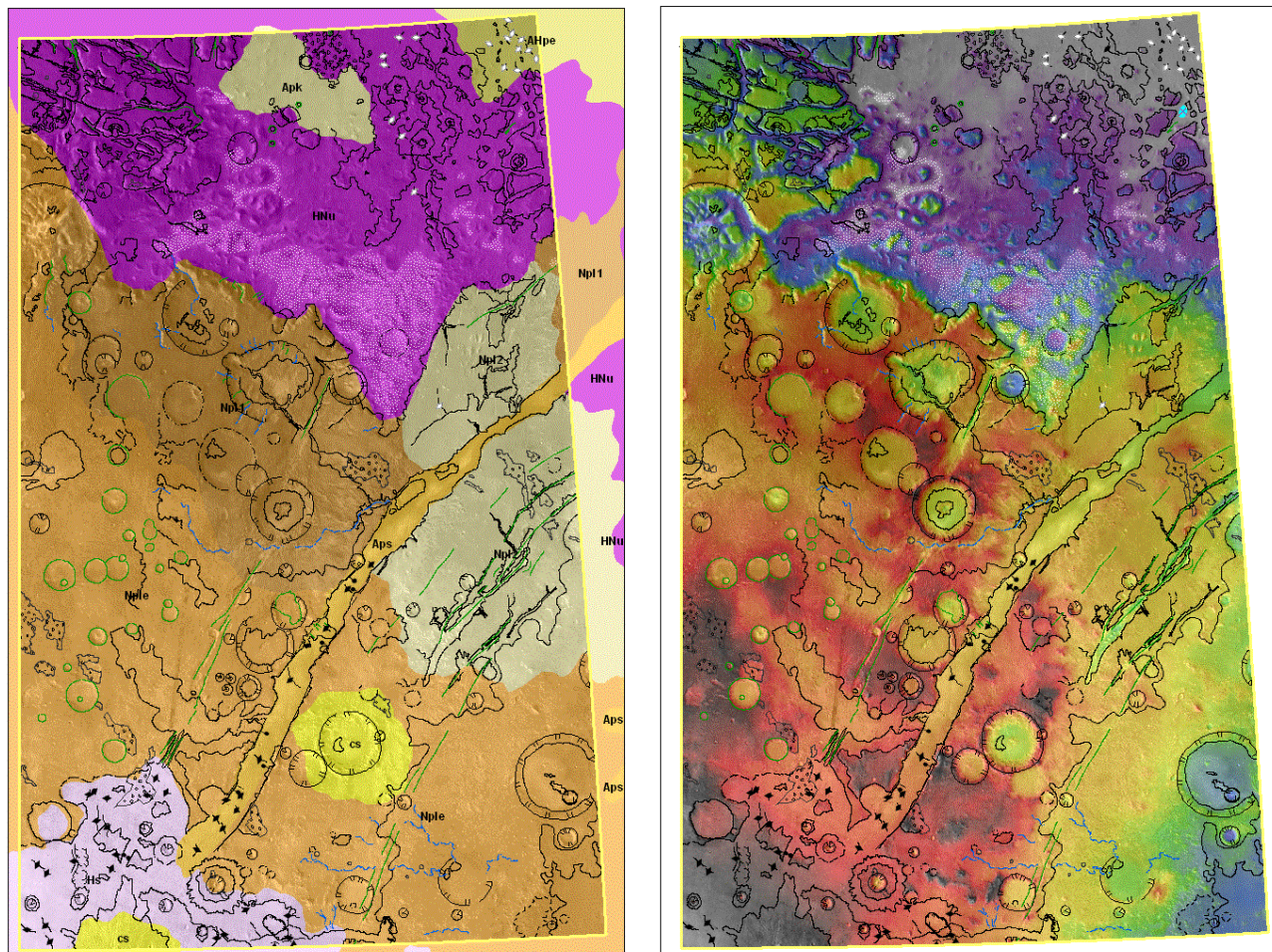


Figure 1. (Left) Present mapping (contacts, linear and surface features) overlain on geologic units (no contacts) of Mars Global Map 1802 [3] (including units, from south to north: **cs** – impact crater material, superposed; **Hs** – Syrtis Major Formation; **Nple** – plateau sequence, etched unit; **Npl2** – plateau sequence, subdued cratered unit; **Npl1** – plateau sequence, cratered unit; **HNu** – undivided material; **Apk** – knobby plains material; and **AHpe** – etched plains material. (Right) Same line work overlain onto MOLA and THEMIS daytime IR basemap.

GEOLOGIC MAPPING OF THE MAWRTH VALLIS REGION, MARS: MTM QUADRANGLES 25022, 25017, 25012, 20022, 20017, and 20012. F.C. Chuang¹ and L.F. Bleamaster III^{1,2}, ¹Planetary Science Institute, 1700 E. Fort Lowell Rd., Suite 106, Tucson, AZ 85719, ²Trinity University Geosciences Dept., San Antonio, TX 78212 (e-mail: chuang@psi.edu).

Introduction: Mawrth Vallis is a 15-25 km wide, 500 km long sinuous channel that winds through the highlands of Arabia Terra and debouches into the lowlands of Acidalia Planitia. The Mawrth Vallis region lies along the gradational zone between southern hemisphere thick crust and northern hemisphere thin crust, a topographically distinct portion of the Martian crustal dichotomy. The origin and age of the dichotomy boundary are controversial [1 and cited references therein] and are further complicated by the multi-stage and multi-process geologic history [2,3] that has modified this ~6000 km section of the highland-lowland boundary (~15 N, 330E to ~30 N, 80 E; herein referred as the Arabia Terra boundary). Furthermore, the Arabia Terra boundary has been subjected to many post-boundary processes such as outflow floods to the west, volcanism and tectonism to the east, and potential volatile deposition and glacial modification to the north. This study seeks to better understand the history of the Mawrth Vallis region by mapping six MTM quadrangles (17.5-27.5 N, 335-350 E) at 1:1M scale using traditional and modern digital geologic mapping techniques [4,5].

Data and Methods: GIS-ready datasets include both Viking and THEMIS day IR basemaps, and 128 pixel/deg MOLA topographic data covering the entire mapping region. We will utilize ESRI ArcGIS software for all mapping work and storage (geodatabase). Our initial mapping will be focused on the units and structures seen in the THEMIS basemap. Refinement of unit contacts, identification of sub-units, and structural boundaries will follow using higher resolution data (e.g., HRSC, CTX, THEMIS VIS, MOC). OMEGA and CRISM data will be used to look for possible correlations between map units and various mineral signatures. Cumulative crater counts for crater-size frequency analyses will also be undertaken to obtain surface ages.

Phyllosilicate Materials: Since the initial discovery of phyllosilicate-bearing materials by the OMEGA instrument [6-7], Mawrth Vallis has been an area of intense study to map the stratigraphic sequence and diversity of clays in the region [8-16]. Three principle clay types are evident: Fe, Mg, and Al-rich smectites.

The Al-rich phyllosilicates, in the form of montmorillonite clays, are located in eroded light-toned outcrops along the flanks of Mawrth Vallis [6]. The Al-rich unit is minimally hundreds of meters thick [6,9,13], layered down to the meter-scale [6,7,9,10,13]

with moderate thermal inertia signatures [9,13], and is eroded into knobby and flat mesa-like cliff forms [6,13]. In some locations along the walls of Mawrth Vallis, the Al-rich unit appears to lie stratigraphically between Fe or Mg-bearing smectite units (e.g., nontronite) [11,12]. A transitional unit with spectral signatures of both Al-bearing and Fe/Mg clays is also observed. The Al-bearing unit has meter-scale polygonally-fractured surfaces while the darker-toned Fe/Mg-bearing clay units have larger polygonal surfaces that are tens of meters wide [9,12]. These surfaces may have formed as a result of thermal and/or dessication contraction [9,12]. Other dark-toned materials present throughout the region are identified as pyroxene-rich materials (i.e., basaltic sand and dust) that mantle the surface (and clay-bearing units) [10,11,13].

The presence of clays in Mawrth Vallis is important as they imply a past aqueous environment in this region of Mars. It is argued that the clay-bearing units were formed early in the history of Mars (also prior to the formation of Mawrth Vallis) as aqueous deposits of sedimentary or pyroclastic materials, or a combination of both [6-13].

Mapping Results: The following describes the geologic units mapped thus far for the Mawrth Vallis region (Fig. 1).

Geologic Units

Highly-degraded crater material (c1) – Partial to discontinuous rim with little or no relief relative to surrounding surfaces; little to no ejecta blanket; several craters have channels along the interior walls. *Interpretation:* Deposits exhibiting extensive degradation that form ejecta, rims, and floors of impact craters.

Moderately-degraded crater material (c2) – Continuous rim with minor relief relative to surrounding surfaces and continuous to semi-continuous ejecta blanket; several craters have channels along the interior walls. *Interpretation:* Deposits exhibiting moderate degradation that form ejecta, rims, and floors of impact craters.

Well-preserved crater material (c3) – Pronounced, continuous rim with significant relief relative to surrounding surfaces and continuous ejecta blanket; several craters with ejecta blankets have rampart margins. *Interpretation:* Deposits exhibiting little degradation that form ejecta, rims, and floors of impact craters.

Ridged plains 1 material (pr1) – Plains with ridges ranging from straight to sinuous in planform

shape with relatively constant widths that occasionally widen and narrow along their length; ridges appear as a simple step or a broad, flat-topped surface with relief; some ridge axes intersect at near right angles (i.e., near-perpendicular). *Interpretation:* Near-surface highland crust modified by tectonic forces producing ridges either by contraction and (or) upwards thrusting along a fault. For intersecting ridges, crustal shortening may have occurred as separate events along each ridge axis or as isotropic contraction activated structures of multiple orientations.

Ridged plains 2 material (pr2) – Smooth material with occasional ridges and abundant secondary craters and crater chains; areas near Mawrth Vallis appear etched where parts of the surface are stripped, exposing a possible lower surface unit. *Interpretation:* Highland crust modified from tectonic forces producing ridges, but in fewer numbers than Ridged Plains material 1. Eolian deflation and (or) weathering processes have eroded the surface, creating rough, knobby-like regions, particularly near Mawrth Vallis.

Acidalia plains material (ap) – Relatively smooth plains covering the lowlands beyond the dichotomy boundary; many locales have clusters or individual polygonal blocks and knobs of highland material; several ridges similar to those in Ridged Plains material are observed. *Interpretation:* Highland materials deposited into the low-lying northern plains by sedimentary processes that may include eolian, mass-wasting, and volcanic airfall deposits. Fluvially-deposited materials may be near the mouth of Mawrth Vallis.

Mawrth channel 1 material (mch1) – Multiple smooth surfaces within the channel floor along the upper and middle reaches of Mawrth Vallis; surfaces have a low abundance of impact craters, are divided into larger polygonal sections in places, and are sometimes incised by one or more channels; darker material is exposed from below this unit in the middle reaches. *Interpretation:* Fluvially-modified surface during the formation of Mawrth Vallis with possible remnant bars and scour features.

References: [1] Watters T.R. and McGovern P.J. (2006) GRL 33, doi:10.1029/2006GL025755; [2] McGill G.E. (2000) JGR 105, 6945-6959; [3] McGill G.E. (2002) USGS Geol. Invest. Map 2746, 1:1M; [4] Wilhelms D.E. (1990) Planetary Mapping, Cambridge Univ. Press, New York, 208-260; [5] Tanaka et al. (2005) USGS Sci. Invest. Map 2888, 1:15M; [6] Poullet et al. (2005) Nature 438, 623-627; [7] Bibring et al. (2006) Science 312, 400-404; [8] Howard A.D. and Moore J.M. (2007) LPSC 38, abstract #1339; [9] Loizeau et al. (2007) JGR 112, doi:10.1029/2006JE002877; [10] Michalski J.R. and Noe Dobrea E.Z. (2007) Geology 35, 951-954; [11] Bishop et al. (2008) Science 321, 830-833; [12] Wray et al. (2008) GRL 35, doi:10.1029/2008GL034385; [13] Michalski J.R. and Fergason R.L. (2009) Icarus 199, 25-48; [14] McKeown et al. (2009) JGR 114, doi:10.1029/2008JE003301; [15] Farrand et al. (2009) Icarus 204, 478-488; [16] Loizeau et al. (2010) Icarus 205, 396-418.

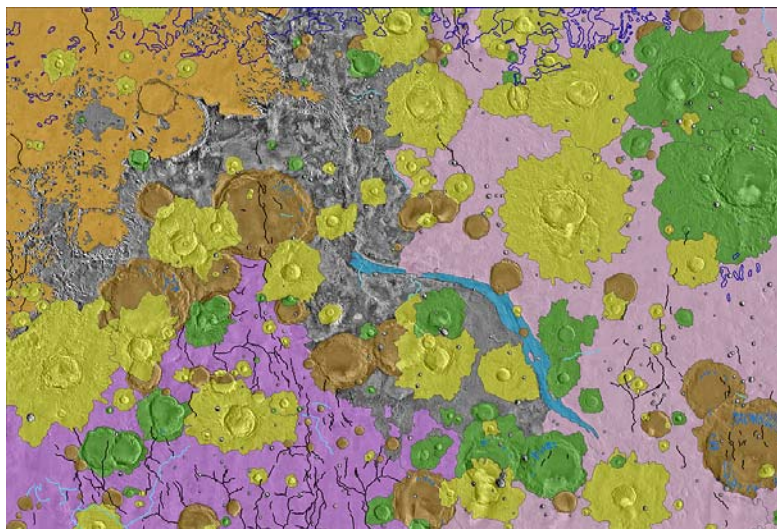


Figure 1. Preliminary geologic map of the Mawrth Vallis region. Geologic units: brown = c1, green = c2, yellow = c3, purple = pr1, pink = pr2, orange = ap, cyan = mch1. Geologic structures: thick black lines = ridge crests, dark blue areas = secondary crater fields/chains, thick cyan lines = sinuous channels, thin blue lines = fluvial channels.

EVIDENCE FOR AN ANCIENT BURIED LANDSCAPE ON THE NW RIM OF HELLAS BASIN, MARS.

David A. Crown¹, Leslie F. Bleamaster III¹, Scott C. Mest¹, John F. Mustard², and Mathieu Vincendon², ¹Planetary Science Institute, 1700 E. Ft. Lowell Rd., Suite 106, Tucson, AZ 85719; crown@psi.edu, ²Dept. of Geological Sciences, Brown University, Providence, RI 02912.

Introduction: Hellas basin is the largest (2000+ km across) well-preserved impact structure on Mars and its deepest depositional sink [e.g., 1]. The Hellas rim and adjacent highlands are of special interest given the possibility of paleolakes on the basin floor [2-4], recent studies of potential localized fluvial/lacustrine systems [2, 5-17], and evidence for phyllosilicates around and within impact craters north of the basin [18-26].

We are producing a 1:1.5M-scale geologic map of eight MTM quadrangles (-25312, -25307, -25302, -25297, -30312, -30307, -30302, -30297) along Hellas' NW rim. The map region (22.5-32.5°S, 45-65°E) includes a transect across the cratered highlands of Terra Sabaea, the degraded NW rim of Hellas, and basin interior deposits of NW Hellas Planitia. No previous mapping studies have focused on this region, although it has been included in earlier global and regional maps [27-29].

Geologic Mapping of NW Hellas: Mapping of the NW Hellas rim initially involved production of geologic maps of two subregions of the larger map area in order to establish a scheme for delineation of geologic units. Research related to the geologic mapping investigation [30-34] has included general terrain characterization, evaluation of geomorphology and stratigraphic relationships, exploration of compositional signatures using CRISM, and investigation of impact crater distribution, morphometry, and interior deposits. These analyses are providing new constraints on the magnitudes, extents, and history of volatile-driven processes as well as a geologic context for mineralogic identifications.

Mapping Results: NE Subregion. Geologic mapping of the NE subregion (22.5-29°S, 57.6-65°E) characterizes the Terra Sabaea plains zone, interpreted to be a depositional shelf formed subsequent to degradation of rugged highland terrain adjacent to the basin rim [30-34]. Terra Sabaea plains are found at elevations intermediate (-1800m – 500m) to those of the highlands of Terra Sabaea proper and the steeper basin rim zone. Eastern Hellas exhibits evidence for widespread deposition at similar elevations, potentially associated with flooding from Reull Vallis, large paleolakes within Hellas, and/or accumulation of atmospheric volatiles due to circulation patterns off of the south pole [e.g., 2, 4, 35-36].

Surface materials in the NE subregion can be divided into the following types: highlands, smooth

plains, crater materials, and crater floor deposits. Subunits within both the highlands and plains may be defined as mapping continues; the plains in particular display significant brightness variations in THEMIS IR images. Small valleys dissect plains surfaces and are concentrated on sloping plains deposits at the margins of highland outcrops. Detailed mapping of this sub-region has resulted in identification of more irregular depressions than were found initially [30]. In some cases, the scarps defining these depressions reveal finely layered outcrops. The occurrence of the irregular depressions and layered outcrops in both crater floor deposits and within the plains may indicate emplacement of sedimentary units on a regional scale. Mapping shows an eroded and extensively buried ancient highland landscape, with partial exhumation indicated by etched surfaces and retreat of plains around eroded massifs and crater rims [32-33].

Mapping Results: NW Subregion. Geologic mapping of the NW subregion (22.5°-30°S, 45-50°E) characterizes the highlands of Terra Sabaea, which typically are found at elevations above 500m and exhibit numerous impact craters with various sizes and degradation states. Irregular depressions exposing layered deposits have been identified in crater interiors [30-34]. This region is located at higher elevations and contains generally larger impact craters with extensive ejecta deposits relative to the NE subregion, and, in general, resembles a typical highland terrain. However, closer inspection during detailed mapping reveals that the units defined for the NE subregion also characterize the surface geology of the NW subregion. MRO Context Camera (CTX; ~5 m/pixel) images show evidence for burial and partial exhumation of what appear to be relatively well-preserved crater rim and ejecta materials (e.g., 24.9°S, 46.1°E) in lower resolution images. CTX images also show that variations in brightness of plains materials seen in THEMIS IR images can be attributed to differential removal of layered sequences. These geologic characteristics are consistent with burial of ancient cratered terrain extending to the higher elevations of Terra Sabaea.

Correlation of CRISM Mineralogy to Geologic Mapping. We are analyzing CRISM multispectral data for the NW Hellas map area for phyllosilicates and Fe-bearing silicates, including smectite, chlorite/prehenite, pyroxene, and olivine. Mineralogic signatures typically consist of 10s to 100s of pixels grouped together in a

localized area. We are examining the distribution of specific compositional signatures to search for correlations with geologic map unit, physiographic setting, elevation, local topography, local geomorphic setting, and the presence of dark deposits.

Fe/Mg smectites are identified in CRISM data by the presence overtones and combinations tones of vibrational absorptions due to water, OH, and coordinating cations near 1.9 and 2.3 μm . Pyroxene and olivine are identified by the presence of ferrous crystal field absorptions between 1 and 2.5 μm and a lack of vibrational overtone bands. We use spectral parameters [26] calculated from the CRISM multispectral mosaics to identify locations of mineral-bearing outcrops. Each occurrence is then validated by examining representative spectra of the occurrences and comparing to library spectra. Spectral ratios are generated to better isolate the mineral absorption features.

From examining the locations of smectite and chlorite/prehnite across the entire map region and for olivine within the NW mapping subregion, we observe that mineral signatures are most abundant in the Terra Sabaea plains zone (-1800m – 500m), common in the Terra Sabaea highlands (above 500m), rare below elevations of -3100 m in the Hellas rim zone, and absent from the floor of Hellas basin. Chlorite/prehnite identifications are much less frequent than the other mineral signatures and are strongly associated with remnants of the highlands found in the Terra Sabaea plains zone. Pyroxene exposures are more numerous and larger in size at the higher elevations of the Terra Sabaea highlands zone than in the Terra Sabaea plains, where they are also found in significant numbers. In comparison, olivine is more evenly distributed across the plains and highlands. There are no obvious correlations between mineralogic signature and geologic map unit, although there are typical settings in which mineralogic signatures most commonly occur. In addition, there are a series of locations within the map area that exhibit exposures of smectite, olivine, and pyroxene. These typically occur in deposits associated with degraded crater rims.

Conclusions: Geologic mapping and investigations of impact craters on the NW Hellas rim [30-34] show evidence for crater infilling and regional resurfacing along with widespread occurrences of phyllosilicates and Fe-bearing silicates in association with highland remnants, including depressions formed by retreat/erosion of plains. The NW Hellas region preserves the record of an extensively buried landscape with sedimentary deposition that extended

beyond the topographic margin of Hellas basin and well into the surrounding highlands.

References: [1] Tanaka, K.L. and G.J. Leonard (1995), JGR, 100, 5407-5432. [2] Crown, D.A. et al. (2005), JGR, 110, E12S22, doi:10.1029/2005JE002496. [3] Moore, J.M. and D.E. Wilhelms (2001), Icarus, 154, 258-276. [4] Bleamaster, L.F. and D.A. Crown (2009), USGS Sci. Inv. Ser. Map 3096. [5] Lahtela, H. et al. (2003), Vernadsky Institute-Brown University Microsymposium 38, MS057. [6] Lahtela, H. et al. (2005), LPSC XXXVI, abstract 1683, LPI (CD-ROM). [7] Ansan, V. and N. Mangold (2004), 2nd Conf. on Early Mars, abstract 8006, LPI (CD-ROM). [8] Ivanov, M.A. et al. (2005), JGR, 110, E12S21, doi:10.1029/2005JE002420. [9] Kortenien, J. et al. (2005), JGR, 110, E12S18, doi:10.1029/2005JE002427. [10] Kraal, E.R. et al. (2005), Role of Volatiles on Martian Impact Craters, abstract 3008, LPI (CD-ROM). [11] Mest, S.C. and D.A. Crown (2005), Icarus, 175(2), 335-359. [12] Mest, S.C. (2005), Role of Volatiles on Martian Impact Craters, abstract 3014, LPI (CD-ROM). [13] Mest, S.C. (2006), LPSC XXXVII, abstract 2236, LPI (CD-ROM). [14] Moore, J.M. and A.D. Howard (2005), JGR, 110, E04005, doi:10.1029/2004JE002352. [15] Moore, J.M. and A.D. Howard (2005), LPSC XXXVI, abstract 1512, LPI (CD-ROM). [16] Wilson, S.A. and A.D. Howard (2005), LPSC XXXVI, abstract 2060, LPI (CD-ROM). [17] Wilson, S.A. et al. (2007), JGR, 112, E08009, doi:10.1029/2006JE002830. [18] Poulet, F. et al. (2005), Nature, 438, 623-627. [19] Bibring, J.-P. et al. (2006), Science, 312, 400-404. [20] Costard, F. et al. (2006), LPSC XXXVII, abstract 1288, LPI (CD-ROM). [21] Murchie, S. et al. (2006), EOS Trans. AGU, abstract P33A-04. [22] Murchie, S. et al. (2007), JGR, 112, E05S03, doi:10.1029/2006JE002682. [23] Mustard, J.F. et al. (2007), LPSC XXXVIII, abstract 2071, LPI (CD-ROM). [24] Mustard, J.F. et al. (2007), 7th Inter. Conf. on Mars, LPI. [25] Pelkey, S.M. et al. (2007), LPSC XXXVIII, abstract 1994, LPI (CD-ROM). [26] Pelkey, S.M. et al. (2007), JGR, 112, E08S14, doi:10.1029/2006JE002831. [27] Scott, D.H. and M.H. Carr (1978), USGS Misc. Invest. Ser. Map, I-1083. [28] Greeley, R. and J.E. Guest (1987), USGS Misc. Invest. Ser. Map I-1802B. [29] Leonard, G.J. and K.L. Tanaka (2001), USGS Geol. Invest. Ser. Map I-2694. [30] Crown, D.A. et al. (2007), EOS Trans. AGU, abstract P41A-0189. [31] Mest, S.C. et al. (2008), LPSC XXXIX, abstract 1704, LPI (CD-ROM). [32] Crown, D.A. et al. (2009), LPSC XL, abstract 1705, LPI (CD-ROM). [33] Crown, D.A. et al. (2010), in NASACP-2010-216680. [34] Crown, D.A. et al. (2010), LPSC XLI, abstract 1888. [35] Colaprete, A. et al. (2004), LPSC XXXV, abstract 2149, LPI (CD-ROM). [36] Colaprete, A. et al. (2005), Nature, 435, 184-188.

NEW GEOLOGIC MAP OF THE ARGYRE REGION OF MARS: DECIPHERING THE GEOLOGIC HISTORY THROUGH MARS GLOBAL SURVEYOR, MARS ODYSSEY, AND MARS EXPRESS DATA SETS. J.M. Dohm¹, M. Banks², D. Buczkowski³; ¹University of Arizona, Tucson, AZ (dohm@hwr.arizona.edu), ²Smithsonian Institution, Washington, D.C., ³John Hopkins University, Washington, D.C.

Introduction: The primary objective of the mapping effort is to produce a geologic map of the Argyre basin and surrounding region at 1:5,000,000 scale in both digital and print formats that will detail the stratigraphic and crosscutting relations among rock materials and landforms (30°S to 65°S, 290°E to 340°E) (Fig. 1). There has not been a detailed geologic map produced of the Argyre region since the Viking-era mapping investigation of [1]. The mapping tasks include stratigraphic mapping, crater counting, feature mapping, quantitative landform analysis, and spectroscopic/stratigraphic investigation feature mapping. The regional geologic mapping investigation includes the Argyre basin floor and rim materials, the transition zone that straddles the Thaumasia plateau, which includes Argyre impact-related modification, and the southeast margin of the Thaumasia plateau using important new data sets from the Mars Global Surveyor, Mars Odyssey, Mars Express, and Mars Reconnaissance Orbiter. The geologic information unfolded by this new mapping project will be useful to the community for constraining the regional geology, paleohydrology, and paleoclimate, which includes but is not limited to the assessment of: (1) whether the Argyre basin contained lakes, (2) the extent of reported flooding and glaciation, (3) existing interpretations of the origin of the narrow ridges located in the southeast part of the basin floor, and (4) the extent of Argyre-related tectonism and its influence on the surrounding regions.

Methodology: The mapping investigation will include stratigraphic mapping, crater counting, feature mapping, quantitative landform analyses, and stratigraphic/spectroscopic investigation.

Stratigraphic mapping. Identification, characterization, and relative-age analyses of map units with presently available data will be vastly improved over those based solely on Viking images. Using the new data, the stratigraphic and crosscutting relations among rock materials and landforms can be mapped, characterized, and interpreted. Geologic cross sections will cover mountainous impact crater rim materials (Charitum Montes and Nereidum Montes) and adjoining highland materials of Noachis Terra, valleys and elongated basins that are radial and concentric about the primary Argyre basin, and faults, sinuous ridges, lobate debris aprons, polygons, and valley networks. The mapping effort will also characterize the stratigraphic relations among basin infill materials (e.g., massive vs. layered vs. sequence stratigraphy). The mapping results will provide the planetary science community with better constraints on regional geology, paleohydrology, and paleoclimate.

Crater counting. Careful interpretation of crater density data is required due to the following factors: (a) crater density reflects a mean surface age (some grasp of potential relative-age range can be obtained by performing crater counts in multiple locations); for example, total crater counts of a map unit can help constrain its emplacement history, while counts of only superposed craters (pristine ejecta blankets that overlie the map unit and/or erosional, depositional, and/or tectonic structure) reflect an upper time limit for the resurfacing of that particular unit [e.g., 2]); (b) resurfacing

activity causes degradation and/or embayment of craters as well as inflections and roll-offs in crater-size distributions due to crater obliteration [e.g., 3]; (c) possible secondary and non-impact craters, particularly at smaller diameters, which can alter crater size-frequency distributions [4]. Keeping the above mentioned factors in mind, we intend to produce detailed summary crater counts for all map units, as well as multiple counts for more broadly occurring units. These should help establish ranges and spatial variability of ages of surface and near-surface units, as well as resurfacing ages.

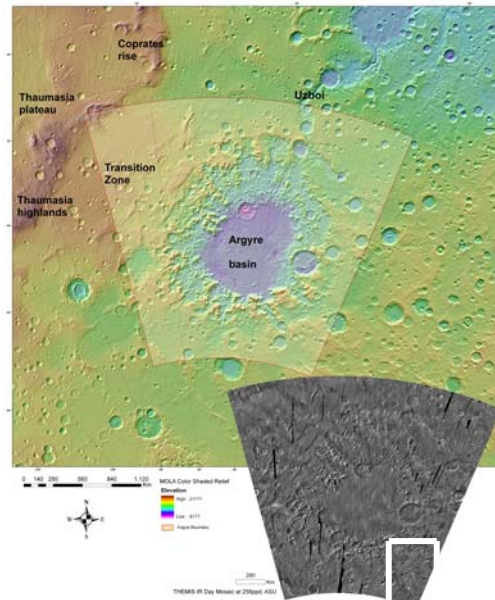


Fig. 1. MOLA color shaded relief map centered on the Argyre region (transparent outline). The image on the bottom right shows a 256 pixels/degree THEMIS IR day mosaic, to show the coverage available for mapping. Our regional 1:5,000,000-scale mapping investigation will include the Argyre floor and rim, transition zone, and the southeast margin of the Thaumasia plateau [2].

Structural and feature mapping. Tectonic, collapse, depositional, and erosional features will be mapped in detail including wrinkle ridges, lobate scarps, faults, fluvial channels, enigmatic ridges, lobate debris aprons, polygons, and valley networks, to help unfold the geological history (e.g., Fig. 3). Detailed crater statistics and MOLA-based cross-sectional information will assist in the determination of stratigraphic and crosscutting relations among rock materials and landforms. This includes Argyre basin infill materials (massive vs. layered vs. sequence stratigraphy), mountainous impact crater rim materials (Charitum Montes and Nereidum Montes) and adjoining highland materials of Noachis Terra, valleys and elongated basins that are radial and concentric about the primary Argyre basin, and faults, enigmatic ridges, lobate debris aprons, polygons, and valley networks.

Quantitative landform analyses: Multiple modern datasets will be used to identify landforms in the Argyre region, and various techniques will be implemented to quantitatively analyze these landforms to constrain the processes involved in their formation and to compare them with terres-

trial analogs (Fig. 2 based on [5]). Such analyses will provide important insight into possible formation mechanisms of the various landforms observed in the region and, based on the distribution and abundance of the landforms, indicate how active and widespread these formation processes are/were. In assessing different formation mechanisms, a “landsystems” approach will be used similar to [5]. In this approach, landforms will be considered in context and relation to each other, and the entire pattern and regional assemblage of landforms will be considered in regard to a typical terrestrial landscape. Altogether, this will provide important insight into the geologic history of the Argyre region.

Spectroscopic/stratigraphic investigation. Comparative analyses among the stratigraphic information based from this mapping investigation and the CRISM data will be performed to further unfold the geologic history of the Argyre region. Fig. 3 based from the work of [6], for example, shows a laterally-extensive, phyllosilicate-enriched deposit on the western wall of a shallow graben related to the seventh (of eight) ring structures associated with the Argyre basin, as mapped by [7].

Summary: The proposed investigation will have a direct bearing on the understanding of the geologic evolution of Mars. Furthermore, a new regional geologic map of the Argyre region of Mars will have wide-ranging significance and application, including: (1) the establishment of a spatial and temporal geologic context for local to regional geologic, geophysical, geochemical, hydrologic, and climatic studies, (2) the refinement of the regional stratigraphic scheme for establishing chronology and estimating rates of geologic activity, and (3) spatial and temporal information from which to assess whether the Argyre basin contained lakes [e.g., 8] and whether flooding and glaciation contributed significantly to the geologic and paleohydrologic records of the Argyre region [e.g., 7,9,10], as well as determining the extent of Argyre-related tectonism [2].

References: [1] Scott, D.H., et al., 1986-87, USGS Map I-1802-A-C. [2] Dohm, J.M., et al., 2001a, USGS Map I-2650. [3] Tanaka, K.L., et al., 2006, Workshop on Surface Ages and Histories: Issues in Planetary Chronology, Houston, Lunar and Planetary Institute, #6014. [4] McEwen, A.S., et al., 2005, Icarus, 176, 351-381. [5] Banks, M.E., et al., 2008, J. Geophys. Res., 113, E12015, doi:10.1029/2007JE002994. [6] Buczkowski, D.L., S. Murchie, R. Clark, K. Seelos, F. Seelos, E. Malaret, C. Hash and the CRISM Team (in revision), Investigation of an Argyre basin ring structure using MRO/CRISM, J. Geophys. Res. [7] Hiesinger, H., and J.W. Head, 2002, Planetary and Space Sci. 50, 939-981, 2002. [8] Parker, T.J. and D.S. Gorsline, 1993, Am. Geophys. Union Spring Meeting, 1pp. [9] Kargel, J.S., and Strom, R.G., Ancient glaciation on Mars, Geology, 20, 3-7, 1992. [10] Parker, T.J., et al., 2000, LPSC 31, abstract 2033.

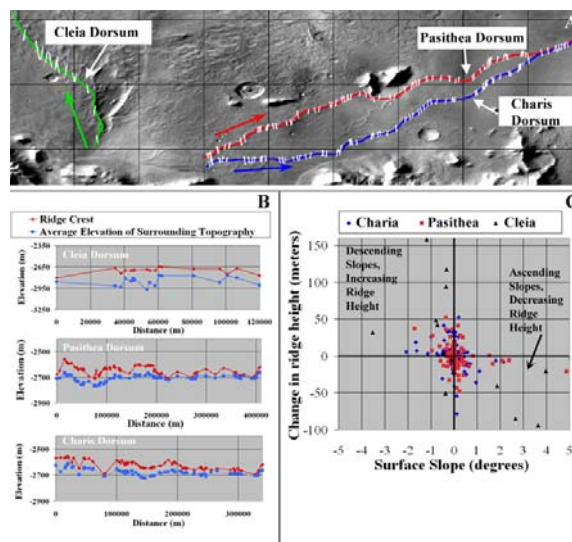


Fig. 2. Topographic analysis of the Argyre sinuous ridges. A) The locations of the three ridges used in the topographic analysis are marked in green (Cleia Dorsum), red (Pasithea Dorsum), and blue (Charis Dorsum) on a THEMIS daytime IR mosaic [http://jmars.asu.edu]. Multiple cross sectional profiles were derived from MOLA PEDR tracks along the extent of the three ridges. White lines in the mosaic indicate the location of the MOLA tracks on each of the ridges. The direction along each ridge in which the data was plotted in B is indicated by colored arrows next to the three ridges. B) The elevation of the surrounding surface was averaged at each profile location in A and plotted as a function of distance along the extent of each ridge (blue lines). For each of the ridges, the overall elevation at which they occur varies along trend indicating that the Argyre ridges cross topography. The height of each ridge was also plotted (red lines) and found to vary along the extent of each ridge. The vertical exaggeration differs for each plot. C) The change in ridge height between successive MOLA tracks along each ridge was plotted against the average slope of the surrounding surface. For slopes greater than 1°, ridge height generally increases with descending slopes and decreases with ascending slopes. This a characteristic observed in terrestrial eskers that is related to flow processes.

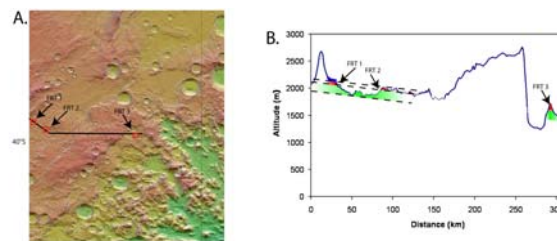


Fig. 3. Example of combining CRISM-based information with MOLA data for spectroscopic/stratigraphic investigation [6]. A) MOLA colorized topography draped over THEMIS daytime IR mosaic of the northwest part of the Argyre region. Red boxes indicate the CRISM observations noted in the text. Black line shows transect line of the topographic profile shown in B. B) Locations of CRISM FRT images are shown on a MOLA profile (vertical exaggeration = 67x). Steep peak separating FRT 3 from the other observations is a ridge used to infer the location of the sixth Argyre impact ring structure [7]. Red indicates phyllosilicate identifications, green high-calcium pyroxene, and blue low-calcium pyroxene. Dashed lines indicate probable layering of materials across the graben.

Introduction: Hesperia Planum, characterized by a high concentration of mare-type wrinkle ridges and ridge rings [1-4], encompasses > 2 million km² in the southern highlands of Mars (Fig. 1). The most common interpretation is that the plains were emplaced as “flood” lavas with total thicknesses of <3 km [4-10]. The wrinkle ridges on its surface make Hesperia Planum the type locale for “Hesperian-aged ridged plains” on Mars [e.g., 9], and wrinkle-ridge formation occurred in more than one episode [4]. Hesperia Planum’s stratigraphic position and crater-retention age [e.g., 9, 11-12] define the base of the Hesperian System. However, preliminary results of geologic mapping reveal that the whole of Hesperia Planum is unlikely to be composed of the same materials, emplaced at the same geologic time. To unravel these complexities, we are generating a 1:1.5M-scale geologic map of Hesperia Planum and its surroundings (Fig. 1). To date, we have identified 4 distinct plains units within Hesperia Planum and are attempting to determine the nature and relative ages of these materials (Fig. 2) [13-15].

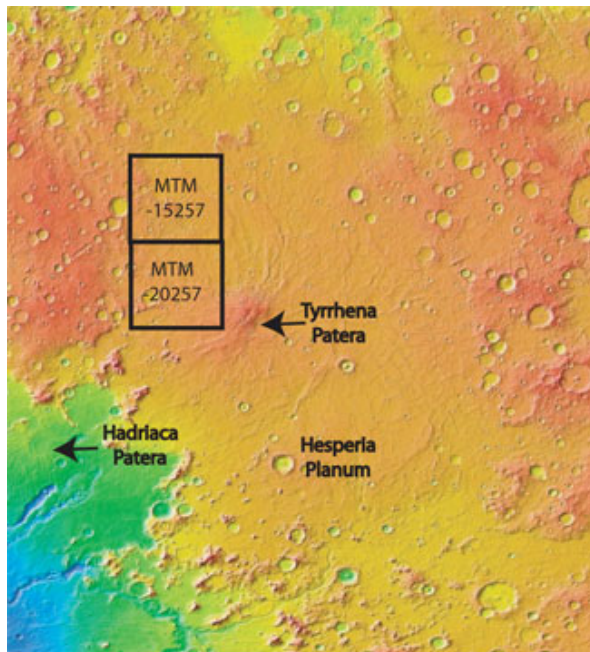


Figure 1. Gridded MOLA data (128 pixels/degree) of the Hesperia Planum region being mapped at 1:1.5 million. Reds are topographic highs (Tyrrhena Patera summit is ~3 km above mean planetary radius) and blues are lows. Locations of MTM quadrangles -15257 and -20257 noted.

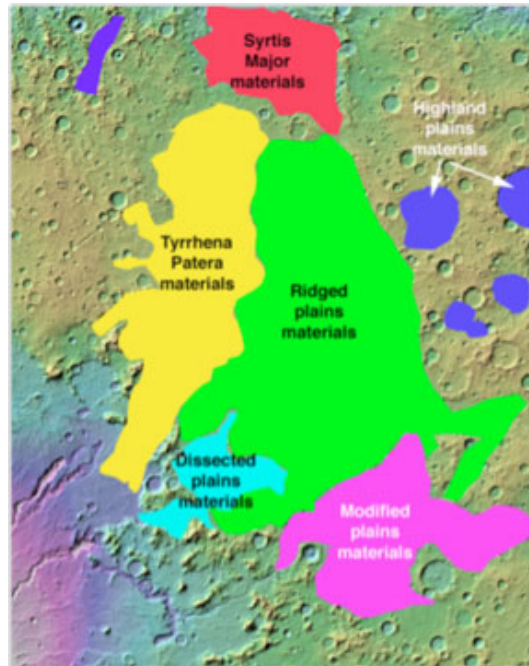


Figure 2. Rough boundaries of identified plains materials within Hesperia Planum. Portions of these materials were originally mapped as “Hesperian-aged ridged plains” at 1:15 million [9].

Hesperia Planum contains the volcano Tyrrhenus Mons, and embays the eastern flanks of the volcano. A large (~1000 km x 300 km) lava flow field, connected to the Tyrrhena Patera summit caldera complex via a volcano-tectonic rille, is superposed on the surrounding plains materials [16, 17]. Thus, the volcanic activity at Tyrrhenus Mons both pre-dates and post-dates the emplacement of at least some Hesperia Planum materials. To constrain and elucidate the relation between Hesperia Planum and Tyrrhenus Mons deposits, we are completing the geologic mapping of Mars Transverse Mercator (MTM) quadrangles -20257 and -15257 (Figure 3) at 1:500,000 [18]. These quadrangles are located to the west of the Tyrrhenus Mons summit, and contain the western boundary of Hesperia Planum as well. Mapping is almost completed for these quadrangles. Important discoveries as a result of geologic mapping include the extent of Tyrrhenus Mons eruptive materials, and the erosional morphology of these materials.

Hesperia Planum Materials: The region of Hesperia Planum located to the east of Tyrrhenus Mons (Fig. 2) is the typical “Hesperian ridged plains” [7, 9]. Aside from Tyrrhena Patera, no obvious volcanic vents

have been found within Hesperia Planum [cf. 4, 12, 17-20]. Lava flows can be seen at available image resolutions in the Tyrrhenus Mons lava flow field [17] that post-date the ridged plains, but they are not readily apparent within the ridged plains. In eastern Hesperia Planum, we have identified the following plains units: *highland knobby plains*, *smooth plains*, *highland smooth plains*, and *knobby plains*. Less than a dozen narrow (<100 m wide), linear to sinuous channels have been observed within Hesperia Planum (approximately 6 have been seen within the Tyrrhenus Mons MTM quadrangles -15257 and -20257). These channels have no obvious source or deposits associated with them, and regrettably High Resolution Imaging Science Experiment (HiRISE) images (25 cm/pixel) reveal that these channels are covered with secondary aeolian bedforms. Although their origin remains unclear, their morphology is most similar to terrestrial lava channels.

There are few obvious cross-cutting or superposition relations between the Hesperia Planum materials, and it is possible that the compositions of these units are similar, and the morphologic contrasts are caused by different styles and degrees of modification.

Within MTM quadrangles -15257 and -20257, Hesperia Planum materials can be further divided. In particular, northeast of Tyrrhenus Mons there is a “dark lobate plains” material that is best observed in THEMIS daytime infrared images. The lobate margins of these plains clearly overlie the lighter plains material to the west, and embay Tyrrhenus Mons edifice materials. The lobate margins of this unit show no shadows or bright cliffs, indicating a thin deposit. The deposit planform suggests that this material flowed from the north to the south, but we have not been able to identify a source. This material could be a thin lava flow or mudflow, and appears to be the youngest material within these MTM quadrangles.

Tyrrhenus Mons Materials: MTM quadrangles -15257 and -20257 were originally mapped by M. Farley, a M.S. candidate under Gregg’s advisement [18]. We are currently modifying her contacts, using images from the Context Imager (CTX) with resolutions of ~6 m/pixel to confirm or deny contacts originally identified on the basis of THEMIS visible and daytime infrared images.

Previous mapping efforts centered at the Tyrrhenus Mons summit [17] identified 2 units comprising the main edifice. Within MTM quadrangles -15257 and -20257, we have identified 2 additional units that are stratigraphically beneath those previously mapped (Fig. 3). These newly mapped units have a similar morphology to each other and to the previously mapped edifice units: they display stair-step erosional patterns; layers become thinner with distance from the

Tyrrhenus Mons summit; and the materials commonly occur as isolated mesas. Similar to the previously mapped Tyrrhenus Mons edifice units, we interpret these to be formed of pyroclastic deposits erupted from Tyrrhena Patera [cf. 19].

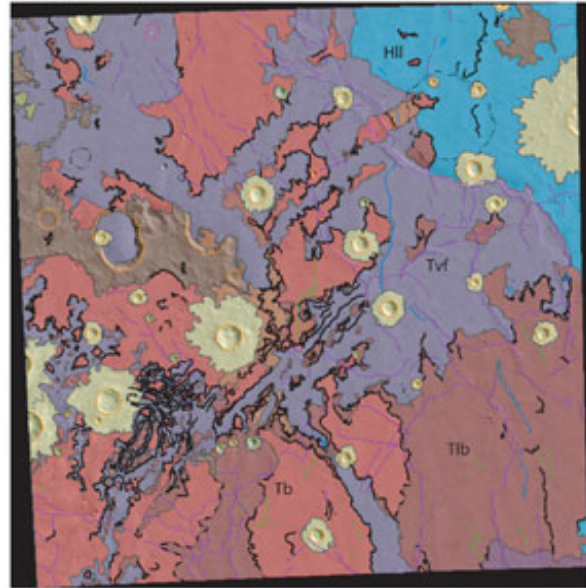


Figure 3. MTM Quadrangle -15257. Hll = Hesperian light lobate plains; Tvf = Tyrrhena valley fill; Tb = Tyrrhena basal edifice material; Tlb = Tyrrhena lower basal edifice material.

- References:** [1] Scott, D.A. and M. Carr (1978) *USGS Misc. Series I-1083*. [2] Chicarro, A.F., P.H. Schultz and P. Masson (1985) *Icarus* 63:153. [3] Watters, T. and D.J. Chadwick (1989) *NASA Tech. Rpt.* 89-06:68. [4] Goudy, C., R.A. Schultz and T.K.P. Gregg, 2005, *J. Geophys. Res.* 110: E10005 10.1029/2004JE002293. [5] Potter, D.B. (1976) *USGS Misc. Series I-941*. [6] King, E.A. (1978) *USGS Misc. Series I-910*. [7] Greeley, R. and P. Spudis (1981) *Rev. Geophys.* 19:13. [8] Scott, D.A. and K. Tanaka (1986) *USGS Misc. Series I-1802A*. [9] Greeley, R. and J. Guest (1987) *USGS Misc. Series I-1802B*. [10] Leonard, J.G. and K. Tanaka (2001) *USGS Misc. Map Series I-2694*. [11] Tanaka, K.L. (1986) *Proc. LPSC 17th, JGR Suppl.* 91, E139-E158. [12] Tanaka, K. (1992) in *Mars*, U. Arizona Press, p. 345. [13] Gregg, T.K.P. and D.A. Crown (2007) *Lun. Planet. Sci. Conf. 38th*, Abstract #1190. [14] Crown, D.A., D.C. Berman and T.K.P. Gregg (2007) *Lun. Planet. Sci. Conf. 38th*, Abstract #1169. [15] Jones, T.K., T.K.P. Gregg and D.A. Crown (2007) *Lun. Planet. Sci. Conf. 38th*, Abstract #2156. [16] Greeley, R. and D.A. Crown (1990), *JGR* 95(B5):7133-7149. [17] Gregg, T.K.P., D.A. Crown and R. Greeley (1998) *USGS Misc. Map Series I-2556*. [18] Farley, M.A., T.K.P. Gregg and D.A. Crown (2004) *USGS Open File Rpt. 2004-1100*. [19] Gregg, T.K.P. and M.A. Farley (2006) *J. Volcanol. Geophys. Res.* 151:81-91. [20] Ivanov, MA et al. (2005) *JGR* 110, E12S21.

GEOLOGIC MAPPING OF THE MERIDIANI REGION OF MARS. B. M. Hynek^{1,2} and G. Di Achille³

¹Laboratory for Atmospheric and Space Physics, ²Department of Geological Sciences (392 UCB, Univ. of Colorado, Boulder, CO 80309), ³now at Research and Scientific Support Department, ESA-ESTEC (Noordwijk, The Netherlands).

Introduction: The Mars Exploration Rover Opportunity observed an upper layer of a more than 600-m-thick sequence of light toned outcrops that characterize the Meridiani region of Mars. Results from the rover analyses have shown that the bedrock contains mineral and textural characteristics that require the interaction of, and possibly an overall formation by, water-related mechanisms in order to be explained [1]. Additionally, remote sensing studies of the region have suggested that the rocks sampled in places by the MER rover consist of many distinct layers extending over an area of more than 3×10^5 km² spanning 20° of longitude [2].

Geologic Mapping: To address the origin and history of these unique materials, we are completing a PG&G-funded geologic, stratigraphic, and thermophysical properties study of this widespread terrain. Specifically, we have drafted a geological map covering the full extent of these water-related deposits that will be ready for peer-review within a month. This task serves several purposes including gaining an understanding of the complex nature of these materials, their potential sources region(s), and the timing of their emplacement, as well as to place the observations by the Opportunity Rover in a broader context.

We have completed a detailed geologic mapping at 1:2M-scale in the Meridiani region. The study area is defined here as 5°S-15°N, 15°W eastward across the prime meridian to 15°E. This covers portions of the quadrangles MC-11, MC-12, MC-19, and MC-20. The numerous units in the study area were refined from recent works [2-4] and new data and analysis. Formal geological mapping used a 100-m-resolution THEMIS base map combined with MOLA gridded data. Additional data for mapping included MOC WA images, THEMIS daytime and nighttime IR data, some THEMIS visible data, HRSC mosaics and topography, MOLA topography, TES and THEMIS thermal inertia, MOC NA, and CTX and HiRISE images. We also mapped valley networks to understand their potential link to the layers. Additionally, we have identified and characterized all craters in the region down to 1.5 km diameter for age-dating.

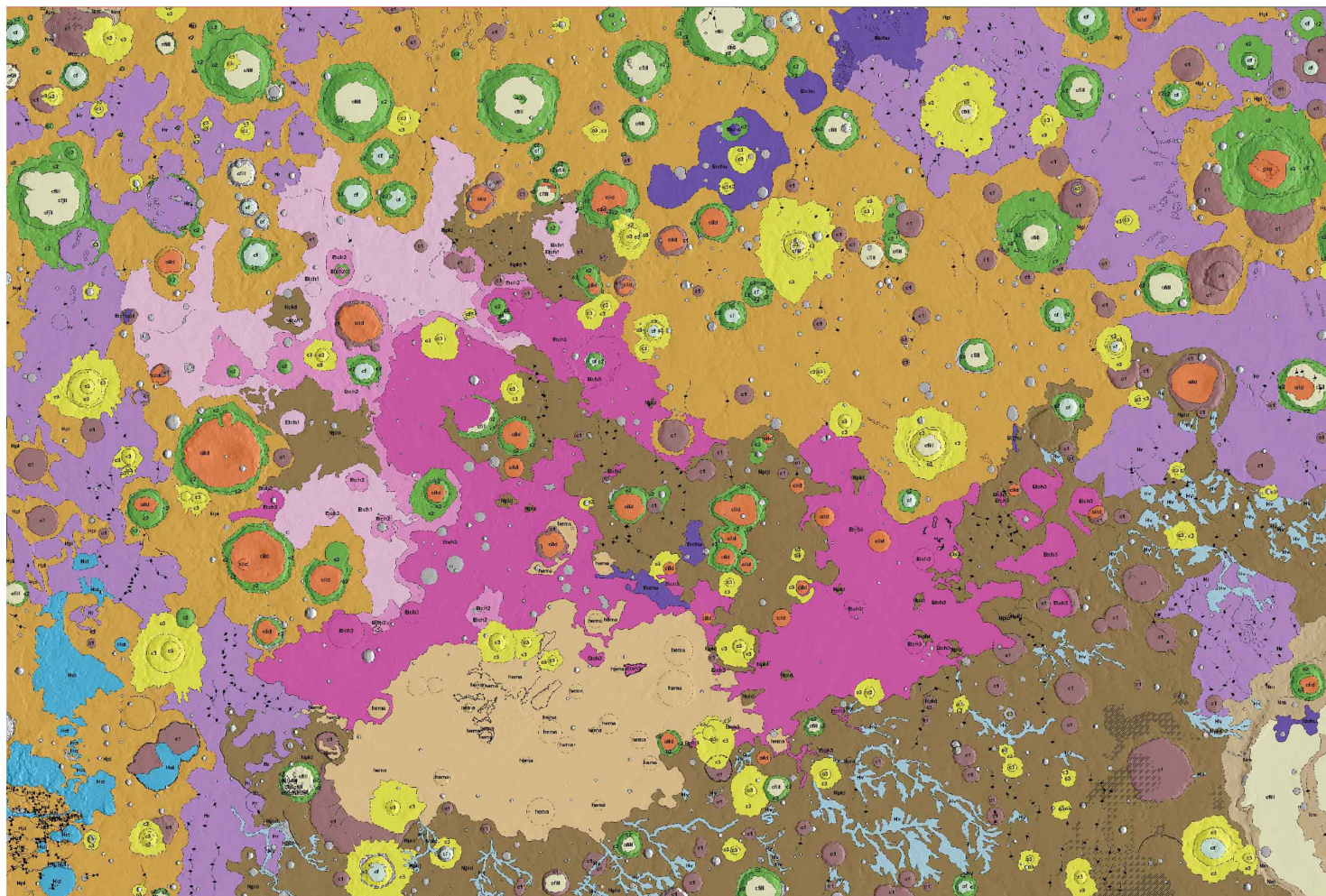
Geologic History Determined from Mapping (Figure 1): From our mapping, the geologic history of the region can be ideally reconstructed as follows. The heavy bombardment period is still preserved in the uplifted crustal materials found around the rim of large impact craters, resulting in the formation of the *Nm*

unit. Impacts continued during the remainder of the Noachian and accompanied the formation of the *Nc* and *Ncd* units (in analogy with the *Npl2* and *Npld* units described in ref. 5). The *Ncd* shows evidence of erosional features and deposits produced by fluvio-lacustrine processes. The latter processes formed unit *Nv* in the southern part of the map area.

Etched terrains (see *Etch1*, *Etch2*, *Etch3*, and *Etchu* units) likely formed from the Middle-Late Noachian to the Early Hesperian. Several hypotheses have been put forth to explain the deposition of these sub-horizontal highly erodible materials including eolian, lacustrine, groundwater, ice-related, and/or volcanic depositional processes. The occurrence of many outliers of these materials throughout the central part of the map region suggests that the deposits could have had a larger and more contiguous extent. The *Ilcd* unit is found in craters surrounding the etched terrains, suggesting its correlation with the latter units. Subsequently the unit has been likely affected by intense eolian erosion. Crater statistics and stratigraphic relationships suggest that the hematite-rich *Hema* unit likely formed during the Early Hesperian. The unit is exclusively associated with the etched terrains and its outcrops represent smooth surfaces overlying the *Etch3* unit. *Hema* could have formed as a primary or alteration product from either water-related (e.g. precipitation from solutions or groundwater alteration) or volcanic processes. The occurrence of isolated patches around the main extensive outcrop suggests that the deposits could have had a larger and more contiguous extent over the region.

Almost contemporarily to the *Hema* unit, the *Hr* unit likely started to form around the Early Hesperian in the low-lying plains surrounding the central region of the map. The unit of almost certain multisource volcanic origin generally overlies all the units of the highlands group. Finally, the *Hct* unit is cropping out only in the southwestern portion of the map area as an eastern extension of the large chaotic complex of Iani Chaos located just west of the mapped region.

References: [1] Squyres, S. W., et al., *Science*, DOI: 10.1126/science.1170355, 2004. [2] B. M. Hynek and R. J. Phillips, *Earth and Plan. Sci. Lett.*, 274, 214-220, 2008. [3] B. M. Hynek et al., *J. Geophys. Res.*, doi:10.1029/2002JE001891, 2002. [4] Edgett, K. S., *Mars*, doi:10.1555/mars.2005.0002, 2005. [5] Scott D. H. and K. L. Tanaka, *U.S. Geol. Surv. Misc. Invest. Ser., Map I-1802-A*, 1986.



DESCRIPTION OF MAP UNITS

CRATER UNITS

- c1- Highly eroded craters**—Intensely degraded crater material preserves little to no relief with respect to the surrounding units and lacks of a crater rim. The depression shows a flat floor without central peak or peak ring structures. Craters are not visible around the craters. Crater shapes are successively filled by channels. Erosion crater floors are overlain by internal layered deposits (see Red unit). Type location: lat 2°N, long 13°E. Interpretation: Old impact craters whose craters and rim have been almost completely eroded. The associated floorward flows have been filled by fluvio-lacustrine, or volcanic deposits.
- c2- Moderately eroded craters**—Consists of mostly complex craters exhibiting topographic evidence for rim, terraces, and/or central peakings. Crater shapes and secondary ridges of small impacts occasionally preserved in the surroundings of the craters. Crater floor shows either flat floor and evidence for infilling (off unit) or relatively fresh central peak structures (see off unit). In places crater floors are overlain by internal layered deposits (Red unit). Type location: lat 1°N, long 21°E. Interpretation: Impact craters moderately affected by erosional processes. Old impact craters whose shape and rim have been partially eroded. The majority of the crater floors have been infilled by fluvio-lacustrine, or volcanic deposits.
- c3- Well preserved craters**—Overlie all the surrounding units and exhibit almost pristine, subhorizontal crater rims and overall morphology with pronounced central peakings structures in complex craters. Ejecta blankets are always visible and typically continuous. Most crater floors are not modified or infilled (see off unit), occasionally, however, crater floors show evidence for resurfacing (see off unit), and rarely, from internal layered deposits (see Red unit). Type location: lat 0°N, long 3°E. Interpretation: Relatively young impact craters not or slightly affected by erosional processes.
- c4- Crater floor units**—Form the surface of roughness from the fluvio-lacustrine, mostly of the c3 unit. Typical features include ridges along the crater slopes, internal ring structures and scarps, and/or central peak. Type location: lat 1°N, long 10°E. Interpretation: Floor of the eroded impact craters or of craters not affected by later infilling processes.
- c5- Internal crater deposits**—Form smooth, flat, and almost unscoured surfaces of the interior of all craters of the c1, most of the c2, and rarely also of the c3 units. Typical secondary features include visible ridges, chaotic terrain-like fractures, scarps or depositional features. The basal flows and dunes, alluvial fans, and/or central peakings (see Red unit) lobes and talus slope deposits. Type location: lat 4°N, long 14°E. Interpretation: Sedimentary deposits filling the crater floor and resulting from resurfacing processes, such as mass wasting, eolian, fluvio-lacustrine, glacial, or volcanic activities. Hydrothermal deposits also possible.
- c6- Internal layered crater deposits**—Form smooth, mound-like, or outcrops of usually bright (in visual images) layered concepts topographically rising over the surrounding crater floor (sometimes also above the crater rim). The unit shows relatively high values in TES and THEMIS-derived thermal inertia data. In places, the floor rises up to more than a thousand meters that suggests of deposits (e.g., Channelized craters, lat 1°N, long 10°E). Its surface is often sculpted by intersecting fractures and gullies. In places, the outcrops are associated with small ring and/or small dunes, and with small-scale topography (see Red unit) craters. Typical secondary features are represented by yardangs showing the same direction as those of the basal wind streaks. Occurs in several places but appears more extensive close

to the Meridiani units (see Eshk1, Eshk2, Eshk3, and Eshk4 units). It is not visible within craters of the c3 unit. Type location: Comandaria crater lat 3°N, long 10°E. Interpretation: Sedimentary deposits filling the crater floor and of possible eolian, volcanic, fluvio-lacustrine, glacial, or groundwater origin, subsequently affected by eolian erosion and/or other resurfacing processes, such as mass wasting, eolian, fluvio-lacustrine, or volcanic activity. Hydrothermal or spring deposits also possible.

HIGHLAND UNITS

- Nu- Meridiani units**—Form high relief, scattered blocks and ridges mostly in association with the rim and the floor of large craters (e.g., Schiaparelli). In places, exhibit channel dissection and winkle ridges. Type location: lat 1°N, long 17°E. Interpretation: Ancient crater material uplifted during the formation of impact craters (Tanaka and Scott, 1987). Channels suggest later modification by fluvio processes.
- Nu1- Dissected units**—Form extensive surface in the southeastern part and is generally characterized by moderate relief. The unit is heavily modified by impact craters and shows evidence for relatively well-integrated river valley networks or troughs (see Be unit). Winkle ridges are often visible. Overlain by the Meridiani units (see Eshk1, Eshk2, Eshk3, and Eshk4 units), in visible within local eroded outcrops and has also been largely eroded in the central part of the map where inverted channels and winkle ridges are represented by the overlying Meridiani units. The latter are extremely eroded and as small isolated mass knobs over the eroded portion. Type location: lat 4°N, long 5°E (southern part) lat 8°N, long 14°E (central eroded part). Interpretation: Formed during the heavy bombardment period, the materials are likely a mixture of volcanic deposits (both low and pyroclastic flows), impact breccias, and erosional deposits produced and transported by fluvio-lacustrine processes. Unit is similar to Nu2, as described in Scott and Tanaka (1986).
- Nu2- Cratered units**—Form widespread and relatively smooth surfaces in the northern part of the map area and is generally characterized by moderate to low relief. The unit is extensively modified by impact craters, in places enhanced by the smoother surface of the overlying Be unit. Some winkle ridges and scarps observed. Rare channels or troughs. In the southeastern part it continues to be broken by the occurrence of chaotic terrain (see Be unit). Type location: lat 1°N, long 6°E. Interpretation: Formed during the heavy bombardment period, the materials are likely a mixture of volcanic deposits (both low and pyroclastic flows) and impact breccias. Unit is similar to Nu1, as described in Scott and Tanaka (1986).
- Nu3- Valley network units**—Form smooth low lying surfaces filling the numerous eroded valley networks and encompassing eolian river networks associated with the Nu2 unit in the southern part of the map area. The valleys typically show well integrated catchments with up to the first-order level of tributaries. Valley floor rarely preserve evidence for inner channels. The unit can be seen in the Nu2 and Be units but is expressed by the eroded terrain (see Eshk1, Eshk2, Eshk3, and Eshk4 units) and the Hema units, which are embaying, in places, the third part of the drainage system. Type location: lat 4°N, long 44°E. Interpretation: Sedimentary deposits eroded from the surrounding units and deposited by water flowing into the double valley network. Probably later infilling by eolian and/or fluvio-lacustrine. End of the hydrological activity in this area has been dated to the Late Noachian-Early Hesperian (Baker and Hyatt, 2009).

PLAINS UNITS

- Be- Chaotic units**—Form quasi-circular or irregular, in places partially and linear patches of terrain characterized by intense fracturing that produces elongated plateaus, mass knobs, buttes, and linear ridges of higher height and mostly closely spaced by intervening, mostly east-west oriented troughs. Mapped in the southeastern map border, close to the large chaotic complex of Iani Chae. Type location: lat 31°N, long 144°E. Interpretation: Plains terraces eroded and dissected by water-related, eolian, and/or volcanic processes. Not associated with the hydrological activity in the southern map area.
- Be1- Ridge unit**—Form irregular patches of smooth and extensive plains surface characterized by long, parallel, linear to sinuous, and in places closely spaced, macro-type (winkle) ridges. Occurs within and outside craters, embaying low-lying plains throughout the map area. Generally overlies all the units of the highland group. However, in the southeastern part of the map area, the unit is dissected and disrupted by the Nu and Be2 units. Type location: lat 40°N, long 10°E. Interpretation: Widespread low-lying plains floor probably eroded from many different local sources. Ridges may be either volcanic constructs or compressional features (Scott and Tanaka, 1986).

MERIDIANI UNITS

- Eshk1- Eshk1 units**—This group of units forms a roughly extensive (thousands of km, kilometers) hundreds of meters thick sequence of subhorizontal layered deposits occurring in the central part of the map area (see Eshk1, Eshk2, Eshk3, and Eshk4). All the units exhibit evidence for intense erosion (mostly eolian), which resulted in the shaping of the typical eroded nature of these materials. Eshk1 with generally exhibit high values in TES and THEMIS-derived thermal inertia data relative to the surrounding units. In addition to the locally extensive outcrops, the units also consist of numerous cliff-banded blocks, mesas, outcrops and irregular patches of layered outcrops overlying the Nu2 unit. Dissected and eroded units (see Nu2 and Nu3). This suggests that the sequence was likely more extensive and continuous over at least the entire central part of the map area. Additionally, eroded outcrops throughout the unit expose, in places, the underlying Noachian cratered terrain. Based mainly on the structural relief data (reconstructed from derived MOLA topography) and differential erosion characteristics (secondary features), the layered sequence can be divided into three units, described below starting from the bottom to the top of the stratigraphic sequence.
- Eshk1- Lower etched unit**—Form generally phase and low relief surfaces occurring in the northwestern part of the Meridiani plains' unit and overlying the eroded Nu2 unit. The otherwise smooth texture of the unit is often made rugged by the occurrence of relatively small (a few kilometers) winkle ridges, mesas, and outcrops typically cliff-banded and with some heights. These occur as isolated, concentrated patches, and sometimes aligned to form ridge outcrops. Superimposed fault craters are rare, whereas other local craters observed. Contains the lowest values of thermal inertia among all the Meridiani units. Type location: lat 4°N, long 44°E. Interpretation: The unit could have formed as a result of eolian, lacustrine, and/or volcanic depositional processes. The intense erosion and occurrence of an abundance of outcrops suggest that the deposits could have had a larger and more continuous extent over the region. Older Noachian units (Nu2, Nu3) have been marked by eolian, fluvio-lacustrine, or volcanic deposits, the Meridiani plains units (see Eshk1, Eshk2, Eshk3, and Eshk4 units), which have been subsequently eroded mainly by eolian activity.
- Eshk1- Middle etched unit**—Form steep cliff-banded plain and generally smooth surfaces rising above the Eshk1 unit. Knobs, mesas, and outcrops are less common with

respect to the Eshk1 unit itself (to the last) secondary features concentrate only on the 'scarp' margins separating the unit from the underlying units. Eshk1, where a few but large in few tens of km irregular phase patches are scattered over the Eshk1 unit. The differential erosion with respect to Eshk1 suggests a more competent nature of this unit. However, the sharp unit margins and the presence of isolated outcrops suggest widespread erosion and a wider original and/or coverage. Shows intermediate values of thermal inertia among all the etched units. Type location: lat 2°N, long 44°E. Interpretation: The unit could have formed as a result of eolian, lacustrine, and/or volcanic depositional processes. The intense erosion and occurrence of an abundance of outcrops suggest that the deposits could have had a larger and more continuous extent over the region. Older Noachian units (Nu2, Nu3) have been marked by eolian, fluvio-lacustrine, or volcanic deposits, the Meridiani plains units (see Eshk1, Eshk2, Eshk3, and Eshk4 units), which have been subsequently eroded mainly by eolian activity.

Eshk1- Upper etched unit—Forms the uppermost, most extensive and laterally continuous of the etched units, showing a distinctly high thermal inertia values. Data in THEMIS IR day images, the surfaces are rugged, whereas visual high-contrast images (e.g., MOC, CTX, and THEMIS) show that the deposits are composed of many horizontal to sub-horizontal bright layers. Selective erosion of the later units likely determined the characteristic etched aspect of the surfaces with knobs, mesas, and outcrops, which are less common with respect to the Eshk1 and Eshk2 units, suggesting the occurrence of more competent rocks than those units. Secondary eroded features concentrate mostly on the 'scarp' margins separating the unit from the underlying units, whereas a few but large (a few tens of km) isolated irregular patches are observed in the eastern part of the map area. Stratigraphic relationships show that this unit overlies the central and dissected Noachian units Nu2 and Nu3 (erosional windows throughout the map and exposure in places) and also overlies the eroded part of the valley networks (see Be unit), suggesting that the unit was likely formed after the cessation of the hydrological activity within the area. Type location: lat 1°N, long 6°E. Interpretation: The unit could have formed as a result of eolian, lacustrine, and/or volcanic depositional processes. The intense erosion and occurrence of isolated outcrops suggest significant eolian erosion and that the deposits likely had a larger and more continuous extent over the region.

Eshk1- Eshk1 undisturbed unit—Form isolated and irregular patches showing intermediate primary characteristics with respect to the other etched units. Is not laterally continuous with other etched units or is observed at different elevations. More extensive on the southern part of the map area, surfaces are subhorizontal and intensely affected by eolian erosion. Typical secondary features include some height and steep-sided knobs, mesas, outcrops, and NW-SE outcrops. Some patches are also present in the eastern Schiaparelli crater and in association with the main etched units within local deep depressions. Type location: lat 14°N, long 44°E. Interpretation: The unit could have formed as a result of eolian, lacustrine, and/or volcanic depositional processes. The intense erosion and occurrence of isolated outcrops suggest that the deposits likely had a larger and more continuous extent over the region.

Hema- Hema unit—A few tens of meters thick, smooth surface unconformably overlying the Eshk1 unit (approximate contact). Dark in visual images, shows distinct domes, buttes, mesas, or volcanic deposits, the Meridiani plains units (see Eshk1, Eshk2, Eshk3, and Eshk4 units) are embayed, in places, the third part of the drainage system. Additional outcrops (in form of irregular or quasi-circular patches with lobate margins) are scattered over the unit, but not in the main low-lying areas. Secondary features include extensive dark covering, eolian features (ripples and dunes) and a paucity of topographic features. Contrastly, the unit shows a large number of partially buried and filled relatively

large (up to 50-km-diameter) craters, likely inherited from the underlying crater units (Eshk1, Nu2 and Nu3). Type location: lat 1°N, long 44°E. Interpretation: The unit could have formed as primary or alteration product both from water-related (e.g., precipitation from eolian or groundwater alteration) or volcanic processes. The occurrence of isolated patches around the main extensive

SYMBOL EXPLANATION

- Small crater**—Approximate location of minor (diameter < 5 km) impact features.
- Contour of a level crater**—Showing the approximate location of subhorizontal craters visible only from MOLA topography.
- Crater rim**—Showing preserved and defined craters. Hatchures point toward the core of the crater.
- Depression margin**—Line delineates the scarp of topographic low. Hatchures point into the depression.
- Fault**—Certain.
- Fault**—Approximate.
- Winkle ridge**—Line delineates crest, certain.
- Winkle ridge**—Line delineates crest, approximate.
- Shallow flat ridges**—Line delineates raised features interpreted as eroded craters.
- Secondary crater chain**—
- Trough margin**—Line delineates the scarp of topographic low. Hatchures point into the depression.

TYPE OF CONTACTS

- Certain**—Contact is confidently located.
- Approximate**—Contact with undoubted confidence due to data quality, surface expression, and/or unique stratigraphic relationships.
- Gradational**—Contact is transitional at map scale.

Figure 1. Draft version of updated geologic map of the Meridiani region, Mars. See text for details. Zoom in on map to see features.

GEOLOGIC MAPPING IN SOUTHERN MARGARITIFER TERRA. R. P. Irwin III¹ and J. A. Grant²,
¹Planetary Science Institute, 1700 E. Ft. Lowell Rd., Tucson AZ 85719. ²Center for Earth and Planetary Studies, National Air and Space Museum, Smithsonian Institution, 6th St. at Independence Ave. SW, Washington, DC 20560, irwin@psi.edu.

Introduction: Margaritifer Terra records a complex geologic history [1-5], and the area from Holden crater through Ladon Valles, Ladon basin, and up to Morava Valles is no exception [e.g., 6-13]. The 1:500,000 geologic map of MTM quadrangles –15027, –20027, –25027, and –25032 (Figs. 1 and 2 [14]) identifies a range of units that delineate the history of water-related activity and regional geologic context.

Mapping Results: Within the map area (Figs. 1 and 2), the degraded Ladon and Holden multi-ringed impact basins [15] are the oldest features with ring structures reduced to isolated mountains (Nm). The most widespread unit is the Noachian Terra unit (Nt), which includes basaltic bedrock [16], impact ejecta, weathered rocks [17], fluvially reworked sediments, airfall or eolian traction materials, and perhaps other rocks. Fluvial dissection is common, and layering is evident in places. Terra unit surfaces are reworked by impacts [18], typically rolling, and retain small craters poorly relative to smooth basin fills [19, 20].

Late Noachian-Early Hesperian channel materials of Uzboi, Ladon, and Morava Valles include exposed bedrock outcrops, eroded Terra unit (Nt), and alluvial veneers. The Channel 1 unit (HNch₁) represents initial dissection that was abandoned when the main channels were downcut (HNch₂).

The Early-to-mid Hesperian ejecta (Hc) of Holden (26.0°S, 325.8°E) and Ostrov (26.5°S, 332°E) craters postdate these units and resurfaced most of the southwestern part of the map area (Fig. 1). Megabreccia in Holden crater is exposed along the southern crater wall [11]. In the Holden impact basin, a superimposed thick fill unit (HNb₂) is interpreted as moderately to strongly indurated alluvial, volcanic, or eolian materials, where origin and composition may vary.

After Holden crater formed, Holden and Eberswalde (23°S, 327°E) craters accumulated phyllosilicate-bearing light-toned layered deposits (LTLDS) (Hh₂ and HNe) with broadly similar stratigraphy [11, 13, 21], suggesting a similar depositional environment. In both cases, beds are often <1 meter thick and can be traced laterally for hundreds of meters. The deposits are confined to low elevations and do not drape exterior surfaces, favoring low-energy alluvial or lacustrine deposits over airfall materials or volcanic ash.

The origin of phyllosilicates observed in LTLDS of Holden crater (Hh₂), Eberswalde crater (HNe), Ladon impact basin (H1), and other depressions has

implications for habitability [11, 13], as it reflects prolonged weathering. Holden crater initially drained internally, so phyllosilicates were either eroded from sedimentary rocks exposed on the crater walls, or chemical weathering occurred in the crater [13].

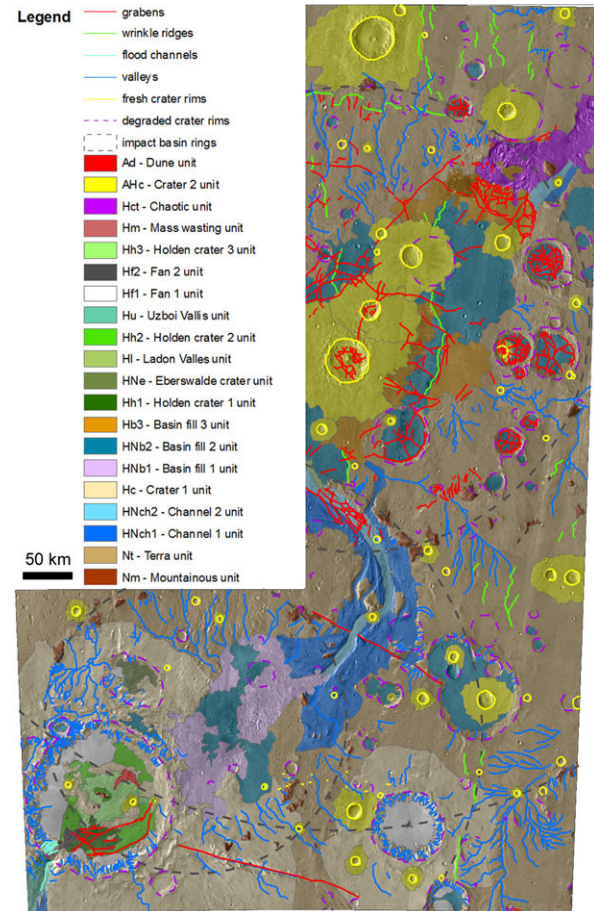


Figure 1. Geologic map and abbreviated legend for MTM quads –15027, –20027, –25027, and –25032 completed at 1:500,000 [14].

Holden and Ostrov craters include some of the most extensive alluvial fans on Mars (Hf₁). Large alluvial fans formed preferentially along the rims of deep, Late Noachian to Early Hesperian impact craters that were not substantially modified by Noachian erosion [22, 23]. Ostrov crater has unusually deep rim dissection, sourcing an alluvial bajada that spans the circumference of the crater. These fans ramp down to the central peak, and a paucity of evidence for deep ponding suggests that the groundwater table was typically

below the crater floor, consistent with infrequent precipitation runoff in an arid paleoclimate around the Noachian-to-Hesperian transition. By contrast, Holden crater contains a fringing bajada along its higher western wall, but the lower eastern wall experienced very little erosion or deposition. The bajada has a relationship between contributing area and slope that is consistent with fluvial rather than debris-flow-dominated fans, and the inverted channels on fan surfaces show that inter-channel deposits were dominantly composed of sand and fines [22], so high-magnitude runoff may have been uncommon.

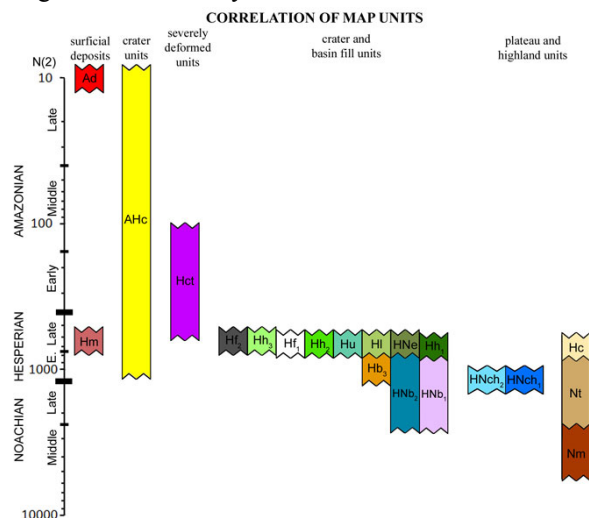


Figure 2. Correlation of map units for the completed geologic map shown in Figure 1 [14].

The putative delta in Eberswalde crater consists of alluvium sourced from a basin to the west, which had been resurfaced by Holden crater ejecta. The alluvium likely includes Holden crater ejecta, weathered Terra unit rocks, and materials from the Eberswalde rim, similar to those occurring in the Holden crater fans. Finally, Holden and Eberswalde craters record variable water levels. In Holden, LTLDs on the floor and > 200 m up the wall suggest a deep lake. In Eberswalde, lateral migration of channels suggests base-level stability over at least century timescales [14, 24].

The youngest layered deposits in Holden crater are the Fan 2 unit (Hf₂) and the Holden crater 3 unit (Hh₃). The Fan 2 unit is coarse-grained with visible boulders in HiRISE images, despite the low gradient of the fan, and it has a multi-lobed planform emanating from a breach where Uzboi Vallis enters the crater. These characteristics suggest origin during a large flood when a paleolake in Uzboi Vallis drained into the crater. The Holden crater 3 unit is interpreted as more distal, fine-grained deposits from the same event modified by more recent eolian activity.

Water-driven erosion and sedimentation may have extended well into the Hesperian, which was also characterized by resurfacing of certain basin floors by eolian or volcanic activity that was concentrated in and around Ladon basin. Amazonian activity was largely confined to a dune field (Ad) inside Holden crater.

Summary: The mapped units and events defined during the recently completed effort describe widespread Noachian to mid-Hesperian aqueous activity in southern Margaritifer Terra that shaped large channels, valley and alluvial systems, and even lakes. The preserved landscape holds important clues related to the early history of Mars and whether habitable conditions may have occurred. Nevertheless, the existing maps are only a part of the story related to understanding the cause, timing, and extent of aqueous degradation of the region and how it relates to a global hydrologic cycle.

References: [1] Saunders S. R. (1979), *USGS Map I-1144, MC-19*. [2] Parker T. J. (1985), *Geomorphology and Geology of the Southwestern Margaritifer Sinus-Northern Argyre Region of Mars*, M.S. Thesis, UCLA. [3] Grant J. A. (1987), *NASA TM 89871*, p. 1-268. [4] Grant J. A. (2000), *Geology*, 28, 223. [5] Hynek B. M. and Phillips R. J. (2001), *Geology*, 29, 407. [6] Grant J. A. and Parker T. J. (2002), *JGR*, 107, 10.1029/2001JE001678. [7] Moore J. F. et al. (2003), *GRL*, 30, E06001 doi:10.1029/2003GL019002. [8] Malin M. C. and Edgett K. S. (2003), *Science*, 302, 1931. [9] Pondrelli M. et al. (2005), *JGR*, 110, doi:10.1029/2004JE002335. [10] Pondrelli M. A. et al. (2008), *Icarus*, 197, 429, doi:10.1016/j.icarus.2008.05.018. [11] Grant J. A. et al. (2008), *Geology*, 36, 195, doi:10.1130/G24340A. [12] Irwin R. P. III and Grant J. A. (2009), in *Megaflooding on Earth and Mars*, Burr D. M. et al., eds., Cambridge Univ. Press, 209–224. [13] Milliken R. E. and Bish D. L. (2010), *Phil. Mag.*, 1478, doi:10.1080/14786430903575132. [14] Irwin R. P. III and Grant J. A. (2010), *USGS map*, 1:500,000 (submitted). [15] Schultz P. H. et al. (1982), *JGR*, 87, 9803. [16] Bandfield J. L. et al. (2000), *Science*, 287, 1626, doi:10.1126/science.287.5458.1626. [17] Murchie S. L. et al. (2009), *JGR*, 114, doi:10.1029/2009JE003342. [18] Hartmann W. K. et al. (2001), *Icarus*, 149, 37. [19] Malin M. C. (1976), in *Studies of the surface morphology of Mars*: CalTech, Ph.D. thesis. [20] Malin M. C. and Edgett K. S. (2001), *JGR*, 106, 23,429. [21] Lewis K. W. and Aharonson, O. (2006), *JGR*, 111, doi:10.1029/2005JE002558. [22] Moore J. M. and Howard A. D. (2005), *JGR*, 110, doi:10.1029/2005JE002352. [23] Kraal E. R. et al. (2008), *Icarus*, 194, 101. [24] Bhat-tacharya J. P. et al. (2005), *GRL*, 32, doi:10.1029/2005GL022747.

Introduction: Geologic mapping of MTM -30247, -35247, and -40247 quadrangles is being used to characterize Reull Vallis (RV) and examine the roles and timing of volatile-driven erosional and depositional processes. This study complements earlier investigations of the eastern Hellas region, including regional analyses [1-6], mapping studies of circum-Hellas canyons [7-10], and volcanic studies of Hadriaca and Tyrrhena Paterae [11-13]. Key scientific objectives include 1) characterizing RV in its “fluvial zone,” and evaluating its history of formation, 2) analyzing channels in the surrounding plains and potential connections to RV, and 3) examining young, possibly sedimentary plains along RV.

Methodology: This analysis includes preparation of a geologic map of MTM -30247, -35247, and -40247 quadrangles compiled on a single 1:1M-scale base. Crater size-frequency distributions compiled for regional analyses [5,6] will be used in conjunction with newly generated statistics for units mapped in the current study using new datasets (e.g., MOC, THEMIS, CTX and HiRISE).

Mapping Results: This section describes observations from geologic mapping and integrates new results with previous mapping of this area [e.g., 5,6] to complete MTM-scale mapping of the entire RV system.

Fluvial Modification: Fluvial processes have modified much of the map area. Most “highland” channels (<1 km wide; 10s of kilometers long) are incised within ejecta deposits associated with several large (D>35 km) impact craters. They consist of single channels to small networks, and some channels are braided. Several steep-walled, theater-headed channels are found within the plains adjacent to RV. Most of these channels are only a few tens of kilometers long, but some extend for hundreds of kilometers. Lastly, many highland massifs and the interior walls of many craters are incised with gullies that generally extend from the topographic peak to the base of the feature.

Reull Vallis System: Segment 1 (S1) and the upper part of Segment 2 (S2) of RV are found within the map area. S1 (~240 km long, 8–47 km wide, 110–600 m deep) displays erosional scarps, scarp-bounded troughs, and scour marks on the canyon floor. S1 consists of a series of irregular basins that contain remnant islands of ridged plains material. The morphology of S1 suggests formation by combined surface flow and

collapse of ridged plains. S1 is the source area for at least some of the fluids that carved S2 [5,6,14].

S1 and S2 are not connected directly, but are separated by the edge of a large depression referred to as the “Morpheus” basin. It has been suggested that during the early stages of RV's formation water released from S1 accumulated in this basin and was later released to carve S2 [15,16].

S2 consists of morphologically distinct upper (S2-U) and lower (S2-L) parts. S2-U (6 to 13 km wide, 110-650 m deep) is sinuous and extends for ~240 km through degraded highlands. Layers or terraces exposed along its walls and braided channels incised in its floor suggest that at least this part of RV was formed and/or modified by surface flow [5,6]. Part of S2-L (6 km wide, 140–350 m deep) occurs in the southwest part of the map area and begins where a narrow (1–2 km wide), shallow (~100 m deep) canyon downcuts into the main canyon floor [5,6]. S2-L displays steep walls and a relatively flat floor suggesting formation by fluvial processes and subsequent modification by collapse and mass wasting [7,8].

Regional Stratigraphy: Materials forming highland terrains - *mountainous material* and *highland plateau material* (previously mapped as the basin rim unit) - are found primarily in the southern part of the map area [5,6,17]. *Mountainous material* (unit Nm) is the most rugged and tends to form isolated to clustered knobs and massifs. *Highland plateau material* (unit Nhp) is less rugged and forms more continuous expanses. These units are interpreted to consist of large blocks/ejecta resulting from the Hellas impact event [3-6,17,18]. In THEMIS day IR images both units appear very rugged; however, in high-res images, the peaks are rounded and appear mantled by a fairly continuous deposit [19,20]. At the peaks of some of the steepest highland massifs this mantling unit is being removed downslope via mass wasting.

Ridged plains material (unit Nrp) forms most of the northern part of the map area. This unit contains a high density of NE-SW and NW-SE trending wrinkle ridges and ridge rings. In THEMIS day IR images, inter-ridge areas are relatively featureless except for low-relief scarps and small sinuous channels. High-res images show inter-ridge areas contain dune features, accumulations of smooth materials in low areas, and small knobs [17]. Crosscutting relationships suggest ridge formation occurred after plains emplacement and prior to formation of S1 [5,6]. N(2) and N(5) statistics

suggest this unit is Noachian in age. Collapse and erosion of Nrp to form S1 significantly modified portions of the ridged plains resulting in exposure of *modified ridged plains material* (unit Nmnp). The ridged plains sequence is interpreted to be sedimentary and/or volcanic [17,18,21,22] material that was modified by fluvial and eolian erosion, mobilization and deposition of surficial materials.

Plains in the southern part of the map area occupy low-lying regions and embay highland massifs. *Smooth plains material – upper member* (unit Nspu) is found primarily adjacent to S2-U. These deposits display smooth surfaces in THEMIS IR images, but high-res images reveal low-relief scarps, small channels, pits and scattered knobs suggesting sublimation and collapse of volatile-rich material, as well as modification by fluvial and eolian processes. *Smooth plains material – lower member* (unit Nspl) is stratigraphically lower than the upper member and forms the lower wall along S2-U. These materials were likely exposed during formation of S2. The smooth plains sequence is interpreted to be sediments deposited prior to and during the formation of RV by overflow of the canyon and from erosion via valley networks, and may also include materials deposited via mass wasting [5-8,17].

Two distinct plains units occupy the southeast part of the map area. *Etched plains material* (unit Nep) is found in the location corresponding to the "Morpheus" basin. In THEMIS day IR images, etched plains display a mottled appearance, which in high-res images is due to erosion of low albedo material into yardangs and exposure of underlying higher albedo material [17]. *Mottled plains material* (unit Nmp) occupies much of MTM -40247; these plains appear smooth at most scales and fill low-lying areas around highland massifs and degraded craters. The mottling and lack of detail expressed throughout much of these plains suggests these materials may be eolian in nature, similar to the mantled highlands unit mapped by [6]. Knobby textures along the southeastern edge of the map area consist of small knobs surrounded by smooth plains, and may consist of remnants of ejecta from a 50-km-diameter impact crater to the west [17].

The floors of the RV segments are covered with morphologically distinct materials [17]. S1 contains *smooth Reull Vallis floor material* (unit Nrvfs) that is generally smooth to rough (at MOC scale) and likely includes fluvial deposits, as well as collapsed ridged plains. S2-U contains *upper Reull Vallis floor material* (unit Hrvfu), which displays an overall smooth appearance at all image resolutions, and this entire deposit is incised with narrow sinuous channels. S2-L contains *lower Reull Vallis floor material* (unit Hrvfl) and exhibits pits and lineations that parallel the canyon

walls. S2 floor materials likely consist of sediments eroded from "Morpheus" basin and adjacent highland and plains units [17].

Debris apron material (unit Ada) forms some of the youngest deposits in the map area [1,5-8,17,23-25] along highland massifs and crater walls. These deposits display uniform or mottled albedo, smooth relatively featureless surfaces to ridge-and-groove morphology, lobate frontal morphologies, and appear to be composed of multiple coalescing flows. Some crater floor deposits contain rings concentric to the crater walls, similar to concentric crater fill, suggesting flow of material downslope [26,27].

Impact-related materials cover a large part of the map area and exhibit a range of preservation states (fresh to highly degraded) and ages (Noachian to Amazonian) [17]. *Crater floor material* (unit AHcf) is found on the floors of most craters in the map area. In THEMIS day IR images, crater floor material appears smooth and featureless; however, in high-resolution images these deposits display a variety of albedos and surface textures, including knobby, pitted, "stucco"-type, "brain"-like, and ridge-and-groove. This unit is interpreted to consist of sediments emplaced via fluvial, eolian and/or mass wasting processes. The differences in albedo and surface textures suggest emplacement by a combination of processes and/or post-emplacement modification of the deposits.

References: [1] Crown, D.A., et al. (1992) *Icarus*, **100**, 1-25. [2] Crown, D.A., et al. (2005) *JGR*, **110**, E12S22, doi:10.1029/2005JE002496. [3] Tanaka, K.L. and G.J. Leonard (1995) *JGR*, **100**, 5407-5432. [4] Leonard, G.J. and K.L. Tanaka (2001) USGS GISM I-2694. [5] Mest, S.C. (1998) M.S. Thesis, Univ. of Pittsburgh. [6] Mest, S.C., and D.A. Crown (2001) *Icarus*, **153**, 89-110. [7] Mest, S.C. and D.A. Crown (2002) USGS GISM I-2730. [8] Mest, S.C. and D.A. Crown (2003) USGS GISM I-2763. [9] Price, K.H. (1998) USGS MISM I-2557. [10] Bleamaster, III, L.F. and D.A. Crown (2010) USGS, in review. [11] Greeley, R. and D.A. Crown (1990) *JGR*, **95**, 7133-7149. [12] Crown, D.A. and R. Greeley (1993) *JGR*, **98**, 3431-3451. [13] Gregg, T.K.P., et al. (1998) USGS MISM I-2556. [14] Crown, D.A. and S.C. Mest (1997) LPSC XXXVIII, 269-270. [15] Ivanov, M.A., et al. (2005) *JGR*, **110**, doi:10.1029/2005JE002420. [16] Kostama, V.-P., et al. (2007) *JGR*, **112**, doi:10.1029/2006JE002848. [17] Mest, S.C. and D.A. Crown (2010) LPSC XLI, #1945. [18] Greeley, R., and J.E. Guest (1987) USGS MISM I-1802B. [19] Mustard, J.F., et al. (2001) *Nature*, **412**, 411-414. [20] Milliken, R.E., et al. (2003) *JGR*, **108**, E6, doi:10.1029/2002JE002005. [21] Potter, D.B. (1976) USGS MISM I-941. [22] Greeley, R. and P.D. Spudis (1981) *Rev. Geophys.*, **19**, 13-41. [23] Pierce, T.L., and D.A. Crown (2003) *Icarus*, **163**, 46-65, doi:10.1016/S0019-1035(03)00046-0. [24] Crown, D.A., et al. (2006) LPSC XXXVII, #1861. [25] Berman, D.C., et al. (2006) LPSC XXXVII, #1781. [26] Squyres, S.W., and M.H. Carr (1986) *Science*, **231**, 249-252. [27] Carr, M.H. (1996) *Water on Mars*, Oxford Un. Press, NY.

THE INTERACTION OF IMPACT MELT, IMPACT-DERIVED SEDIMENT, AND VOLATILES AT CRATER TOOTING, MARS. P. Mouginis-Mark¹ and J. Boyce¹, ¹HIGP, Univ. Hawaii, Honolulu, HI 96822. <pmm@hawaii.edu>

We are producing a 1:200K geologic map of Tooting crater, Mars. This work has shown that an incredible amount of information can be gleaned from mapping at even larger scales (1:10K – 1:25K) using CTX and HiRISE data. We have produced two new science papers (Morris et al., 2010; Mouginis-Mark and Boyce, 2010) from this mapping, and additional science questions continue to arise from our on-going analysis of Tooting crater:

1) What was the interplay of impact melt and volatile-rich sediments that, presumably, were created during the impact? Kieffer and Simonds [1980] predicted that melt would have been destroyed during impacts on Mars because of the volatiles present within the target – we seek to understand if this is indeed the case at Tooting crater. We have identified pitted and fractured terrain that formed during crater modification, but the timing of the formation of these materials in different parts of the crater remains to be resolved. Stratigraphic relationships between these units and the central peak may

reveal deformation features as well as overlapping relationships.

2) Morris et al. [2010] identified several lobate flows on the inner and outer walls of Tooting crater. It is not yet clear what the physical characteristics of the source areas of these flows really are; e.g., what are the sizes of the source areas, what elevations are they located at relative to the floor of the crater, are they interconnected, and are they on horizontal or tilted surfaces?

3) What were the details of dewatering of the inner wall of Tooting crater (Fig. 1)? We find evidence within Tooting crater of channels carved by water release, and the remobilization of sediment (which is inferred to have formed during the impact event). Sapping can be identified along the crest of unit 8 near the floor of the crater (Fig. 2a, 2b). This unit displays amphitheater-headed canyons that elsewhere on Mars are typically attributed to water leaking from the substrate [Laity and Malin, 1985; Malin and Edgett, 2000].

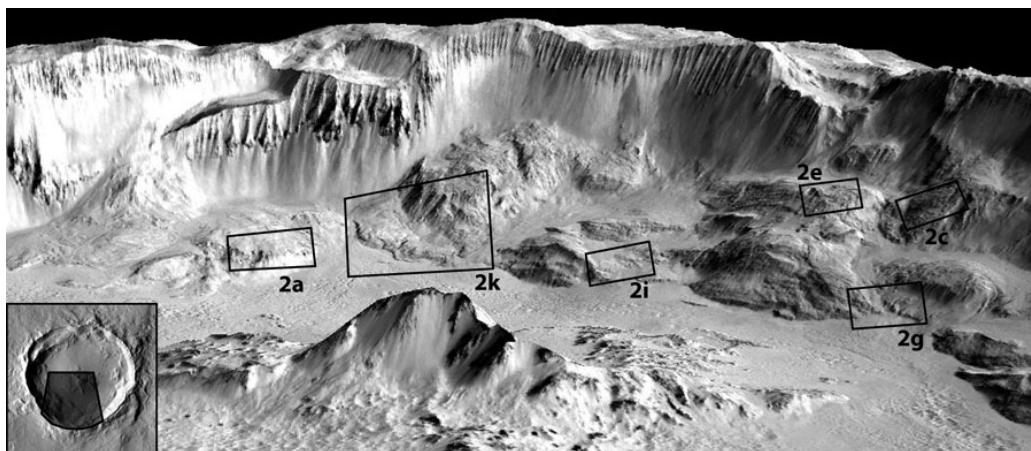


Figure 1: Oblique view looking south at the interior of Tooting crater. The kilometer-high central peak is in the left foreground. Boxes delineate the locations of the HiRISE subscenes presented in Fig. 2. Base image is CTX frame P01_001538_2035, vertical exaggeration is 1.9x. Height of rim rises ~2,100 m above the crater floor. Shaded area within insert at lower left shows the large image location within Tooting crater.

Canyons in Tooting crater are the source of debris that is superposed on the pitted terrain on the crater floor (Fig. 2a), and hence post-dates its formation, whereas in other places

(Fig. 2c) the chronology is the opposite with canyons carved before pitted terrain formed. Slump blocks reveal several episodes of water release, with theater-headed canyons

pre-dating the formation of some units of pitted material (Fig. 2c, 2d), and channels within other blocks (Fig. 2e, 2f). At several levels on the inner wall, we find evidence for the mobilization of sediments. For example, based on their superposition relationships, there is a sequence of three episodes of flow lobes emplaced on top of pitted terrain on the floor of Tooting crater (Fig. 2g, 2h). These flow lobes (units 2-4 in Fig. 2h) are confined by two terrace blocks and are the distal portions of the leveed-flow described by Morris et al. [2010]. The mobilization of sediment deposits fed smaller (<500 m-long) discrete flows at the edge of terrace blocks (Fig. 2i, 2j). Some of these terrace blocks (unit 7, Fig. 2l) have also slumped during cavity modification; a

series of thick (35 - 55 m) flow lobes extend toward the crater floor and appear to pre-date the formation of sediment flow units 3 and 4 because these flow lobes do not disrupt the sediment flow units.

References: Kieffer, S.W. & C.H. Simonds (1980) The role of volatiles and lithology in the impact cratering process. *Rev. Geophys. Space Phys.* 18: 143 – 181. Laity, J. E., & Malin, M. C. (1985) Sapping processes and the development of theater-headed valley networks on the Colorado Plateau: *GSA Bull.* 96: 203 – 217. Malin, M.C., & Edgett, K.S. (2000) Evidence for recent groundwater seepage and surface runoff on Mars: *Science* v. 288, p. 2330 – 2335. Morris, A.R., Mougini-Mark, P.J., & Garbeil, H. (2010) Possible impact melt and debris flows at Tooting crater, Mars, in press, *Icarus*. Mougini-Mark, P.J. & J.M. Boyce (2010) Protracted dewatering of the cavity of Tooting crater, Mars. Submitted to *Geology*.

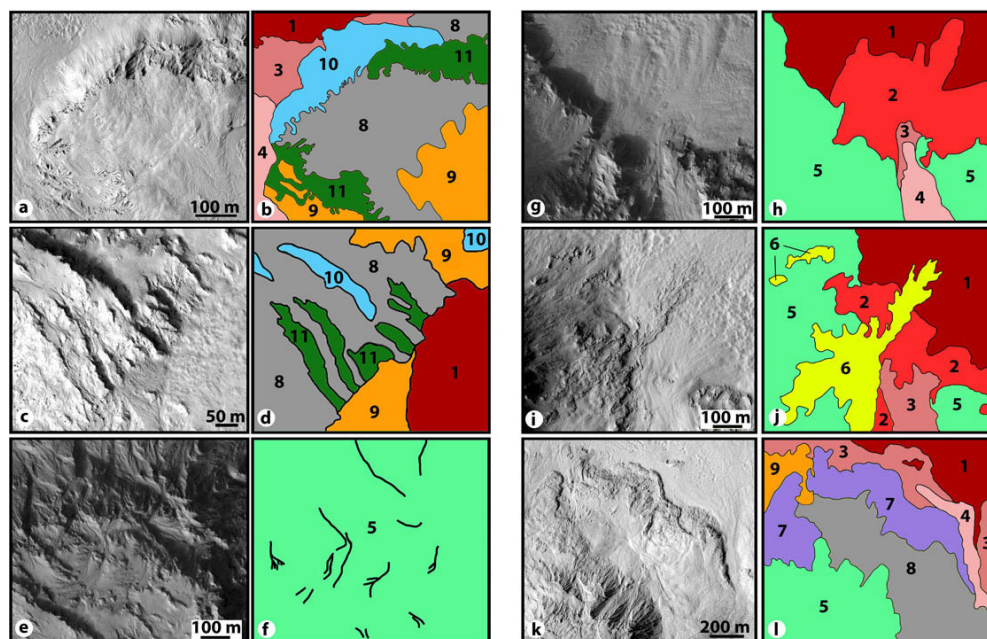


Figure 2: Left two columns, examples of erosion on wall blocks suggestive of water release, along with interpretive sketches. North is towards the top of each image and the illumination is from the left in all images. Locations are indicated in Fig. 1. Numbered units in figures b, d, f, h, j and l are morphologically similar in all images: “1” pitted terrain; “2,” “3” and “4” sediment flows; “5” eroded terrain blocks; “6” flow originated from terrace block; “7” massive flow units; “8” sediment plateaus; “9” smooth units with channels carved into surface cut; “10” scree slopes; and “11” canyonlands. Attributes to note are: (a) scarps with sapping headwalls cut into sediment plateau to produce canyons. HiRISE image PSP_001538_2035; (c) theater-headed canyons (unit “11”) that pre-date the pitted terrain unit “1.” HiRISE image PSP_003569_2035; (e) braided channels within wall block. HiRISE image PSP_005771_2035. Right two columns, examples of features interpreted to be sediment flows generated by up-slope dewatering, along with interpretive sketches. Key attributes to note are: (g) multiple episodes of sediment fans spreading out of pitted terrain. HiRISE image PSP_005771_2035; (i) single lobe superposed over sediment fan which is itself on top of pitted terrain. Central portion of lobe is 55 m thick, eastern margin is 35 m thick. HiRISE image PSP_007406_2035; (k) massive flow lobes from terrace block. HiRISE image PSP_001538_2035.

GEOLOGIC MAP OF THE OLYMPIA CAVI REGION OF MARS (MTM 85200): A SUMMARY OF TACTICAL APPROACHES. J. A. Skinner, Jr. and K. Herkenhoff, Astrogeology Science Center, U.S. Geological Survey, 2255 N. Gemini Drive, Flagstaff, AZ 86001 (jskinner@usgs.gov).

Introduction: The 1:500K-scale geologic map of MTM 85200—the Olympia Cavi region of Mars—has been submitted for peer review [1]. Physiographically, the quadrangle includes portions of Olympia Rupēs, a set of sinuous scarps which elevate Planum Boreum ~800 meters above Olympia Planum. The region includes the high-standing, spiral troughs of Boreales Scopuli, the rugged and deep depressions of Olympia Cavi, and the vast dune fields of Olympia Undae. Geologically, the mapped units and landforms reflect the recent history of repeated accumulation and degradation. The widespread occurrence of both weakly and strongly stratified units implicates the drape-like accumulation of ice, dust, and sand through climatic variations. Similarly, the occurrence of layer truncations, particularly at unit boundaries, implicates punctuated periods of both localized and regional erosion and surface deflation whereby underlying units were exhumed and their material transported and re-deposited. Herein, we focus on the iterative mapping approaches that allowed not only the accommodation of the burgeoning variety and volume of data sets, but also facilitated the efficient presentation of map information. Unit characteristics and their geologic history are detailed in past abstracts [2-3].

Tactical Approach: Like many recent Mars geologic maps, this map was completed during a time of especially high data flux and evolving digital mapping techniques. The 2009 Mappers Handbook [4] provided guidance for the construction of geologic maps, focusing on temporally and fiscally efficient drafting, review, and production. We adhered to the general structure of these recommendations, as outlined below.

GIS Parameters. We used ArcGIS to co-register and analyze available datasets. Vector linework was digitally streamed at a constant scale of 1:125K (25% of the publication map scale), which is sufficiently detailed for both hard-copy and digital map publications. Linework was streamed directly into a GIS database in Polar Stereographic projection using a digital mapping tablet. Vertices were placed every 125 meters (1 vertex per 1 mm at 1:125K digitizing map scale) and attributes were assigned using an attribute domain stored within the geodatabase. Geologic map symbols were derived from FGDC Digital Cartographic Standards for Geologic Map Symbolization and adapted where necessary to convey the geologic information unique to the quadrangle. Contact linework was cleaned, smoothed, and used to build unit polygons. Subsequent editorial iterations of the digitized linework allowed for refinement of contact placement and unit descriptions based on cross-comparison between the map base and supplemental data sets.

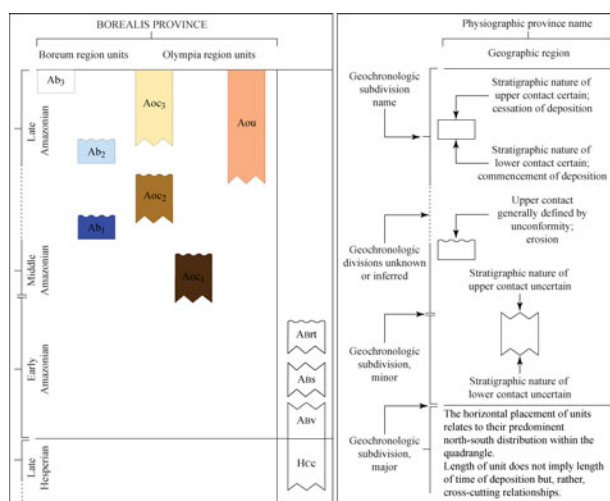


Figure 1. COMU organization, reference units, and key.

Base Maps. The primary base map for this geologic map was a Viking Orbiter mosaic constructed from frames acquired during the 1976 Martian northern summer (L_S from 133 to 135; 50 m/px). The original intent of the Viking base mosaic was to provide a time-controlled view of the polar ice during its presumed minimal extent and with the absence of obscuring seasonal frost [5]. However, to include the topographic detail afforded by MOLA, we overlaid the Viking mosaic with the MOLA polar DEM (115 m/px). Unit delineation and description was explicitly tied to the blended base map due to its near-complete areal coverage of the selected quadrangle (~0.4° latitude of data non-existent for MOLA at the northern boundary of the map region due to orbit of Mars Global Surveyor).

Supplemental Data. Base map linework was refined by integrating other data sets, including MOLA-derived products (cell-to-cell slope, aspect, and color-shaded relief maps) and the full range of THEMIS, MOC, HiRISE, and CTX images via web-linked image footprints. The areal discontinuity of high resolution data sets along with the scale of geologic detail (compared to published map scale) reduced their utility to an important, but supplemental, role in geologic mapping. High-resolution data sets were strategically and selectively employed to delineate and define geologic units and assess stratigraphic relationships. Their use was limited to those instances where critical geologic characteristics were consistently observable despite incomplete spatial coverage.

Unit Names and Symbols. We named geologic units with non-morphologic, non-genetic terms and grouped these into two regions. The “Boreum region units” are

those that comprise the polar flats and troughs of Planum Boreum, generally located north of the Olympia Rupēs (3 units). The “Olympia region units” are those that occur within and adjacent to the Olympia region of Mars, generally located south of the Olympia Rupēs (4 units). Unit names reflect their geographic occurrence as well as their stratigraphic relationship to one another. Unit symbols identify (1) the chronologic period (**A**=Amazonian period), (2) the geographic region unit (**o**=the Olympia region), (3) physiographic feature name where more than one geologic unit occurs in a region (**c**=Olympia Cavi), and (4) the interpreted stratigraphic sequence (1=the first of two or more related geologic units). Therein, the geologic symbol “**Aoc₁**” refers to the Amazonian-age, stratigraphically-lowest unit that occurs within and/or adjacent to Olympia Cavi. This scheme differs from that applied by [6] due to a lack of global physiographic province in MTM 85200.

Description of Map Units (DOMU). We compiled unit descriptions in tabulated format, adhering to the recent guidelines [4]. Unit groupings, appearance, and stratigraphic relationships were determined based primarily on their appearance in the base map, which provided the most consistent areal extent and resolution; supplemental data sets provided unit characteristics where they were consistently observed and critical to the interpretation (see above sections). The tabulated description of map units uses bulleted “primary” and “supplemental” characteristics, which are consistently listed for each unit. Supplemental characteristics include high resolution image numbers for reference. In addition, we included an “other names” field that listed alternative published names for mapped units (or variants thereof) located both within and outside of the quadrangle boundary [7]. We also produced a classical, prose-based DOMU, which included equivalent information.

Correlation of Map Units (COMU). The paucity of impact craters within the map area precluded the confident assignment of stratigraphic divisions using crater statistics. As such, epochs were assigned based on the contextual work of previous publications [6-10]. Units were organized within the COMU based on their occurrence and distribution within each region. For reference and textual clarity, we included reference units from past work as well as a “key.” The latter provided a guide to the visual depiction of stratigraphic relationships between units mapped within the quadrangle. We also compiled a table showing relative ages, areas, and superposition relationships.

Figures. We used three figures to summarize the contextual geologic and stratigraphic information. One figure showed regional topography of the map region via a MOLA color shaded relief image, which included IAU-approved nomenclature. In addition, two figures were constructed from CTX image excerpts that showed key

unit outcrops and stratigraphic relationships. The figures are annotated with geologic contacts and figure locations and extents are shown on the map. We submitted multiple annotated figures based on excerpted high resolution images that we suggest be published solely as digital supplements. The intent was to minimize map size as well as production costs by supplementing the map with figures deemed important but not necessarily critical to the conveyance of map information. Supplemental figures are referenced as such within the geologic map text.

Conclusions: Digital data volumes and mapping environments allow for the characterization of geologic units and relationships well below the limitations of the expected publication scale of geologic maps. A balanced mix of scale-based observations and succinct descriptions is critical for the efficient production of geologic maps. From a tactical standpoint, we conclude:

- Consistent use of a map scale and digitizing parameters provides a documentable means for delineating and describing geologic materials and relationships using several, overlapping, multi-scale data sets.
- Map scale necessitates a conscious division between primary and supplemental data sets. The volume, type, resolution, and areal diversity of available data necessitate thoughtful preference and down-selection so that maps are completed in a timely manner.
- The naming and symbolizing of geologic units is scale dependent and is assisted by including physiographic province and region.
- Including reference units (from previous map publications) and a “key” in the COMU diminishes the need for equivalent explanation in the geologic map text.
- Annotated figures showing key outcrops and unit relationships are critical to conveying the map information. Digital supplements assist with limiting text size.
- DOMU tabulation is an extremely helpful way to collate and efficiently present unit characteristics from both primary and supplemental data sets.
- Geologic mapping strategies require continued optimization so that best practices are employed for the production of clear, consistent geologic map information.

References: [1] Skinner and Herkenhoff, Geologic Map of the Olympia Cavi region of Mars, 1:500K scale (in review). [2] Skinner and Herkenhoff (2007) *PGM 2007 abstract volume*. [3] Skinner and Herkenhoff (2006) *PGM 2006 abstract volume*. [4] Tanaka *et al.* (2009) Plan. Geo. Map. Handbook, *PGM 2009 abstract volume*. [5] Herkenhoff (2003) *USGS I-2753*, 1:500K scale. [6] Tanaka *et al.* (2005) *USGS SIM 2888*, 1:15M scale. [7] Tanaka *et al.* (2008) *Icarus* 196, 318-358. [8] Blasius *et al.* (1982) *Icarus* 50, 140-160. [9] Herkenhoff and Plaut (2000) *Icarus* 144, 243-253. [10] Tanaka (2005) *Nature* 437, 991-994.

GEOLOGY OF THE TERRA CIMMERIA-UTOPIA PLANITIA HIGHLAND LOWLAND TRANSITIONAL ZONE: FINAL TECHNICAL APPROACH AND SCIENTIFIC RESULTS. J. A. Skinner, Jr. and K. L. Tanaka, Astrogeology Science Center, U. S. Geological Survey, 2255 N. Gemini Drive, Flagstaff, AZ 86001 (jskinner@usgs.gov).

Introduction: The southern Utopia highland-lowland transitional zone extends from northern Terra Cimmeria to southern Utopia Planitia and contains broad, bench-like platforms with depressions, pitted cones, tholi, and lobate flows [1-2]. The locally-occurring geologic units and landforms contrast other transitional regions and record a spatially partitioned geologic history [2-5]. We systematically delineated and described the geologic units and landforms of the southern Utopia-Cimmeria highland-lowland transitional zone for the production of a 1:1,000,000-scale geologic map (MTMs 10237, 15237, 20237, 10242, 15242, 20242, 10247, 15247, and 20247). Herein, we present technical and scientific results of this mapping project.

Technical Approach: Below are the tactics and strategies that we employed during construction and presentation of this geologic map.

Mapping Methods. Unit delineation and description was based primarily on a USGS-produced THEMIS daytime IR mosaic (100 m/px). Versions of the map base-derived contacts and units were refined through comparison with MOLA-derived products as well as the full range of THEMIS VIS, CTX, MOC, and HiRISE images via web-linked image footprints. This iterative approach provided an important step in refining the location and description of geologic units as well as their lateral spatial and temporal relationships. Despite the use of supplemental data sets, the overall fidelity of the linework was held to those required by map scale (vertex spacing of 250 meters).

Unit Names and Symbols. We generally adhere to the recommendations outlined in the 2009 Geologic Mapping Handbook [6]. We developed unit names that reflect spatial occurrence within three physiographic provinces (Utopia, Nepenthes, and Cimmeria) as a means to avoid the stratigraphic inspecificity of using morphology as primary unit descriptors [7]. Unit symbols identify (1) the chronologic period (**AH**=Amazonian/Hesperian period), (2) the physiographic province (**N**=Nepenthes province), (3) the geographic region (**np**=Nepenthes Planum region), and (4) the interpreted stratigraphic order (₁=the first of two or more related geologic units). Therein, the geologic symbol "**AHnp₁**" refers to the Amazonian/Hesperian-age, stratigraphically lowest unit that occurs within and (or) adjacent to Nepenthes Planum, which is located within the Nepenthes province of the highland-lowland transitional zone. Deviations from the scheme presented herein are likely to be incorpo-

rated during final editorial stages and (or) based on map reviews.

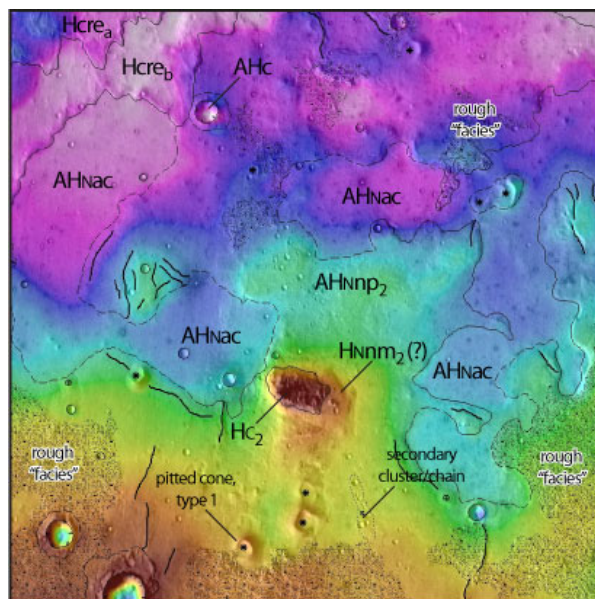


Figure 1. Excerpt of geologic map showing key units and geomorphic features. A “rough facies” surface of the Nepenthes Planum 2 unit (**AHnp₂**) is shown by stipple pattern. Frame is approximately 100 km on each side and centered at 16.52°N, 111.87°E. MOLA DEM overlain on THEMIS base.

Geomorphic Features. We mapped a variety of geomorphic features, including two types of pitted cones, very small tholi, ridges (with terminal truncations), narrow ridges, flow fronts, radially grooved ejecta, shallow linear depressions, fractures, exposed crater rims, buried/degraded crater rims, scarps, raised rims of impact craters ($1 \leq D < 5$ km), secondary crater clusters, and rugged surfaces (applied only to a single geologic unit) (**Fig. 1**). Inclusion of these features provided an opportunity to give local geologic information without adding additional units. Symbols adhere to the Federal Geographic Data Committee recommendations for planetary features [e.g., 6].

Stratigraphic relationships. Similar to past geologic maps, regional cross-cutting relationships show that geologic units become progressively younger at lower elevations [1,8]. Map-based temporal relationships were iteratively merged and refined with crater counts using all craters ≥ 1 km diameter. Crater statistics are ongoing and will be reported as cumulative size-frequency values for diameters of 1, 2, 5, and 16 kilometers.

Figures and Tables. In order to streamline the compilation, review, and production of planetary maps, recent guidelines emphasize the need for reducing (where possible) text and figures [6]. For critical geologic context, we included three figures that we recommend for inclusion on the map sheet (MOLA topography with nomenclature, annotated lowland boundary margin, and annotated pitted cones and mounds). Map area and surrounding regional context will be provided in the pamphlet figure. We are also in the process of compiling supplemental figures that we recommend be included in the digital product only (type locality panels for geologic units and landform features). Tables include a description of map units, stratigraphic relationships, and cumulative crater counts.

Science Results: The goal of this project was to clarify the geologic evolution of the Terra Cimmeria-Utopia Planitia highland-lowland transitional zone by identifying the geologic, structural, and stratigraphic relationships of surface materials. Below are key topical results regarding this evolution.

Lowland margin. The northern part of the map area is defined by the Utopia Planitia marginal unit (**AHum**), which forms a planar to slightly undulating surface. The unit's margin consists of overlapping, south-facing lobes that commonly ramp onto (or terminate against) small knobs and plateaus that are tens of meters high [1-3]. Arcuate ridges and pitted cones dominate the surface of the unit within 50 km north of its margin. Ridges are nested and roughly parallel the marginal lobes. The lobe-forming margin is consistently traceable for >2800 kilometers [1-2]. We interpret the Utopia Planitia marginal unit as a Late Hesperian/Early Amazonian sedimentary sequence perhaps formed as mass flows or quiescent subaqueous (submarine?) deposition [3]. We interpret the characteristic "ridge and cone" morphology of the unit as landforms formed by the shoaling of a mass flow unit during emplacement or as secondary landforms related to seismically-induced liquefaction [3]. Alternatively, the features may represent moraine-like landforms related to de-volatilization and marginal retreat of the unit [9].

Lobate materials. We mapped three types of lobate materials within the central part of the map area [4]. The Nepenthes Mensae 3 unit (**AHnp₃**) contains south-facing bright lobes that occur between knobs and plateaus of Nepenthes Mensae. Shadows and onlap relationships suggest these are <10 meters thick. The Nepenthes Planum 2 unit (**AHnp₂**) contains rugged and smooth lobes that complexly overlap one another. Locally, these are >100 meters thick and emanate from pitted cones and tholi. The Amenthes Cavi unit (**AHnac**) consists of smooth materials that form within cavi floors and are sourced from narrow (<500-

meter-wide) fractures that ring individual cavi. We interpret these units as Hesperian to Amazonian-age materials that were emplaced through various flow-related processes, likely associated with the mobilization and release of subsurface volatiles [3].

Crater facies. Because impact cratering appears to be a fundamental aspect of the regional geologic history, we subdivide crater units into facies, using the approaches employed in pre-Apollo lunar geologic maps [e.g., 10]. We use an undivided unit (**AHc**) for impact craters with rim diameters ≥ 3 and < 15 km throughout the map region. Noachian craters in this diameter range are heavily-eroded and are identified by line symbol only. There are 21 impact craters with rims ≥ 15 , which are generally considered "complex" impact craters [11]. Of these, 12 craters have mappable facies, including distal ejecta, proximal ejecta, rim, wall, floor, and peak materials. The remaining 9 complex craters are eroded and identified either as rim material or by symbol. Crater material for impacts with rim diameters < 3 km are not mapped as separate geologic units.

Summary: Geologic mapping has largely been completed and map components are currently undergoing technical and scientific edits. These efforts have resulted in advances that we hope will further the consistent production and use of geologic maps not only as tools for future research but also as high quality stand-alone scientific products. In an effort to streamline the geologic map text and minimize the more interpretive preferences of the map-based scientific study, we are scheduled to submit two peer reviewed articles in tandem with the geologic map. These will focus on the geologic and stratigraphic characteristics of (1) the Utopia Planitia marginal unit [3] and (2) the Nepenthes Planum Formation [2,4]. These articles will provide a formal mechanism for referencing key topical components of the geologic evolution without burdening the geologic map text [6]. We expect the map edits and supportive products to be completed by August 2010 and the map package to be submitted for formal review by October 2010.

References. [1] Tanaka et al. (2005), *USGS SIM* 2888, 1:15M scale. [2] Skinner et al. (2007), *Icarus*, 186, 41-59. [3] Skinner et al. (2008), *39th LPSC*, abstract #2418. [4] Skinner et al. (2009), *40th LPSC*, abstract #2459. [5] Skinner and Mazzini (2009), *Marine Pet. Geo.*, 26, 1866-1878. [6] Tanaka et al. (2009), *Plan. Geo. Map. Handbook, PGM 2009 abstract volume*. [7] Tanaka et al. (2010), *this volume*. [8] Scott et al. (1986-87), *USGS I-1802A-C*, 1:15M scale. [9] Grizzaffi and Schultz (1989), *Icarus*, 77, 358-381. [10] Schmidt et al. (1967), *USGS I-515*, 1:1M scale. [11] Melosh (1989), *Impact Cratering: A Geologic Process*, Oxford University Press.

GEOLOGY OF LIBYA MONTES AND THE INTERBASIN PLAINS OF NORTHERN TYRRHENA TERRA, MARS: FIRST YEAR RESULTS AND SECOND YEAR WORK PLAN. J.A. Skinner, Jr.¹, A.D. Rogers², and K.D. Seelos³, ¹Astrogeology Science Center, U.S. Geological Survey, 2255 N. Gemini Drive, Flagstaff, AZ 86001 (jskinner@usgs.gov); ²Stony Brook University, 255 Earth and Space Science Building, Stony Brook, NY 11794; ³Johns Hopkins Applied Physics Laboratory, MP3-E140, 11100 Johns Hopkins Road, Laurel, MD 20723.

Introduction: The Libya Montes-Tyrrhena Terra highland-lowland transitional zone of Mars is a complex tectonic and erosional region that contains some of the oldest exposed materials on the Martian surface [1-3] as well as aqueous mineral signatures that may be potential chemical artifacts of early highland formational processes [4-5]. Our 1:1M scale mapping project includes the geologic materials and landforms contained within MTMs 00282, -05282, -10282, 00277, -05277, and -10277, which cover the highland portion of the transitional zone. The map region extends from the Libya Montes southward into Tyrrhena Terra and to the northern rim of Hellas basin and includes volcanic rocks of Syrtis Major Planum and a broad low-lying plain (palus) that forms a topographic divide between Isidis and Hellas basins. The objective of this project is to describe the geologic history of regional massif and plains materials by combining geomorphological and compositional mapping observations. This abstract summarizes the technical approaches and interim scientific results of Year 1 efforts and the expected work plan for Year 2 efforts.

Data Sets and Methods: We are following the mapping recommendations outlined in the 2009 Geologic Mappers Handbook [6] as well as approaches used in recent and ongoing geologic maps [7-9] to iteratively produce and refine the geologic map using primary and supplemental data sets. The primary geomorphologic base map is a THEMIS daytime IR mosaic (100 m/px). Compositional information is critical to the objectives of this project and regional THEMIS DCS images (100 m/px) and CRISM summary parameters (231 m/px) are considered primary products wherein geologic units are being delineated and defined. Supplemental data sets include MOLA topography (and derivative products) as well as the full range of THEMIS VIS, CTX, MOC, and HiRISE images via web-linked image footprints. Compositional characterizations will be supplemented by local TES and CRISM hyperspectral observations.

Year 1 Results: The Year 1 work plan consisted of managerial aspects, geologic mapping, feature mapping (including impact craters), nomenclature reviews, and exploratory mapping for Year 2.

Project management. Year 1 efforts included managerial steps that addressed technical/scientific and organizational/financial aspects. We established guiding parameters in order to produce geologic linework of

consistent fidelity (*e.g.*, vertex spacing and digital map scale), identified the role of specific data (*e.g.*, primary

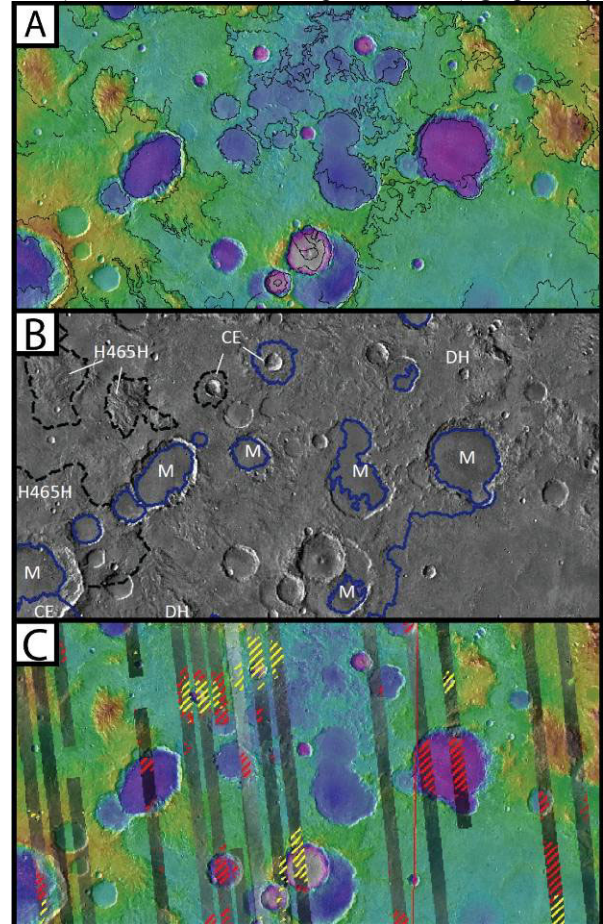


Figure 1. Excerpts from center two quads showing Year 1 geomorphologic and compositional map results. (A) Massif, intermediate, and low-lying geomorphic and stratigraphic units. (B) THEMIS IR-based mafic plains ("M"), pyroxene-depleted impact materials ("CE"), high-silica highlands ("H465H"), and undivided highlands ("DH"). (C) CRISM-based summary parameters showing olivine- and phyllosilicate-bearing units (red and yellow, respectively). Panels are approximately 400 kilometers wide.

versus supplemental), and produced and packaged the necessary data sets within a dedicated GIS. A project GIS DVD containing primary base maps and relevant supplemental data sets was compiled and distributed to team members in March 2009. CTX images, THEMIS DCS mosaics, and CRISM summary parameters were subsequently added to the project GIS and will be up-

dated as necessary. In addition, we acquired the requisite agreements for conveyance of funds to cooperating institutions (Stony Brook and JHU-APL).

Geologic mapping. In order to identify the pervasively occurring geologic surfaces, onlap relationships, landforms, and units, we focused Year 1 geomorphologic and compositional mapping efforts on materials and landforms that occur within the center two quadrangles (**Fig. 1**). These quads were selected because they contain the three geologically, stratigraphically, and topographically distinct surfaces within the study region: high-standing massifs, intermediate elevation dissected plains, and low-lying plains.

Geomorphologic mapping resulted in the preliminary identification of six highland units, including a single “massif” unit, a single “intermediate plains” unit, three “low plains” units, and a channel unit (**Fig. 1A**). Of particular note, the currently identified “low plains” sequence appears to contain traceable topographic benches, which show some evidence of confinement to broad topographic warps as well as lateral thinning against older materials. Further mapping efforts and supportive topical research will investigate evidence for syntectonic deposition within the intermediate and low-lying plains. We also began mapping seven impact crater facies, in similar fashion to [8].

Compositional mapping resulted in the identification of multiple unique surfaces using both thermal and visible range spectral data sets. TES surface emissivity provided first-order spectral variability in the region, which was refined using morphology, thermophysical properties, and THEMIS DCS mosaics. These assessments led to the identification of five surface units: younger degraded plains, older degraded highlands, flat-floored craters with high thermal inertia fill, crater ejecta, and high-silica degraded highlands (**Fig. 1B**). CRISM-based summary parameters led to the identification of two pervasive surface units: an olivine-bearing unit (generally located in crater floors and low-lying plains) and a phyllosilicate-bearing unit (generally located in crater rims and ejecta deposits) (**Fig. 1C**). Generalized compositional mapping will segue into targeted spectral deconvolutions of “type surfaces” to provide key information for the delineation, description, and interpretation of geologic units.

Feature mapping. Feature mapping, including topographic features and tectonic structures, intentionally lags the identification of preliminary geologic units so as not to unnaturally bias unit delineation. The THEMIS daytime IR base map is particularly well suited to identifying geologic features at digital mapping scale (1:250,000). We began cursory examination of mappable features during unit mapping phases and noted those features that are likely to be delineated during Year 2 and 3 and incorporated into the final

map. In addition to the pervasively applied channel, ridge, and trough features, we are likely to map narrow grooves (associated with massifs), small tholi (located in low-lying plains), “albedo” boundaries (where not associated with geologic contacts), and secondary crater clusters (with parent crater, if identifiable [10]). We digitized impact craters ≥ 1 km in diameter using the USGS Crater Helper Tool, which will be used to compile crater-based relative age information and supplement map-based cross-cutting observations.

Nomenclature. The use of approved nomenclature is critical for geologic mapping because it allows succinct identification and description of units and features. Though we identified several surface features that may require a formal name (including the palus features located between large massifs), we did not submit any formal nomenclature requests during Year 1.

Exploratory mapping. We began preliminary geomorphologic mapping of the northern two quadrangles, extending the units delineated in the center two quads where possible. Where the units were sufficiently varied between quads, we noted the key variations and subdivided geologic units. Later stages of mapping are likely to result in the grouping of similar units, particularly where stratigraphic evidence is sparse. Key differences in single units will be identified in the description of map units.

Year 2 Work Plan: The second year of the project is underway and closely follows Year 1 scientific mapping tasks. The Year 2 efforts include the following:

- Collating geomorphologic and compositional line-work into a master project GIS for re-distribution
- Continuing geologic unit mapping efforts, including TES and CRISM/OMEGA spectral deconvolutions for unit type localities
- Tabulating preliminary description of map units, to include primary and supplemental characteristics as well as unit type locality figures
- Mapping of geologic features located within all six quadrangles and begin compiling feature descriptions and type locality figures
- Refining the crater data set and begin first-order crater statistics for preliminary units, as necessary
- Drafting a letter-sized manuscript describing the key units and their geomorphologic and compositional characteristics as well as their implied evolution

References: [1] Greeley and Guest (1987), *USGS I-1802-B*, 1:15M scale. [2] Crumpler and Tanaka (2003), *JGR*, 98. [3] Tanaka et al. (2005), *USGS SIM 2888*, 1:15M scale. [4] Bibring et al. (2005), *Science*, 307. [5] Bishop et al. (2007), *7th Int. Conf. Mars*, #3294. [6] Tanaka et al. (2009), *Plan. Geo. Map. Handbook, PGM 2009 abstract volume*. [7] Skinner and Herkenhoff (2010), *this volume*. [8] Skinner and Tanaka (2010), *this volume*. [9] Tanaka et al. (2010), *this volume*. [10] Nava et al. (2010), *40th LPSC*, abstract #2530.

MARS GLOBAL GEOLOGIC MAPPING PROGRESS AND SUGGESTED GEOGRAPHIC-BASED HIERARCHICAL SYSTEMS FOR UNIT GROUPING AND NAMING. K.L. Tanaka¹, J.M. Dohm², R. Irwin³, E.J. Kolb⁴, J.A. Skinner, Jr.¹, and T.M. Hare¹, ¹U.S. Geological Survey, Flagstaff, AZ, ktanaka@usgs.gov, ²U. Arizona, Tucson, AZ, ³Planetary Science Inst., Tucson, AZ, ⁴Google, Inc., CA.

Introduction: We are in the fourth year of a five-year effort to map the global geology of Mars at 1:20M scale using mainly Mars Global Surveyor, Mars Express, and Mars Odyssey image and altimetry datasets. Previously, we reported on details of project management, mapping datasets (local and regional), initial and anticipated mapping approaches, and tactics of map unit delineation and description [1-2]. Last year, we described mapping and unit delineation results thus far, a new unit identified in the northern plains, and remaining steps to complete the map [3].

Progress: This past year, mapping of much of the highlands, northern plains, and polar regions have been completed in preliminary form, including linework, unit naming, and definition (including type localities). However, considerable mapping remains for Tharsis and parts of the highlands. For map-unit dating, we have shown with the help of Stephanie Werner (U. Oslo) how some of the units in the northern plains appear to be regionally time-transgressive [4]. In addition, Werner and Tanaka are preparing a paper addressing how to more precisely tie crater size-frequency distributions to the Martian epochs [5] for both Hartmann and Neukum crater production functions [6]. This paper will make age assignments for Mars a bit more clear, although the great disparity between the Hartmann and Neukum distributions continues to be problematic.

Unit-group naming scheme: Various systems of unit groupings and hierarchies appear in geologic maps of Mars. In comparing Mars maps, as shown in Table 1, we find a disparity in the terminology used, which leads to ambiguity and confusion [7-12].

For example, the Viking-based global geologic map of Mars [7] and the post-Viking map of the northern plains region [8] are both widely referenced and show why the current approaches need clearer definition. The highest unit rank in [7] includes “lowland terrain, highland terrain, and north and south polar region units,” as well as “materials occurring throughout map area.” The second order groups include various assemblages and a “channel-system and eolian materials” grouping. The third level includes formations, materials, units, deposits, a plateau sequence, and a paterae category. In turn, formations are divided into members, and polar deposits are subdivided. In the case of [8], the regional designations are all named “provinces,” and all map units are designated “units,” including those that would be included at both the formation and member levels.

Other Mars maps add further labels used in unit rankings, such as “material(s)” and “deposits” for the

second rank in Table 1 [e.g., 9-11]. Additional designations are used that reflect lithotype for third- and fourth-rank names, such as “ejecta” [12].

Terrestrial lithostratigraphic unit rankings of higher orders as shown in Table 1 are constructed where the stratigraphic sequences are defined and varied for a considerable period in a particular regional setting. If the basic unit, the formation, is closely related to one or more other formations, they may be assigned to a group. A supergroup may arise from a collection of groups and individual formations. For example, the Precambrian Grand Canyon Supergroup in Arizona includes the Unkar and Chuar Groups along with the Nankowap and Sixtymile Formations. In turn, the supergroup is overlain by another 16 formations that occur in the Grand Canyon, several of which comprise the Tonto and Supai Groups [13]. Thus, not every formation belongs to a group or a supergroup and not every group belongs to a supergroup. Also, formations may or may not include members and other subunits.

In similar fashion, the grouping of units on Mars and other planetary surfaces should be performed judiciously; this includes not grouping units (and groups of lower order) in cases where geologic, morphologic, and/or geographic associations with other units appear to be weak, coincidental, or non-existent. In other words, one should place a unit into a group (or group into a higher order group) only when there is a clear fit. In addition, a unit may be located within a particular geographic zone or province but may be so geologically distinct from the other units in the group that it should be excluded.

Given this understanding that not all units need to be included in a hierarchy, we suggest the following scheme based primarily on geographic and geomorphic associations, as summarized in Table 1. (1) The first geographic level is the “zone,” which is the broadest grouping used in global mapping. These may include for Mars highland, lowland, transition (highland/lowland boundary), polar, basin, rise (volcanic), and ubiquitous (including scattered craters and volcanoes, etc.) zones. (2) The second level—provinces—would include subdivisions of the zones, such as individual plains, poles, basins, and rises. These would use applicable geographic names (e.g., Amazonis, Tharsis, and Borealis provinces, as used in [8]). (3) The third-level rank would consist of a geographic locality. (4, 5) The fourth and fifth levels would each include either a geographic feature or stratigraphic position.

Unit naming scheme: Scale is a major factor in how units are identified and named. Thus, unit names should be approached consistently with the scale-dependent rankings in Table 1. Based on this premise, we make the following recommendations for global, regional, and local unit names (see Table 2 for examples):

Global units (<1:15M scale): In previous global maps, unit names either have [7] or have not [14] included geographic features. The inclusion of units based on local features greatly increases the number of map units and thus complicates the map. For our global map, we are using the simpler approach in which unit names and symbols consist of the unit's zone and either or both a morphologic (or other) identifier, and a stratigraphic position [3]. Given our preliminary mapping results, we anticipate that we will complete our global map of Mars at 1:20M scale with ~40 map units [3].

Regional units (1:2M to 1:15M): These follow largely the scheme used in [8]. The units are grouped into provinces and named for a related or nearby geographic locality and optionally a definitive feature type or stratigraphic position. The unit names do not include province names, but the province is indicated by a small-cap letter.

Local units (>1:2M): These are similar to regional units but ignore the province designation, because the majority of units occur within a province and thus can be ignored (with the exception of maps that straddle province boundaries, which would require the use of province designators in unit symbols).

Regional- and local-scale maps might include some units of higher order, such as global-scale units, when such are not subdivided.

Remaining work for the map product: We anticipate completing our Mars global geologic map for review by the Fall of 2011, which includes following the latest submission guidelines and, for the GIS product, organizing mapping layers and creating metadata [15].

References: [1] Tanaka K.L. et al. (2007) *7th Intl. Conf. Mars* Abs. #3143. [2] Tanaka K.L. et al. (2008) *LPSC XXXIX*, Abs. #2130. [3] Tanaka K.L. et al. (2010) in Bleamaster et al. (eds.), *Abs. Ann Mtg. Planet Geol. Mappers, San Antonio, TX, 2009, NASA/CP—2010-216680*, p. 41-42. [4] Werner S.C. et al. (submitted) *Planet. Space Sci.* [5] Tanaka K.L. (1986) *JGR 91, suppl.*, E139-158. [6] Hartmann W.K., and Neukum G. (2001) *Space Sci. Rev.*, 96, 165-194. [7] Scott D.H. et al. (1986-87) *USGS Maps I-1802A-C*. [8] Tanaka K.L. et al. (2005) *USGS SIM-2888*. [9] Chapman M.G. and Tanaka K.L. (1993) *USGS Map I-2294*. [10] Chuang F.C. and Crown D.A. (2009) *USGS SIM-3079*. [11] Dohm J.M. et al. (2001) *USGS Map I-2650*. [12] McGill G.E. (2005) *USGS Map I-2811*. [13] Beus S.S. and Morales M. (1990) *Grand Canyon Geology*, Oxford U. Press, NY. [14] Scott D.H. and Carr M.H. (1978) *USGS Map I-1803*. [15] Tanaka K.L. et al. (2010) in Bleamaster et al. (eds.), *Abs. Ann Mtg. Planet Geol. Mappers, San Antonio, TX, 2009, NASA/CP—2010-216680, Appendix*, 21 p. [16] The North American Commission on Stratigraphic Nomenclature (2005) *Amer. Assoc. Petrol. Geol. Bull.*, 89, 1547-1591.

Table 1. Categories and ranks of terrestrial lithostratigraphic units and of Mars map units until now as well as proposed herein.

Lithostratigraphic [16]	Mars maps [e.g., 7-12]	Proposed here (example(s))
Supergroup	Terrain, Region	Zone (lowland zone)
Group	Assemblage, System, Province, Material(s), Deposits	Province (Borealis province)
Formation	Formation, Unit, Material, Deposits, Other	Locality (Planum Boreum)
Member (or Lens, or Tongue)	Member, Unit, Deposits	Feature/Position (bright, ridged/1, 2)
Bed(s) or Flow(s)		Feature/Position (layered/1, 2 or a, b)

Table 2. Proposed unit naming schemes for geologic maps of Mars at various scales.

Map scale	Unit name scheme (unit name examples)
Global, <1:15M	Zone and feature ¹ and/or position ¹ (polar dune unit, basin 4 unit, transition knobby 2 unit)
Regional, 1:2M-1:15M	Province ² , locality, and feature ¹ or position ¹ (Simud Valles unit, Planum Boreum cavi unit, Planum Boreum 1 unit)
Local, >1:2M	Locality, primary ¹ and secondary ¹ feature or position feature/position (Olympia Undae unit, Scandia Colles 2 unit, Amazonis Planitia 1 flow unit, Alba Mons 3b unit)

¹If needed.

²Highest rank noted; in unit symbol but not in unit name.

PROGRESS IN THE SCANDIA REGION GEOLOGIC MAP OF MARS. K. L. Tanaka¹, J. A. P. Rodriguez², C. M. Fortezzo¹, R. K. Hayward¹, and J. A. Skinner, Jr.¹ ¹U. S. Geological Survey, Flagstaff, AZ 86001 (ktanaka@usgs.gov), ²Planetary Science Institute, Tucson, AZ (alexis@psi.edu).

Introduction: We are in the second year of a four-year project to produce a geologic map of the Scandia region of Mars at 1:3,000,000 scale for publication in the USGS Scientific Investigations Map series. The primary objective of the map is to analyze and reconstruct the resurfacing history of this region in much greater detail than achieved by the previous northern plains-wide mapping effort [1-2]. This region includes (1) a broad swath of the Vastitas Borealis plains that includes various Scandia landforms and the Phoenix lander site; (2) part of the margin of the north polar plateau, Planum Boreum; and (3) the northern margin of the immense Alba Mons volcanic shield. We rely mostly on Mars Orbiter Laser Altimeter (MOLA) digital elevation models, Thermal Emission Imaging Spectrometer infrared and visual range, and Context Camera images for mapping and topographic analysis.

Background: Resurfacing within the study region is thought to have involved collapse, erosion, mud volcanism, and sedimentary diapirism of fluvial-lacustrine deposits originating from outflow-channel discharges from the Martian highlands into the northern plains [1-2]. Landforms interpreted as having resulted from these processes include Scandia Colles (knobs), Tholi (low rounded plateaus), and Cavi (broad, irregular depressions surrounded by rises). Furthermore, basal materials exposed along the margin of Planum Boreum may source from eroded Scandia materials [3].

Mapping results: Thus far, 20 geologic units mapped include: Alba Mons shield lavas and channelized flows, Vastitas Borealis plains materials, (3) Scandia materials, Planum Boreum rupēs and layered deposit units [4-5], circum-polar dune material, and crater units (Fig. 1). The crater densities for older units register Hesperian surface ages (Table 1).

Table 1. Cumulative densities of craters* for Scandia region units (from [1, 6]).

Unit	N(2)	N(5)
northern Alba Mons	332±23	78±11
Vastitas Borealis	273±10	74±5
Scandia region	336±51	122±31
Planum Boreum rupēs	476±107	148±58

*N(X) = no. craters > X km diameter per 10⁶ km².

We are mapping a variety of structures and landforms. Linear features include classes of ridges, most of which form the wrinkle ridges of Arcadia Dorsa, which become more subdued toward lower elevation parts of the Scandia region. Another set of subtle, linear ridges

trend N in the SE corner of the map region. Some ridges trend down slope and may be degraded flows. Narrow grabens trending NNE make up Alba and Tantalus Fossae and dissect NE Alba Mons. North-facing scarps of irregular form generally trend E-W across the middle of the map, defining a low topographic scarp along which the Scandia Colles knob field occurs. The Phoenix lander site is just below this scarp. North of the scarp, the plains are marked variously by ridges, mesas, and irregularly shaped, nested depressions. The two lowest parts of the northern plains occur immediately south of Planum Boreum. The western part includes the broad, circular domes of Scandia Tholi and the irregular depressions surrounded by rises that form Scandia Cavi. The eastern low is partly included along the NE margin of the map region and includes the conical features known as Abalos Colles. Each of these low regions includes plains that are cut by networks of troughs that bound polygons several to ~20 km across.

We also have mapped all 17,472 knobs in the region that can be defined by at least two enclosed 20-m-interval elevation contours. They are distributed throughout the map region and are particularly concentrated in Scandia Colles, Tholi, and Cavi and around Milankovič and Korolev craters. Impact crater morphologic types and significant albedo boundaries, including one locally defining the boundary of Vastitas Borealis units, are also being mapped.

Formational hypotheses: Geologic mapping provides a basis to assess the spatial, temporal, and geologic relationships that enable creation and testing of hypothetical reconstructions of the process history and events that shaped the landscape. Based on our initial mapping results for the Scandia region, we are formulating working hypotheses that may account for the major aspects of geologic activity recorded during the Hesperian for the map region. Here are a few intriguing hypotheses based on our preliminary observations that we plan to further develop and test (see also [7-8]):

(1) The major endogenic geologic materials, structures, and landforms of Hesperian age in the map region may have developed in an integrated, regional basin environment that includes the lowest part of the northern plains. The major components were: (a) Alba Mons magmatism, which drove tectonic deformation, heating, and hydrothermal groundwater circulation in the Scandia region; and (b) northern plains outflow-channel sediments that included an ice-rich, impermeable upper permafrost zone underlain by water-saturated material and

thus were subject to hydrogeologic, tectonic, and periglacial processes.

(2) Crustal rocks bounded by thrust faults underlying wrinkle ridges N and NW of Alba Mons could be zones of groundwater collection, aquifer development, and elevated fluid pore pressure (especially within topographically lower zones of aquifers) [9-10]. In addition, upward groundwater and ice flow may have been enhanced along such buried faults. Such flow could have led to diapirism and the formation of cavi and tholi, especially with the development of superlithostatic fluid pore pressure and/or intense seismic shaking associated with large impact events. Buried salt deposits might also participate in similar activity [cf. 11].

(3) NE of Alba Mons, resurfacing was relatively moderate and may relate to a cluster of grabens that cut the shield. The grabens may define a zone of enhanced crustal cooling due to heat dispersion through hydrothermal convection along deep-seated fractures, resulting in downward propagation of a cooling front. As a result, thickening of the cryosphere along fractures underneath

this terrain could have reduced aquifer connectivity and hydraulic head.

Knobs, pedestal craters, albedo variations, and mantles in the map region record additional aspects of the geologic history that remain poorly understood, but we are studying them [e.g., 7-8]. As with the other features in our study, we will consider how they fit into the regional geologic context.

References: [1] Tanaka K.L. et al. (2005) *USGS SIM-2888*. [2] Tanaka K.L. et al. (2003) *JGR*, 108, 8043. [3] Tanaka K.L. (2005) *Nature*, 437, 991-994. [4] Tanaka K.L. et al. (2008) *Icarus*, 196, 318-358. [5] Putzig N.E. et al. (2009) *Icarus*, 204, 443-457. [6] Tanaka K.L. and Fortezzo C.M., map in review. [7] Rodriguez J.A.P. and Tanaka K.L., (2010) *LPSC* 41, #2387. [8] Skinner J.A. Jr. and Tanaka K.L., (2010) *LPSC* 41, #2734. [9] Rodriguez J.A.P. et al. (2007) *Icarus*, 191, 545-567. [10] Skinner J.A. Jr. and Mazzini A. (2009) *Marine Petrol. Geol.*, 26, 1866-1878. [11] Adams J.B. et al. (2009) *Geology*, 37, 691-694.

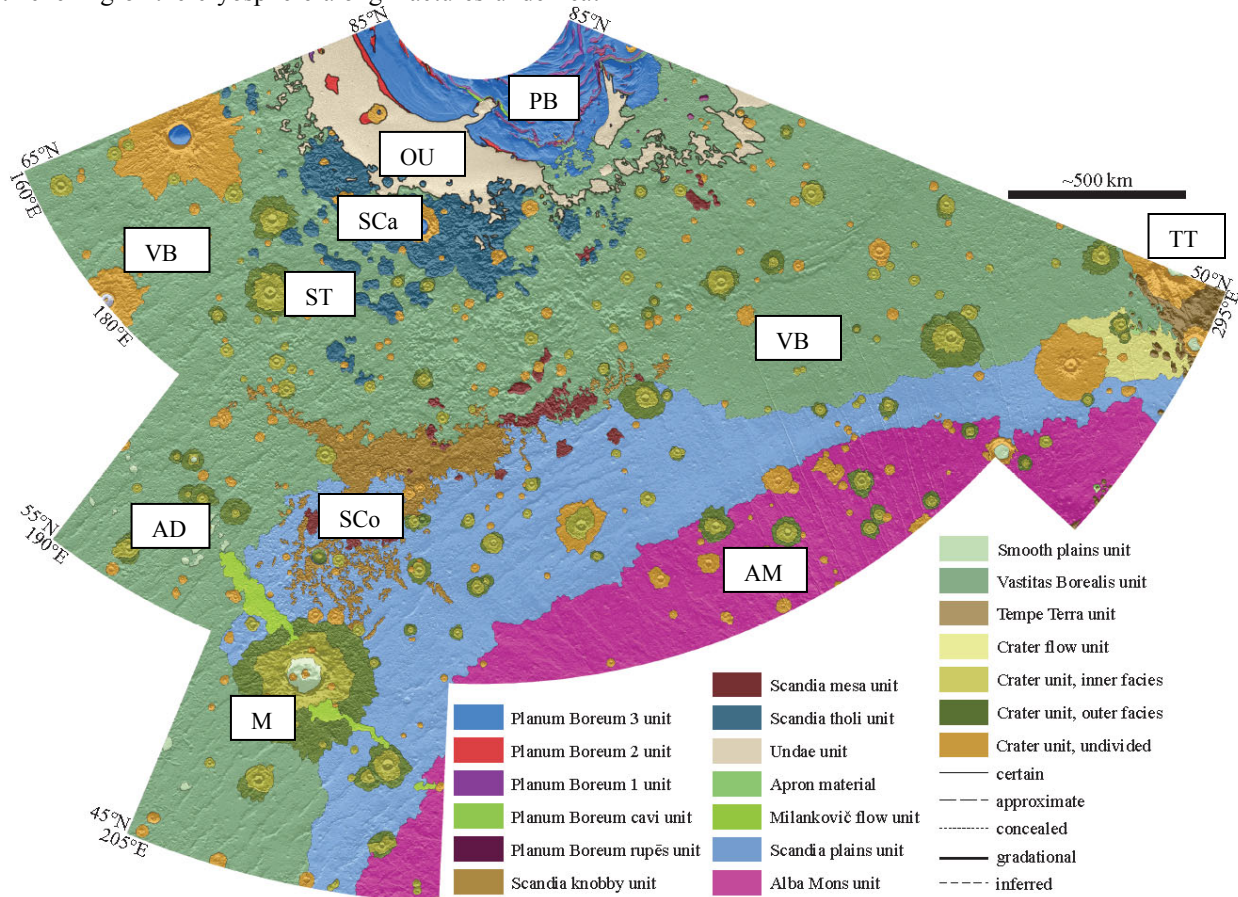


Fig 1. Preliminary geologic map of the Scandia region of Mars showing map units and contact types. Background image is MOLA shaded relief view in Polar Stereographic projection (45-85° N., 160-295° E.); scale varies with latitude. AM=Alba Mons, SCa=Scandia Cavi, ST=Scandia Tholi, SCo=Scandia Colles, M=Milanković crater, VB=Vastitas Borealis, PB=Planum Boreum, OU=Olympia Undae, TT=Tempe Terra, AD=Arcadia Dorsa.

Introduction: Geomorphic mapping at 1:500,000 scale within three quadrangles in Margaritifer Terra, Mars, is nearing completion (Fig. 1) [e.g., 1 – 4]. This region was previously studied [5-9] because of the combination of geomorphic processes that have shaped its surface, and the current mapping has revealed details that were not visible in Viking Orbiter images used by those previous studies. The large Uzboi-Holden-Ladon-Margaritifer megaoutflow system has shaped the western part of Margaritifer Terra (Fig. 1), and flow in the Samara and Paraná-Loire valley systems merged with UHLM in MTM -15022 [3]. The area in MTMs -20022 and -20017 has also been shaped by many impact craters, including an outer ring of Ladon basin and the relatively young Jones crater. Fluvial erosion associated with Loire Valles and Samara Valles and their tributaries has influenced much of the surface, and many areas are covered by resurfacing deposits (possibly fluvial, volcanic, and/or aeolian).

MTMs -20022 and -20017 include Jones crater, the confluence of Himera Valles and Samara Valles, and a significant portion of Loire Valles (Fig. 1). One of the main objectives of this mapping is to determine the relative timing of fluvial activity and impact cratering, specifically the impact that created Jones.

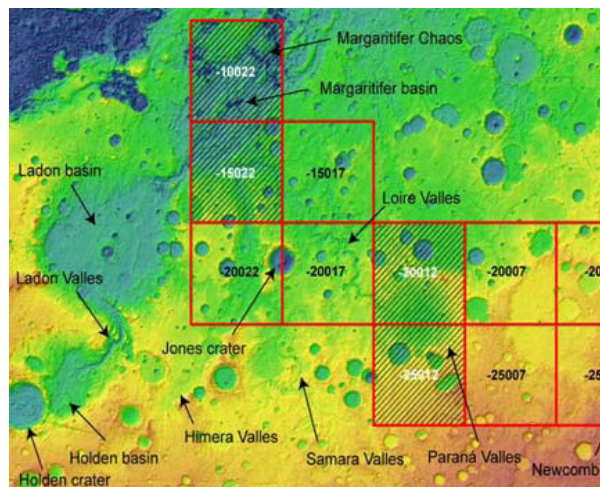


Fig. 1. Areas within Margaritifer Terra mapped at 1:500K shown on the 128 pixel/degree MOLA topography. The shaded red boxes are areas whose maps are in revision and second submission. The open red boxes are those currently being mapped. MTM quadrangles -20022 and -20017 (the focus of this abstract) are in the center of the figure.

Methods: Geomorphic mapping utilized ESRI's ArcMap GIS software to register Viking, THEMIS IR and VIS, HiRISE, and CTX images as well as MOLA topography. Together, these data sets allowed for the delineation of geomorphic contacts and structures. Standard crater counting techniques were also used to estimate ages of the surfaces.



Fig. 2. THEMIS daytime IR image I23141002. Image is ~30 km across. [NASA/JPL/ASU]

Summary of Observations: The area to the southwest and southeast of Jones crater was not well imaged by Viking; however, much better resolution images now provide the detail needed to address the history of geomorphic processes affecting the area. Figure 2 shows a reach of Loire Valles in which there is now an impact crater. There is some evidence that this crater might have occurred while fluvial processes were still active in Loire.

The relative timing of fluvial activity in Samara Valles is also of interest. Figure 3 shows a portion of Samara Valles almost directly south of Jones crater. The effects of ejecta from Jones can be seen in the top of the image, but it appears as though fluvial erosion within Samara may have continued after the impact that created Jones. Other images west of Jones suggest that fluvial activity in Samara did cut through ejecta from Jones. Today, much of Samara Valles is filled by aeolian deposits, but details shown in the images are allowing the geomorphic history to be unraveled.

In addition to erosion, several resurfacing deposits have been mapped in this area. At least one of the resurfacing units embays portions of Loire, helping to determine the relative timing of fluvial activity in the three main valleys in this area

References: [1] Grant J. A. and D. A. Clark (2002) *Planetary Mappers Meeting*, Tempe, AZ. [2] Williams K. K. et al. (2005) *LPS XXXVI*, Abstract #1439. [3] Williams K. K. and J. A. Grant (2007) submitted map, USGS. [4] Fortezzo C. M. et al. (2008) *LPS XXXIX*, Abstract #2244. [5] Saunders S. R. (1979) *USGS I-1144*, USGS. [6] Parker T. J. (1985) Masters Thesis, CA State Univ., L.A. [7] Parker T. J. (1994) Ph.D. Thesis, USC, L.A. [8] Grant J. A. (2000) *Geology*, 28, 223. [9] Grant J. A. and T. J. Parker (2002) *JGR*, 107(E9), 5066.

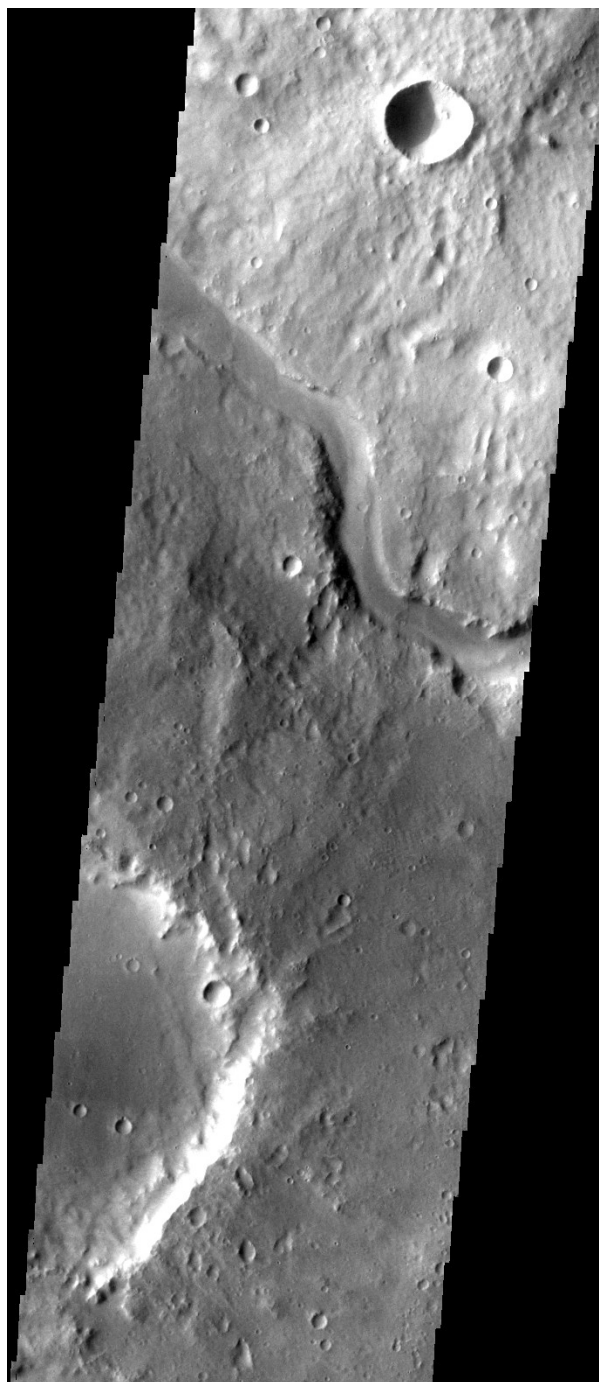
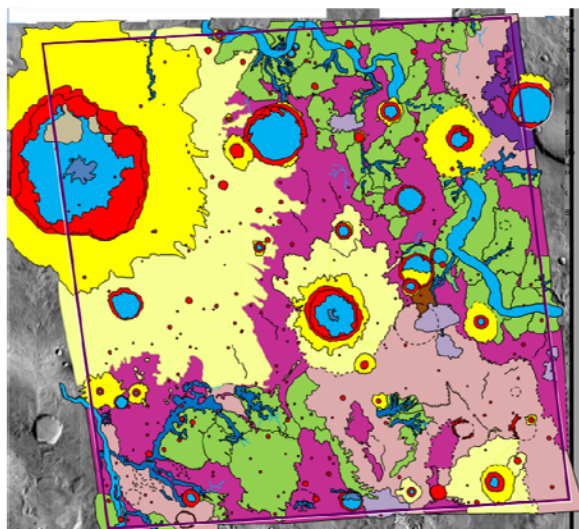


Fig. 3. THEMIS Visible image (V27147006) showing a portion of Samara Valles directly south of Jones crater. Image is ~35 km across. [NASA/JPL/ASU]

Fig. 4. Preliminary geomorphic map of MTM -20017 to the southeast of Jones crater. Shades of purple are resurfacing units, and the lighter purple unit is younger than the darker purple unit. Fluvially etched terrain (green) is younger than the resurfacing units.

Introduction: This report summarizes the status of mapping projects supported by NASA grant NNX07AP42G, through the Planetary Geology and Geophysics (PGG) program. The PGG grant is focused on 1:2M-scale mapping of portions of the Medusae Fossae Formation (MFF) on Mars. Also described below is the current status of two Venus geologic maps, generated under an earlier PGG mapping grant.

Medusae Fossae Formation, Mars: Work on mapping of the heavily eroded western portions of MFF continues to progress, only hampered by the PI's learning about ArcGIS. Attributes of MFF as documented in Mars Orbiter Camera images were used in a reevaluation of the numerous hypotheses about the origin of MFF, with the conclusion that an ignimbrite origin is most consistent with observations [1]. Yardangs are abundant within an intensely eroded component of the lower member of MFF (which we label as unit Aml₂), and they provide insights into the friable nature of Aml₂ [2], as evidenced by differences in competency resulting from erosion and mass wasting, a result that appears to be most consistent with variable degrees of welding often present within volcanic (ignimbrite) deposits [1]. A preliminary geologic map of the MC-23 NW quadrangle (Fig. 1) covers the southwestern margin of the globally mapped large

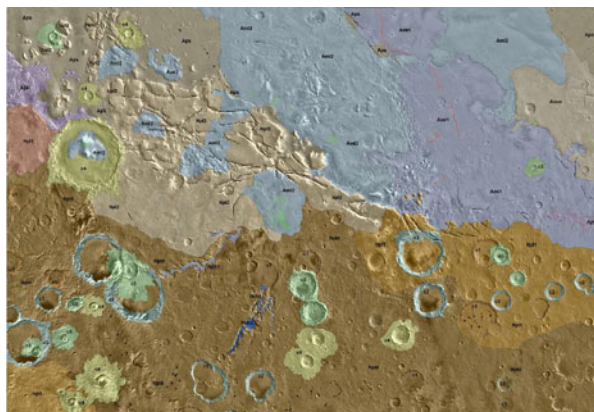


Figure 1. 2009 version of the MC-23 NW geologic map (MFF are the blue, violet, and light tan units).

exposures of MFF [3]. Mapping has revealed several outliers interpreted to be isolated remnants of Aml₂ (Fig. 2), suggesting that the previous extent of MFF materials may have been much larger than what is expressed by the present-day MFF exposures [4].

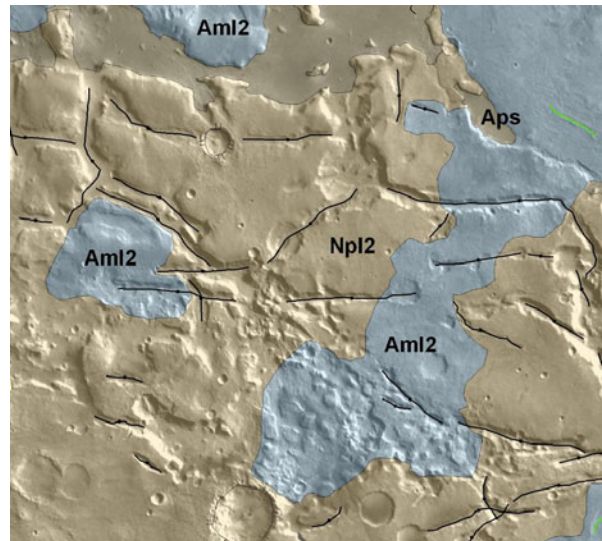


Figure 2. Detail of MC-23 NW map (center-left of Fig. 1) showing outliers of Aml₂ materials, located south and west of broad Aml₂ exposures.

A distinctive feature thus far restricted to the westernmost MFF exposures is the occurrence of sinuous positive-relief ridges [5], which in MC-23 NW are restricted to the topographically lowest portions of Aml₁, what we interpret to be the lowest stratigraphic component of global unit Aml [2; Aml is described in 3]. These sinuous ridges are interpreted to be inverted paleochannels [5, 6] which may represent prolonged flow of a liquid coincident with the emplacement of the stratigraphically lowest component of MFF [2, 5, 6].

Since early 2009, the PI has been learning to use ArcGIS software, obtained through a licensing agreement with the Smithsonian Institution. The learning curve for ArcGIS continues to be very steep, and after a full year the PI is still getting familiar with the intricacies of the software. Unfortunately, at the 2009 mappers meeting, the PI learned that all ArcGIS mapping he had done to date was incorrect, and he is still in the process of trying to get polygons and line attributes all sorted out. The map of MC-23 NW is the first geologic map that will be produced by the PI using ArcGIS, and thus it remains a work in progress at present. The unit contact locations are likely to not change by much, but the symbology and the contact attributes for this map are not yet in USGS format, as of the time of this writing.

Mapping of MC-16 NW (Fig. 3) has barely begun, but it is already clear that this map will provide some



Figure 3. MDIM base map for MC-16 NW.

important new insights into both the lower and middle members of MFF [3]. To illustrate some of the stratigraphic relationships evident here, it is apparent that the global units will be able to be divided into multiple subunits, based on distinctive levels expressed in the erosion of the MFF materials (Fig. 4). Results from

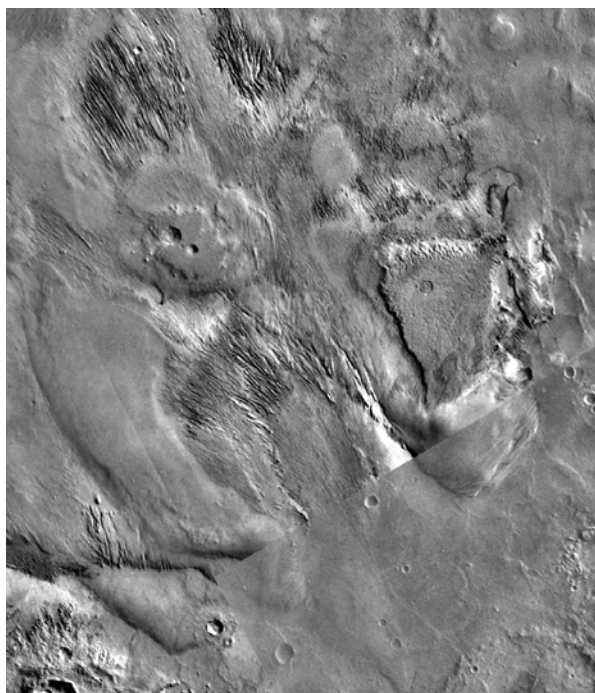


Figure 4. Detail of cliff-forming subunits within MFF (from center-left of Fig. 3).

MC-16 NW are expected to provide valuable new insights into both the emplacement and the erosional characteristics of all three of the globally mapped members of MFF. When mapping of both MC-23 NW and MC-16 NW is successfully completed using ArcGIS, the PI will work on producing an ArcGIS ver-

sion of a geologic map for MC-8 SE, using an earlier (Illustrator 9) mapping product [7] as a guide to the newly mapped geology.

Northern Lowland Plains, Venus: The map and text for the Kawelu Planitia quadrangle (V-16) have been in review with the USGS for many years [8]. A revised version, addressing all reviewer comments, was submitted to the USGS in 2008, at which time it became apparent that the linework (which dated from mapping carried out on unstable hardcopy base materials) was not uniformly registered to the digital photobase that is the current standard for production of published maps. Careful review of all of the linework revealed that no single shift or warp could correct the situation, due to map revisions that were made at different times to various sections of the map. During 2009, all of the V-16 linework was manually adjusted to register with the digital photobase, through the helpful assistance of NASM volunteers. We have not yet regenerated the unit polygons in Adobe Illustrator 9, the software used to make the current version of the map, but we hope to do so later this year. Once the adjusted linework is reconstituted into a map registered to the digital base, V-16 should be able to continue through the revision process. The Bellona Fossae quadrangle (V-15) was mapped preliminarily several years ago [9] under a previous PGG grant, also initiated on hardcopy base materials like V-16. When the V-16 map is finally through review, we will redo the V-15 geology in ArcGIS, using the prior map as a guide while generating the new linework in ArcGIS.

Future Plans: Plans for a no-cost extension of funding include submission of the MC-23 NW map to the USGS and preparation of a preliminary map for MC-16 NW, followed by production of revised versions of the geologic maps for MC-8 SE and V-15 using ArcGIS.

References: [1] Mandt, K.E., et al. (2008) JGR-Planets, 113, E12011, doi: 10.1029/2008JE003076. [2] Zimbelman, J.R., and Griffin, L.J. (2010) Icarus, doi: 10.1016/j.icarus.2009.04.003. [3] Greeley, R., and Guest, J.E. (1987) USGS Misc. Invest. Series Map I-1802-B. [4] Zimbelman, J.R., et al. (2009) Geol. Soc. Am. Abs. Prog. 95-1. [5] Burr, D.M., et al. (2009) Icarus 200, 52-76, doi: 10.1016/j.icarus.2008.10.014. [6] Williams, R.M.E., et al. (2009) Geomorphology, doi: 10.1016/j.geomorph.2008.12.015. [7] Zimbelman, J.R. (2007) NASA Mappers mtg, ZIMBELMANa2007PGM.PDF. [8] Zimbelman, J.R. (2007) NASA Mappers mtg, ZIMBELMANb2007PGM.PDF. [9] Zimbelman, J.R. (2004) NASA Mappers mtg, ZIMBELMAN2004PGM.PDF.

VOLCANISM ON IO: RESULTS FROM GLOBAL GEOLOGIC MAPPING. D.A. Williams¹, L.P. Keszthelyi², D.A. Crown³, P.E. Geissler², P.M. Schenk⁴, Jessica Yff², W.L. Jaeger². ¹School of Earth & Space Exploration, Arizona State University, Tempe, Arizona 85287 (David.Williams@asu.edu); ²Astrogeology Science Center, U.S. Geological Survey, Flagstaff, Arizona; ³Planetary Science Institute, Tucson, Arizona; ⁴Lunar and Planetary Institute, Houston, Texas.

Introduction: We have completed a new 1:15,000,000 global geologic map of Jupiter's volcanic moon, Io, based on a set of 1 km/pixel combined *Galileo-Voyager* mosaics produced by the U.S. Geological Survey [1]. The map was produced over the last three years using ArcGIS™ software, and has undergone peer-review. Here we report some of the key results from our global mapping efforts, and how these results relate to questions regarding the volcano-tectonic evolution of Io.

Previous Work: Previously we reported our techniques for global mapping of Io [2] and on the development of an Io database [3] that will include most Io data sets to address the surface changes due to Io's active volcanism. Previously we also reported the percentage of Io covered by each of 14 process-related geologic material units and structures [4], and last year we presented a stratigraphic correlation of these map units [5]. Here we report results from visual, graphic, and statistical analyses of the map units and structures and discuss insights into the formation of plains, lava flow fields, paterae, mountains, and diffuse deposits.

Results I (Plains): Plains units cover 66.6% of the surface, and (with the exception of a few outliers) are geographically distributed on Io. Red-brown plains dominantly occur $>\pm 30^\circ$ latitude, and are thought to result from enhanced radiation-induced alteration of other plains units. White plains (typically enriched in SO₂) occur mostly in the equatorial antijovian region ($\pm 30^\circ$, 90° - 230° W), possibly indicative of a regionally colder part of the satellite to preserve the SO₂. Why is this one region colder such that SO₂ concentrates here? The answer may be related to variations in crustal distribution of magma sources or delivery mechanisms, or perhaps crustal thickness, relative to other parts of Io. Outliers of white, bright, and red-brown plains occurring in other regions likely result from long-term accumulation of white, yellow, and red diffuse deposits, respectively.

Results II (Lava Flows): Lava flows cover 27.8% of the surface, the bulk of which (20.6%) are undivided flows whose original composition (dark silicate or bright sulfur) cannot be determined. Bright flow fields outnumber dark flow fields by a ratio of ~ 1.5 to 1; both of these are presumed to be the freshest and youngest lava flow types on Io. Only 16.8% of the bright flow fields are adjacent to dark flow fields. The association of adjacent bright and dark flows would be

expected if sulfur flows are derived from secondary sulfur volcanism (i.e., melting of sulfur-rich country rock by heat from silicate magmas or lavas [6].) Thus, this result suggests that secondary sulfur volcanism may only have a minor role in Io's current volcanic activity (although there may be a scale-dependence on these processes that requires further investigation). There is an unusual concentration of bright flows at $\sim 45^\circ$ - 75° N, ~ 60 - 120° W, perhaps indicative of past, extensive primary sulfur volcanism in this region. However, this stands in stark contrast to the current correlation of active hot spots with surface materials, in which only 1.7% of hot spots correlate with bright flows, suggesting that at present primary sulfur volcanism has a minor role in Io's current activity. 20.3% of hot spots detected by telescopic and spacecraft observations correlate with dark flow fields and another 9.3% correlate with undivided flow fields. Thus, lava flows make up less than one-third of Io's heat sources.

Results III (Paterae): Paterae are circular to irregular volcano-tectonic depressions on Io, thought to be similar to terrestrial calderas [7]. Evidence suggests some of these contain periodically foundering lava lakes [8], whereas others are resurfaced by bright or dark lava flows. We have mapped a total of 425 paterae on Io, an increase from the 417 previously identified by [7]. Yet even though paterae cover only 2.5% of Io's surface (and dark patera floor material covers only 0.5%), Io's hot spots dominantly occur within paterae (63.9% of all hot spots, with 45.3% correlated with dark patera floor material). The fact that 93.5% of Ionian hot spots correlate with either dark (younger) or undivided (older) patera floors or lava flows suggests that silicate materials are the dominant component of Io's recent volcanism.

Results IV (Mountains): Mountains cover only 3.1% of Io's surface, yet are some of the most dramatic features observed in spacecraft images. A majority of Io's mountains, 37.9%, were mapped as undivided mountain materials, in contrast to mapping 27.1% as Lineated mountains, 22.1% as Layered plains, 3.6% as Tholi (volcanic mountains), and 2.9% as Mottled mountains. These results demonstrate that variable imaging coverage of Io's mountains inhibits more accurate mapping of undivided mountains into the other units. As expected, lineated mountains, thought to be tectonically uplifted crustal blocks [9], are generally taller than the more degraded mottled

mountains and layered plains. Volcanic tholi are less than 2km tall, indicative of mafic to ultramafic materials that tend not to build tall volcanic edifices. We are working on additional correlations, including the locations and areas of mountains with heights and image resolution, to further identify relationships that can provide insights on the genesis of these features.

Results V (Diffuse Deposits): Diffuse deposits (DD) that mantle the other units cover ~18.2% of Io's surface, and are distributed as follows: red (47.2% of all DD), white (37.9%), yellow (11.5%), black (3.3%), and green (~0.1%). Red DD are thought to be derived by condensation of S₂ gas and recrystallization to short-chain sulfur (S₃-S₄ ± chlorides) from volcanic vents. These are dominated by ring-like units resulting from outbursts, except for that found surrounding volcanoes such as Pele that are continuously replenished by ongoing activity. White DD, mostly irregular in shape and often surrounding lava flow boundaries, result from vaporization, condensation, and reaccumu-

lation of SO₂ frosts around warm flow margins. The relative lack of pyroclast-bearing DD, i.e., dark (black) DD (thought to be derived from silicate pyroclasts) and yellow DD (thought to be derived from sulfur pyroclasts) compared to gas-derived White and Red DD (14.8% vs. 85.1%) may suggest that sulfur and SO₂ do not have a major role as volatiles that disrupt or interact with sulfur or silicate magmas.

References: [1] Becker, T. and P. Geissler (2005), *LPS XXXVI*, Abstract #1862. [2] Williams, D.A. et al. (2007), *Icarus*, 186, 204-217. [3] Rathbun, J.A. and S.E. Barrett (2007), *LPS XXXVIII*, Abstract #2123. [4] Williams, D.A. et al. (2008), *LPS XXXIX*, Abstract #1003. [5] Williams, D.A. et al. (2009), *LPS XL*, Abstract #1403. [6] Greeley, R., et al. (1984), *Icarus* 60, 189-199. [7] Radebaugh, J., et al. (2001), *JGR* 106, E12, 33,005-33,020. [8] Lopes, R.M.C., et al. (2004), *Icarus* 169, 140-174. [9] Schenk, P. and Bulmer, M. (1998), *Science*, 279, 1514-1517.

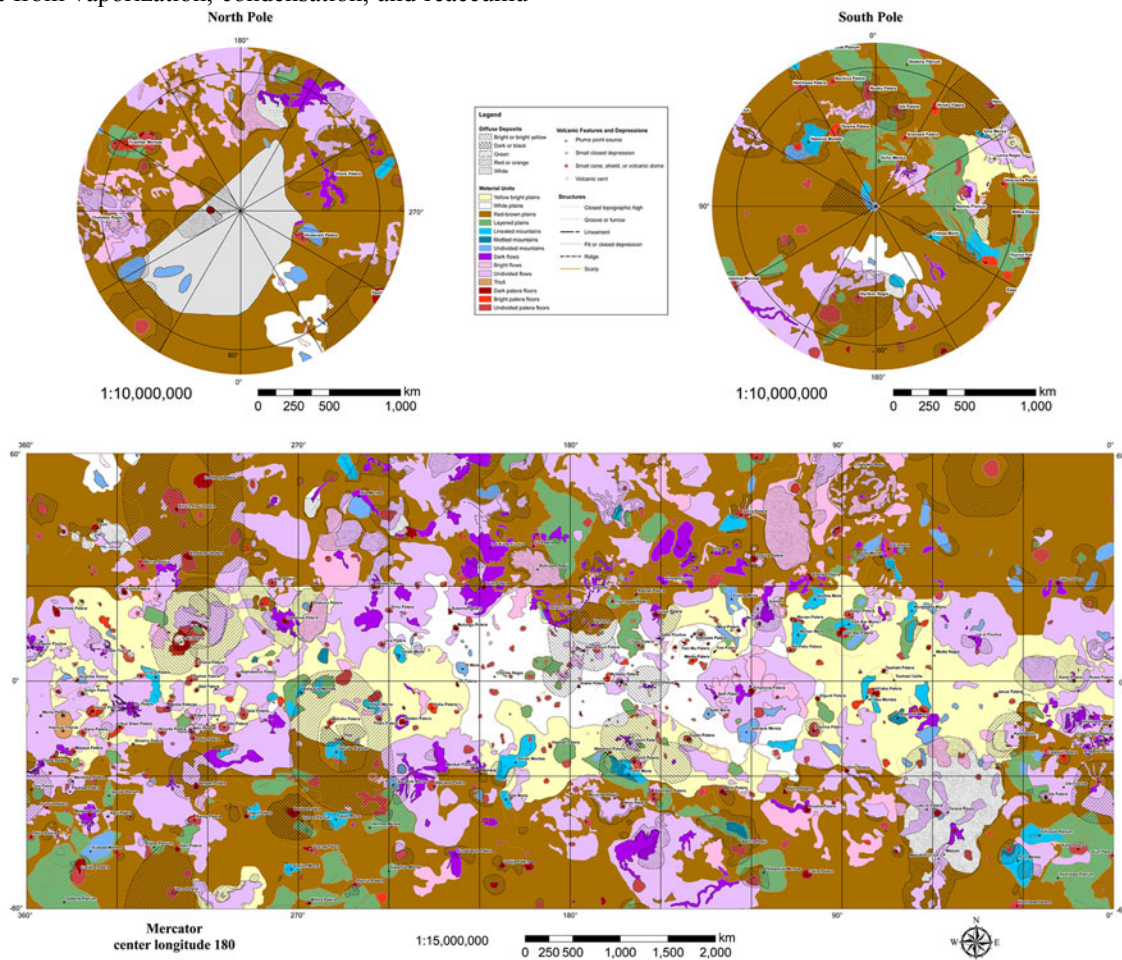


Figure 1. The global geologic map of Io, produced using ArcGIS™ software based on the combined *Galileo-Voyager* mosaics produced by the U.S. Geological Survey [1]. For additional information on mapping strategy, areal coverage of map units, and stratigraphic correlation of map units, see [2, 4, 5].

EMPLOYING GEODATABASES FOR PLANETARY MAPPING CONDUCT – REQUIREMENTS, CONCEPTS AND SOLUTIONS. S. van Gasselt¹ and A. Nass², ¹Freie Universität Berlin, Institute of Geological Sciences, Malteserstrasse 74-100, D-12249 Berlin, Germany (Stephan.vanGasselt@fu-berlin.de); ²German Aerospace Center (DLR), Institute of Planetary Research, Rutherfordstrasse 2, D-12489 Berlin, Germany (Andrea.Nass@dlr.de).

Introduction and Background: Planetary geologic mapping has become complex in terms of merging and co-registering a variety of different datasets for analysis and mapping. But it has also become more convenient when it comes to conducting actual (geoscientific) mapping with the help of desktop Geographic Information Systems (GIS). The complexity and variety of data, however, are major issues that need to be taken care of in order to provide mappers with a consistent and easy-to-use mapping basis. Furthermore, a high degree of functionality and interoperability of various commercial and open-source GIS and remote sensing applications allow mappers to organize map data, map components and attribute data in a more sophisticated and intuitional way when compared to workflows 15 years ago.

Integration of mapping results of different groups becomes an awkward task as each mapper follows his/her own style, especially if mapping conduct is not coordinated and organized programmatically. Problems of data homogenization start with various interpretations and implementations of planetary map projections and reference systems which form the core component of any mapping and analysis work. If the data basis is inconsistent, mapping results in terms of objects' georeference become hard to integrate.

Apart from data organization and referencing issues, which are important on the mapping as well as the data-processing side of every project, the organization of planetary geologic map units and attributes, as well as their representation within a common GIS environment, are key components that need to be taken care of in a consistent and persistent way.

Employing Geodatabases: Today, still very few organizations in the field of planetary mapping seem to employ object-relational geodatabase management systems (GDBMS) although such environments form the backbone of any GIS. ESRI's ArcGIS environment allows each user to create a local database stored directly as part of the computer's file system and managed by ArcGIS without having to set up a server-client-based database management system (DBMS). A file-based geodatabase (FGDB) is transportable (via Extensible Markup Language Metadata Interchange format; XMI) and can be easily migrated, and its layout can be modified and adapted to fit specific requirements. The FGDB layout (model schema) is easily transferable to a DBMS if there is a need to migrate

and set up a larger-scale environment or switch to other GIS applications. The reasons to switch to database-organization (either file-based or based on a server management system) for planetary mapping conduct are twofold. The first reason is concerned with data homogenization and integration as outlined above. The database model provides boundary constraints in terms of reference systems and map projection issues which control and safeguard the proper use of data (e.g., raster or feature datasets form containers with associated reference and map projection definitions to control individual feature class objects).

The second reason is concerned with attribute values for specific feature class objects (a map unit, a contact), feature datasets and relations. Once attributes for feature classes and additional relations are defined they can be imported and utilized without having to set up feature objects manually, thus avoiding inconsistencies. Secondly, once feature classes and relations are defined, they can interact by relationship classes and subtype-driven domain assignments which consequently allow the user to (a) query data in a limited (when FGDB-based) or highly sophisticated (when DBMS-based) way and (b) select only attribute values that are within a given domain and controlled by subtypes. This not only prevents erroneous entries but it also allows working much more efficiently, even collaboratively if required. Furthermore, a rich set of topology classes improves the quality and consistency of mapping work by, e.g., controlling different feature classes covering geologic and/or geomorphologic mapping units.

Key DB-Model Components: We will present the current status and key components of DB-model developments and focus on tasks dealing with (a) organizational and (b) geoscientific mapping issues. The geoscientific parts are covered by relations dealing with stratigraphic issues and surface-material assignments and relationships in the context of chronostratigraphy and model ages (including concepts on selection processes), integration of geologic and geomorphologic mapping units on different object levels and the possible organization and representation of cartographic symbologies beyond proprietary solutions. Additionally, we will discuss the implementation (and benefit) of topologic constraints and the migratability to DBMS and other GIS environments

Planetary Geologic Mapping Handbook – 2010

K.L. Tanaka, J.A. Skinner, Jr., and T.M. Hare
U.S. Geological Survey, Astrogeology Science Center
2255 N. Gemini Dr., Flagstaff, AZ 86001

Endorsed by:

The Geologic Mapping Subcommittee (GEMS) of the NASA Planetary
Cartography and Geologic Mapping Working Group (PCGMWG)
M.S. Kelley¹, L.F. Bleamaster III², D.A. Crown², L.R. Gaddis³, T.K.P. Gregg⁴,
J.R. Johnson³, S.C. Mest², and K.K. Williams⁵

¹NASA Headquarters, Washington, DC

²Planetary Science Institute, Tucson, AZ

³U.S. Geological Survey, Astrogeology Science Center, Flagstaff, AZ

⁴University at Buffalo, Buffalo, NY

⁵Buffalo State College, Buffalo, NY

TABLE OF CONTENTS

<i>What's New</i>	2
1. Introduction.....	2
2. Purpose of this handbook.....	3
3. Map processing	3
a. Proposals	3
b. Map base package	4
c. Digital mapping	5
d. Mappers meetings and GIS workshops.....	5
e. Submission and technical review	6
f. Map Coordinator review	6
g. Nomenclature review	6
h. USGS metadata preparation.....	7
i. USGS Publications Services Center (PSC) editing and production	7
j. Map printing and web posting	7
4. Map contents	8
a. Map sheet components.....	8
b. Text components	10
c. Digital data products	13
5. References	14
6. Useful web pages	15
7. Planetary geologic mapping support personnel	16
8. Abbreviations	16
9. Figures.....	17

WHAT'S NEW: This edition includes a link that provides a tutorial on adding text labels to maps using ArcGIS' annotation tool, which is useful for unit symbols and nomenclature. See sections 4a3 and 4b3c.

1. INTRODUCTION

Geologic maps present, in an historical context, fundamental syntheses of interpretations of the materials, landforms, structures, and processes that characterize planetary surfaces and shallow subsurfaces (e.g., Varnes, 1974). Such maps also provide a contextual framework for summarizing and evaluating thematic research for a given region or body. In planetary exploration, for example, geologic maps are used for specialized investigations such as targeting regions of interest for data collection and for characterizing sites for landed missions. Whereas most modern terrestrial geologic maps are constructed from regional views provided by remote sensing data and supplemented in detail by field-based observations and measurements, planetary maps have been largely based on analyses of orbital photography. For planetary bodies in particular, geologic maps commonly represent a snapshot of a surface, because they are based on available information at a time when new data are still being acquired. Thus the field of planetary geologic mapping has been evolving rapidly to embrace the use of new data and modern technology and to accommodate the growing needs of planetary exploration.

Planetary geologic maps have been published by the U.S. Geological Survey (USGS) since 1962 (Hackman, 1962). Over this time, numerous maps of several planetary bodies have been prepared at a variety of scales and projections using the best available image and topographic bases. Early geologic map bases commonly consisted of hand-mosaicked photographs or airbrushed shaded-relief views and geologic linework was manually drafted using mylar bases and ink drafting pens. Map publishing required a tedious process of scribing, color peel-coat preparation, typesetting, and photo-laboratory work. Beginning in the 1990s, inexpensive computing, display capability and user-friendly illustration software allowed maps to be drawn using digital tools rather than pen and ink, and mylar bases became obsolete.

Terrestrial geologic maps published by the USGS now are primarily digital products using geographic information system (GIS) software and file formats. GIS mapping tools permit easy spatial comparison, generation, importation, manipulation, and analysis of multiple raster image, gridded, and vector data sets. GIS software has also permitted the development of project-specific tools and the sharing of geospatial products among researchers. GIS approaches are now being used in planetary geologic mapping as well (e.g., Hare and others, 2009).

Guidelines or handbooks on techniques in planetary geologic mapping have been developed periodically (e.g., Wilhelms, 1972, 1990; Tanaka and others, 1994). As records of the heritage of mapping methods and data, these remain extremely useful guides. However, many of the fundamental aspects of earlier mapping handbooks have evolved significantly, and a comprehensive review of currently accepted mapping methodologies is now warranted. As documented in this handbook, such a review incorporates additional guidelines developed in recent years for planetary geologic mapping by the NASA Planetary Geology and Geophysics (PGG) Program's Planetary Cartography and Geologic Mapping Working Group's (PCGMWG) Geologic Mapping Subcommittee (GEMS) on the selection and use of map bases as well as map preparation, review, publication, and distribution. In light of the current boom in planetary exploration and the ongoing rapid evolution of available data for planetary mapping, this handbook is especially timely.

2. PURPOSE OF THIS HANDBOOK

The production of high-quality geologic maps is a complex process involving a wide range of data, software tools, technical procedures, mapping support specialists, review steps, and publication requirements. This handbook provides a comprehensive ‘how to’ mapping guide that covers each of these topics to clarify the process for map authors. This guide emphasizes the production of planetary geologic maps in a digital, GIS format, because this format is required by NASA PGG for maps beginning in (1) 2011 that are submitted for technical review and (2) 2013 that are finalized for publication. Because of continual changes in data availability and mapping techniques, it is understood that the geologic mapping process must remain flexible and adaptable within time and budgetary constraints. Users are advised to seek the latest edition of this handbook, which will be updated periodically as an appendix to the annual abstracts of the Planetary Geologic Mappers’ (PGM) meeting (downloadable at the [PGM web page](#); see below for a complete list of web links). Other updates, including recently published maps, will be posted on the USGS Astrogeology Science Center’s (ASC) PGM web page.

First, we describe the steps and methods of map proposal, creation, review, and production as illustrated in a series of flow charts (Figs. 1-4). Second, we include basic formatting guidelines for each map component. Third, we provide a list of web sites for useful information and download.

3. MAP PROCESSING

Planetary geologic maps as supported by NASA and published by USGS are currently released under the ‘USGS Scientific Investigations Maps’ (SIM) series. In this section, we summarize the process of completing USGS SIM series planetary geologic maps from proposal submission to publication (Figs. 1-4; note that the SIM series was formerly named Geologic Investigations Series and Miscellaneous Investigations Series and both used “I” for the series abbreviation for published maps; all I and SIM series share a common, progressive numbering scheme). These processing steps are subject to change as they are dictated in many cases by higher-level organizational policies, budget constraints, and other circumstances. Planetary geologic mapping support personnel are listed in Section 7; these are subject to change on an annual basis.

a. *Proposals.* Planetary geologic maps published by USGS have been sponsored largely by the NASA PGG program. Thus, maps submitted to USGS for publication must have been accepted under a NASA PGG grant (see the [NASA research opportunities web page](#)) and/or have the approval of the NASA PGG Discipline Scientist. Map publication and printing costs are covered by separate PGG funding and thus are not included in PGG research proposals. The proposal submission deadline is generally during the spring, and selections are usually announced by the following winter (depending on when funds can be released from NASA). Those considering proposing for a grant to perform planetary geologic mapping should visit the [USGS Planetary Geologic Mapping web page](#), where information on current mapping programs and projects, map preparation guidelines, and links to published maps can be found. While a variety of map areas, scales, and projections are potentially feasible for publication, some issues may make a conceived map untenable for publication (e.g., NASA PGG has a limited budget and multiple and oversized map sheets may be prohibitive in cost). Mappers are highly encouraged to contact

the [USGS Map Coordinator](#) (MC) regarding the maps to be proposed for prior to proposal submission to ensure that preparation of the desired map base and publication of the final product are feasible. (See table in Section 7 listing PGM personnel names and email addresses). Generally, proposals should address:

- 1) Digital production: Will the map be generated in GIS software compatible with ESRI's ArcGIS® software (the USGS standard)?
- 2) Map base: The proposal should include a description and justification of the desired map base that addresses the following questions: What data set is desired for the map base (which forms the map background) and are all the needed data released? Does USGS have the capability to generate the map base with available capability and resources? (Consult with the [USGS Map base Specialist](#) to find out.) What other data sets are desired and can they also be imported into the GIS geodatabase? Does the work plan allow for adequate time for USGS to construct the base (usually within 6 months after the USGS is notified by the [PGG Discipline Scientist](#) of the proposal's award), depending on complexity?
- 3) Map printing: At the proposed scale and projection, will the map be oversized (i.e., >40x56 inches)? Will multiple sheets be required for a given map area? (Consult with the [USGS Map Coordinator](#) for estimates of potential extra costs.) Proposer should be aware that increased complexity adds considerable time for preparation, review, and publication.
- 4) Map reviews: Proposers should be prepared to review two other planetary geologic maps for each intended map publication. It is appropriate to budget your time to review maps in each new mapping proposal that you submit.
- 5) Supplemental digital products: Digital map supplements may be proposed. These can include helpful figures and ancillary GIS raster and vector layers that can greatly enhance the map product but may not fit on the printed map.
- 6) Additional analyses and products: Detailed and interpretative analyses outside of the scope of the map product may be desired (for example, to test existing and construct new hypotheses, model observations, etc.), but these should be expressed as tasks independent of map generation (best suited for publication in science journals). Maps will no longer contain such material.
- 7) Attendance at mappers meetings: Proposal budgets must include funding for attendance at the annual Planetary Geologic Mappers' meetings and possible GIS workshops.

b. Map base package (Fig. 1). The map base forms the background image (usually in reduced contrast form) upon which the drafted geologic map units, symbols, and nomenclature are superposed. It is a geometrically controlled product that is the fundamental data set upon which map drafting is performed. In some cases, there are adequate data available from a particular data set, but the map base itself does not yet exist when the mapping proposal is submitted. Thus USGS must generate the map base. (In special cases, the proposer may construct the base, with advance permission from the [USGS Map Coordinator](#)). Sometimes, data gores can be filled in with other lower-quality yet useful data. Even if a desirable data set is released, there may be as-yet unresolved issues in radiometric and geometric processing and/or in data volume that prevent USGS from producing a map base with that particular data set. For example, the number and volume of images may be too large to generate a map base with available resources. Alternatively, such data may be readily viewable as individual frames by using image-location

footprints as GIS shapefiles having web links to data repositories. Other ancillary data in various forms may be provided at the request of the author if there is a demonstrated need for the data and if they can be readily integrated into a GIS geodatabase. The [USGS Map base Specialist](#) is tasked by PGG to produce the digital map base and ancillary data products and to satisfy reasonable and tractable mapping requests by map authors.

Typically, the USGS must generate several map base packages in a given year; these are generally compiled in order of increasing complexity and/or areal extent. Map bases for Venus quadrangles are usually the simplest and are thus generated first during each funding cycle. Map bases for Mars quadrangles may require mosaicking of many individual image frames that must be compared visually, stacked in order of quality, and then collectively processed for tone balance. More complex maps may require several months to complete after USGS is notified to produce them.

For GIS mapping projects, the [USGS GIS Project Specialist](#) generates a GIS map template after quality-checking and collating GIS data layers. The template includes map bases and a map-ready geodatabase with pre-populated symbols. These products are compiled and delivered using ESRI's ArcGIS® software. (USGS can import shapefiles produced from other software in some cases, but authors should consult with USGS GIS specialists *prior* to mapping to ensure that their map files will be usable.) In addition, a variety of GIS thematic maps can be downloaded and imported into the project, as well as other GIS tools, as administered by the [USGS GIS PIGWAD Specialist](#) (see [PIGWAD web site](#)). For Mars, Moon, and Venus maps, the mapping projects will include a stand-alone DVD volume (or equivalent compressed, digital file) of global datasets that can be incorporated into the project-specific GIS template.

c. *Digital mapping.* Mappers presently are mapping mostly in Adobe Illustrator or ArcGIS. For proper building of polygons in Illustrator layers, see the [help web site](#). For ArcGIS, contact and structure mapping is generally done first as polyline shapefiles. Vertex snapping is important for later generation of polygons. Point shapefiles can be used to indicate unit identification for each outcrop. At an advanced stage in mapping, the contacts can be cleaned, smoothed, and converted to polygons. We recommend that the final GIS linework have a vertex spacing of ~0.3 mm at map scale (equivalent to 300 m for a 1:1,000,000-scale map). We also recommend that a consistent scale is used to digitize linework, usually a factor of 2 to 5 larger than the published map to ensure adequate precision but not overkill (e.g., map at 1:200,000 to 1:500,000 for a 1:1,000,000 map). GIS tools can be applied to generalize and smooth linework to achieve the desired result, such as rounded corners. Also, outcrops should generally be at least 2 mm wide at map scale. Reasonably sized cutoffs should also be defined for line feature lengths (for example, 1 or 2 cm long at map scale). Point features can be used to show the distribution of important features such as craters and shields that are too small to map (their size ranges should be indicated). For clarity and completeness, we encourage the compilation and summary of digital mapping approaches and settings for inclusion in the map text.

d. *Mappers' meetings and GIS workshops.* These meetings are announced by the [GEMS Chair](#) and are also posted on the NASA Mars Exploration Program Analysis Group ([MEPAG](#)) [calendar web page](#) and the [Planetary Exploration Newsletter \(PEN\) calendar of events](#). While under active NASA mapping grants, mappers are expected to submit and present abstracts for the Annual Meeting of Planetary Geologic Mappers typically held in late June each year. Others are encouraged to attend as a means to benefit from various aspects of the program. At these

meetings, mappers demonstrate their progress and discuss mapping issues and results. Preliminary map compilations are also displayed and informally reviewed by other attendees during poster sessions. In addition, programmatic issues, mapping standards and guidelines, and related scientific issues are presented and discussed. Expert-led GIS workshops and/or geologic field trips to nearby localities of interest are commonly attached to the mappers' meeting. When possible, associated GIS workshops are held prior to or immediately following mappers' or other appropriate workshops (and occasionally as stand-alone meetings) throughout the year. These GIS workshops are customized to assist planetary geologic mappers in developing proficiency in GIS software and tools as applied toward planetary geologic maps published in the USGS SIM series. Abstracts and related reports are published in an abstract volume in either a USGS or NASA publication series, and they can be downloaded from the [USGS Planetary Geologic Mappers web page](#).

e. Submission and technical review (Fig. 2). Mappers are expected to prepare maps in accordance with guidelines herein (see Map Contents section below) as well as with those posted on the [USGS Planetary Geologic Mappers web page](#). Once the map is produced according to required guidelines, it is submitted in digital form to the [USGS Map Coordinator](#) (MC). The MC reviews the map submission for completeness. If the map is incomplete, the MC returns the map to the corresponding author for revision. If the map is complete, the MC assigns two reviewers, with the approval of the [GEMS Chair](#). The MC fills out an Information Product Review and Approval Sheet (IPRAS; Figure 5) in which all reviewers are listed. Both reviewers must approve (in rare cases, a third reviewer may be assigned to help resolve reviewer conflicts). Maps are returned to authors one or more times until review comments are adequately addressed as determined by the MC. The MC may adjudicate some issues that arise (for more challenging cases and in cases of potential conflict of interest, the MC consults with the GEMS Chair). Normally, initial map reviews are expected to be returned within 1 to 2 months and any additional reviews within 2 weeks.

f. Map Coordinator review (Fig. 3). Once the technical reviews are complete, the MC, with assistance from other USGS specialists as needed, performs a review that ensures that (1) the map conforms to the proper scale and projection, (2) final technical reviewer comments were adequately addressed, (3) map materials follow [PSC author submission checklist](#) guidelines, (4) map information conforms to established USGS and GEMS conventions, (5) nomenclature is sufficient, given what the map text discusses, and (6) stratigraphic inferences are properly conveyed and supported by observations. Map authors respond to the MC review comments and resubmit the map package. Name requests for mapped or referenced features are made by the author as needed using the [online form](#); these can be made anytime during the mapping process. New name proposals may take 4 to 8 weeks or longer for approval. Proposed names *may not be used* in publications until they have been approved by the International Astronomical Union.

g. Nomenclature review (Fig. 3). The [USGS Nomenclature Specialist](#) then reviews the map to assess whether the use of nomenclature accurately reflects the current terminology in the [IAU Gazetteer of Planetary Nomenclature](#). The map itself should have a nomenclature layer that presents all available formal names. Note that some exceptions to this naming requirement may apply in special situations; for example, overly small named features may exist only for a sub-

region of the map. (For a brief review of how IAU nomenclature is being managed and developed in the case of the Moon, see [Shevchenko and others \(2009\)](#)).

h. USGS metadata preparation (*GIS maps only; Fig. 3*). Metadata is the necessary ancillary documentation that describes each GIS layer in a geologic map, including rationale, authorship, attribute descriptions, spatial reference, and other pertinent information as required by the metadata standard. This information is archived as part of the map layer. The USGS GIS specialists will oversee metadata preparation and will tap authors for information when needed. Metadata for a map is comparable to the documentation required by NASA's Planetary Data System for digital planetary data, but it is created specifically for geospatial data sets. USGS GIS specialists will oversee incorporation of metadata for the mapped layers according to USGS publication standards and [Federal Geographic Data Standards](#) (FGDC). Metadata and readme files are required when the manuscript is submitted to PSC for publication. The [PSC Digital Map Editor](#) reviews general information (such as correct USGS contact information, information in appropriate fields, etc.).

i. USGS Publications Services Center (PSC) editing and production (*Fig. 3*). The [PGM Administrative Specialist](#) works with other USGS staff to ensure that the product is complete for PSC processing, and sends the product and review materials on CD or DVD and hardcopy form according to PSC guidelines (see [PSC author submission](#) and [Astrogeology submission checklist](#) web pages). PSC contacts the Map Coordinator and estimates costs for PSC editing and production and printing through a contractor selected by the Government Printing Office (GPO). Based on available funds for these costs, maps are put into the editing and production queue for the current or next fiscal year. A USGS PSC Map Editor then is assigned to the map and works with the author to produce the edited copy. Next, the map goes to the [PSC Production Cartographer](#) to produce a printable version in Adobe Illustrator®. The author has an opportunity to proof the map before it is finalized for publication; however, no significant content changes are allowed (authors will be responsible for proofing non-standard items such as special characters (small caps, diacriticals, etc.)). Also, if there is room on the map, the author may be notified by PSC that appropriately sized tables and/or figures can be shifted from the pamphlet and/or digital supplement to the map.

j. Map printing and web posting (*Fig. 3*). The [PSC Production Cartographer](#) submits the completed map to GPO for bid and printing. Generally, 100 copies of the map are sent to authors, and 300 copies are received by the USGS Regional Planetary Image Facility (RPIF) in Flagstaff, Arizona, for distribution to other RPIFs and PGG investigators on a mailing list provided by the [PGG Discipline Scientist](#). Extra copies are kept by the USGS RPIF and can be requested by investigators through the [Map Coordinator](#). Digital files of map materials are posted by the PSC Web Master on a USGS server for downloading, including: (a) PDFs of all printed materials produced by PSC, (b) author-provided Adobe Illustrator® files, and (c) GIS database, metadata, readme, and additional data files provided by PSC (a copy of these final files is provided to the author). Minor corrections and cosmetic improvements of the digital map product can be generated by authors as a new digital version of the map and submitted to the Map Coordinator for review, editing, and posting (however, consult first with the MC before initiating such a product, as authors have to pay for this service). Minor, non-science changes are shown by a decimal number, for example, correcting spelling of a name throughout the

publication or correcting a number in a table would generate a version upgrade from 1 to 1.1. Changing science on the map or adding data would generate a version upgrade from 1 to 2.

4. MAP CONTENTS

Planetary geologic maps in the past have varied widely in content and arrangement, largely at the preference of map authors. Though some flexibility is desirable to convey the geologic data and interpretation in ways that are suitable for each particular geologic map, unnecessary divergences and details come at a cost. Highly complex and uniquely assembled maps require more effort from mappers, reviewers, cartographers, and editors to prepare the map for publication. This handbook, under the direction of GEMS, defines a basic content template for planetary geologic maps, so that they become more uniform in format and thus simpler for users to assimilate and use as well as easier and cheaper to produce. In addition, following established USGS style guidelines in initial text preparation will result in less editing and revision. Mappers should refer to recently published geologic maps for examples of proper style in terms of spelling, word usage, grammar, and formatting, as well as the [USGS Tips web page](#) that addresses common formatting and editing issues. *Doing so will save time and effort!*

a. Map sheet components. To keep the printed map sheet as small as possible, authors are requested to keep map components to a minimum.

- 1) **Map:** Of course, the map itself is the fundamental product. It should be complete with map base at correct scale and projection, outcrops clearly colored and labeled, and structures consistently mapped. (The [PSC Production Cartographer](#) will cosmetically fine-tune these elements, as well as add the map scale and grid and any notes on base, but cannot be expected to complete or decipher any aspects prepared incompletely or unclearly.) To avoid clutter, highly detailed information may be included in the digital product as a layer (see the digital data products section below). Printed maps normally must be contained within a single sheet having a maximum size of 40 x 56 inches (larger or additional sheets result in significant additional printing costs; authors desiring multiple or oversized sheets may choose to pay for the extra costs, with prior approval via the Map Coordinator).
- 2) **CMU/SMU:** Each map will include a Correlation or Sequence of Map Units (CMU/SMU) chart. The chart is organized horizontally left to right showing the following elements:
 - a) *Stratigraphic column:* Formal or informal stratigraphic divisions (where available).
 - b) *Map units:* Units can be arranged in groups according to location or unit type. Units that form groups closely related in provenance and/or definitive characteristics may have similar unit names and symbols (e.g., Utopia Planitia 1 unit, Utopia Planitia 2 unit) and should be juxtaposed horizontally and/or aligned vertically in the CMU/SMU. Also, younger units and unit groups divided by region or morphologic type generally are placed toward the left, and older and diverse (e.g., ‘undivided highland materials’) and widespread (e.g., ‘crater material’) units are placed to the right. If more complex relations are portrayed, such as unconformities, time transgressive contacts, and other juxtaposition relations, they may be explained using a key (e.g., Young and Hansen, 2003; see also [GEMS guidelines for Venus SMUs](#) and [Appendix D](#) in Tanaka and others, 1994).

- c) *Major geologic events (optional)*: Juxtaposed chart to the right of the CMU/SMU showing inferred episodes of geologic activity (such as deposition, erosion, deformation, etc.; e.g., [Tanaka and others, 2005](#)).
 - d) *Crater density scale (where data are available)*: Cumulative density of craters larger than specified diameter(s) (e.g., [Tanaka and others, 2005](#)). Supporting text should be provided in the ‘age determinations’ text section (see below).
- 3) Nomenclature: Published USGS maps are expected to display nomenclature completely (with minor exceptions, such as features that are spatially insignificant at map scale) and accurately according to the International Astronomical Union ([IAU Gazetteer of Planetary Nomenclature](#)). For adding nomenclature labels in ArcGIS, see tutorial on [Annotation & Nomenclature](#). Whenever named features are mentioned anywhere in the map, including the text, they should be properly capitalized and spelled (including the Latin plural forms for [descriptor terms](#)). In this regard, the [IAU recommends that the initial letters of the names of individual astronomical objects be capitalized](#) (e.g., “Earth is a planet in the Solar System”). Also, ‘crater’ is not capitalized: “Mie crater occurs in northeastern Utopia Planitia, north of Elysium Mons and Albor and Hecates Tholi.” Informal terrain terms (e.g., ‘Utopia basin’ and ‘dark lava plains’) should not be capitalized and non-IAU-approved proper names should not be introduced. If a feature needs a name or name redefinition, the [USGS Nomenclature Specialist](#) can assist with a [name proposal](#). Nomenclature needs can be addressed at any time over the course of mapping, but keep in mind that it generally takes one to two months for a name to be approved. Informal names should be identified clearly as such (e.g., ‘the feature dubbed Home Plate...’). Formal names proposed to the IAU should not be used in maps or publications until the approval process is complete. Name proposals should be based on the need to single out for identification as-yet unnamed features in the map area (a need for names for use in journal articles may also qualify). Consult with the [USGS Map Coordinator](#) and [Nomenclature Specialist](#) when nomenclature issues arise.
 - 4) Geologic sections: A limited number of geologic sections can be shown on the map. These must be drafted in ArcGIS® or Illustrator®. Unit colors and symbols and other symbology and nomenclature should be identical to those on the map. The sections should be at the same horizontal scale as the map, and the amount of vertical exaggeration should be indicated and minimized.
 - 5) Map symbol legend: The legend is a chart on the map sheet that includes all line, point, and stipple symbols, with a feature type name and brief explanation (see recently published maps for examples). Where possible, the features should follow official, published USGS cartographic symbols (see [FGDC web page](#) as well as examples recently published in [planetary geologic maps](#)). The [Production Cartographer](#) will assist with converting symbols into final forms when necessary (e.g., when converting from GIS format to Illustrator®). See Tanaka and others (in press) for a discussion of types of tectonic structures found on particular planetary bodies.
 - 6) Unit legend: The unit legend is a list of map units organized by the unit groupings as illustrated graphically in the CMU/SMU. The units include a box showing the unit color (perhaps overlying the base) and are ordered from youngest to oldest exactly as in the Description of Map Units (DMU; see Tanaka and others, 2005). The only text shown is the unit name (this is a new policy); all unit information is included in the DMU table.

However, if the DMU can be included on the map sheet, the unit legend will not be necessary, and colored unit boxes will be added to the DMU.

- 7) Selected figures, tables, and text: During the map sheet layout construction phase, the [USGS Production Cartographer](#) may determine that there is room for additional material on the map sheet, and he/she will notify the author. The author then selects appropriate figures and tables from already submitted material that will fit. For smaller maps with brief text, all the material may fit on the map sheet (e.g., [Price, 1998](#)).
- 8) Map envelope: The map sheet (sometimes accompanied by a pamphlet with descriptive text) is contained within an envelope. In addition to standard publication citation information, the envelope may include an index map showing the map region typically on a hemispherical view of the planet. Digital data generally will be provided on-line only, as inclusion of a DVD in the map envelope is cost prohibitive.

b. Text components. Text will appear in a pamphlet or, when room is available, on the map sheet. Note that unit and feature descriptions are to be put into tables (i.e., delimited text files or other GIS compatible formats), which will encourage concise presentation and easier conversion to metadata for GIS maps.

- 1) Introduction and background: This section of the map text introduces the map area, including its geography and general geologic setting. It also acknowledges previous work for the map area, particularly any published geologic maps. However, it should not expound on existing scientific controversies. The rationale and purpose of the map are also described here. If the description of geography is extensive, a separate section devoted to it may be provided.
- 2) Data: Data sets should be described that were used to construct the map base and that were needed to identify and discriminate elements of map units and features critical to the mapping. Additional data sets that were consulted should also be mentioned, along with how they benefitted the mapping (or not). Relevant parameters and descriptions that affect mapping-related understandings should be stated, including what particular subsets of data were particularly useful for mapping; examples of such include pixel or other spatial resolution, solar incidence angle, solar longitude, wavelength bands, night vs. day time acquisition of thermal data, look-direction for synthetic aperture radar data, etc. Many of the most useful data sets for planetary mapping are available from the USGS [PIGWAD](#) and [Map-a-Planet](#) web sites. Where appropriate, key data sets may be shown in supplemental figures or as GIS layers as digital products. Also, data measurements applicable to the mapping might be shown in tables (e.g., morphometric measurements of landforms, radar properties of map units, etc.).
- 3) Mapping methods: A variety of techniques can be employed in showing unit names, groupings, symbols, colors, and contact and feature types. The actual methods used should be clearly described and consistently applied.
 - a) *Unit names*: Popular approaches to unit naming include morphologic type (e.g., ‘corona material,’ ‘crater material’), geographic names (‘Utopia Planitia material’), relative age/stratigraphic position (‘lower/older crater material’) and combinations thereof. Closely-related units (e.g., units in a sequence or morphologic variations of otherwise similar units) may be mapped as members (e.g., ‘lower member of the Utopia Planitia material’) or units having names showing their close association with other units (‘Utopia Planitia 1 unit, Utopia Planitia 2 unit...’).

- b) *Unit groups*: Units commonly are grouped by their geographic occurrence (e.g., ‘highland materials’) or morphologic type (e.g., ‘lobate materials’). Capitalize only proper nouns in unit and group names (e.g., ‘Alba Patera Formation,’ ‘Utopia basin unit,’ ‘western volcanic assemblage’).
- c) *Unit symbols*: These can indicate chronostratigraphic age (e.g., ‘A’ for ‘Amazonian’), unit group (e.g., ‘p’ for ‘plains materials’), specific unit designations (including morphology, albedo/reflectivity, and associated geographic feature name), and unit member (commonly as subscripts; may include numbered sequences, as in ‘member 1,’ ‘member 2’...). Small capital letters have been used for unit groupings (e.g., ‘E’ for ‘Elysium province’). Also, capital letters have been used for geographic names on Venus (e.g., ‘fG’ for ‘Gula flow material’). On the geologic map, some symbols may be queried to show that the unit assignment is highly uncertain. For adding unit symbols in ArcGIS, see tutorial on [Annotation & Nomenclature](#).
- d) *Unit colors*: Unit color hues may be applied according to suitable precedents, or they may reflect the group they are in (e.g., warm colors for volcanic materials, cool colors for sedimentary rocks, yellows for crater materials, browns for ancient highland materials), or their relative age using a color spectrum for scale (e.g., [Tanaka and others, 2005](#)). Also, color saturation can reflect general areal extent of unit outcrops (low saturation for extensive units and high saturation for small units), which assists in finding smaller units. Colors must follow [USGS publication guidelines](#), which ensure that they will print well. Generally, colors should not be changed after submission to PSC.
- e) *Contact types*: The quality of contacts varies considerably on most maps. Definitions for contact types are not precisely expressed in most geologic maps, including terrestrial ones. Thus, contact types should be used as consistently as possible for a given map and they should also be defined (e.g., Tanaka and others, 2005). For example, (1) a ‘certain’ contact may indicate that the contact is confidently located; (2) an ‘approximate’ contact indicates that the confidence is not well defined (perhaps due to data quality or the surface expression of the juxtaposed units being unclear); (3) a ‘buried’ contact indicates that surficial material buries the contact but morphologically the contact is still traceable, although subdued; (4) a ‘gradational’ contact means that the contact is broadly transitional at map scale (which may reflect a gradually thinning, overlapping unit or a unit margin expressed by gradually thinning out of numerous outcrops too small to map, as in the margin of a dune field or of a field of relict knobs); and (5) an ‘inferred’ contact, which may be used to delineate map units where the validity of the map unit or distinction between the units is hypothetical (e.g., the contact between the Vastitas Borealis interior and marginal units in Tanaka and others (2005) was drawn as inferred, because the marginal unit may be or may not be the same material as the interior unit).
- f) *Feature types*: Mapped geologic features involving line and point symbols and stipple patterns are listed in the map symbol legend. Also, the feature table (see below) provides a format to systematically describe the features and their geologic relationships and interpretations.
- g) *Drafting parameters*: Note minimum sizes of outcrops and linear features mapped, as well as the size range of features mapped with point symbols. For GIS maps, note

the vertex spacing, digitizing scale, line smoothing methods, and any other important digital controls and processing applied.

- 4) Age determinations: Techniques and reliability of relative and absolute-age determinations for map units should be discussed, as they vary widely according to data quality and preservation and exposure state of key features. These include superposition and cross-cutting relations and crater densities. For quantitative approaches, error analysis should be included. As absolute-age models are based on cratering theory, lunar sample dating, and empirical data on bolide populations, they are subject to high uncertainty. Appropriate references should be used throughout. Where possible, crater statistics can be summarized in the unit stratigraphic relations table described below.
- 5) Geologic history: A summary of the geologic history of a map region serves to provide a context for the entire geologic map and is encouraged. The synthesis is intended to be a brief yet informative review of unit development, tectonic deformation, and erosional and other modifications of the surface and shallow subsurface, with first-order interpretations on geologic and climate process histories as appropriate. However, lengthy considerations of previous and new hypotheses and other interpretive discussions that go beyond immediate mapping results and implications are to be left out.
- 6) References: The list of references and reference citations in the text follows USGS style guidelines; see published maps and this handbook for examples. Note that for more than 5 authors in a reference, only the first 3 are listed and “and x others” substitutes the number of unlisted authors for their names (see reference for Tanaka and others, 1994). Also, note formats for commonly used conference publications in the reference list below, as follows: *American Geophysical Union meeting abstract*: Banerdt, 2000; *Lunar and Planetary Science Conference abstract*: Skinner and Tanaka, 2003; *NASA Technical Memorandum abstract*: Grant, 1987; *edited NASA Special Publication*: Howard and others, 1988; *book chapter*: Wilhelms, 1990; *web-posted geologic map*: Young and Hansen, 2003.
- 7) DMU table: To simplify map texts, the Description of Map Units (DMU) table now forms a concise description of the map units, their stratigraphic relations, interpretation, and other pertinent information (previously, most planetary geologic maps provided a separate, stratigraphic narrative resulting in redundant information in the two sections). The DMU table will consist of four columns of information for each unit:
 - a) *Unit symbol and name*
 - b) *Definition*: Defining, primary characteristics essential to identifying and delineating each map unit from all others. In most cases, 2 to 5 characteristics define a unit, including aspects such as morphology/texture, albedo/reflectivity/spectral character, stratigraphic position or relative age, relative elevation, regional occurrence, and source feature. Where not obvious, mention the critical data sets. Type localities are optional and should be placed at the end of the definition.
 - c) *Additional characteristics*: Brief discussion of additional aspects such as relation to units in previous and adjacent maps, local anomalies in unit character, and prominent secondary features (that may obscure or be partly controlled by primary features).
 - d) *Interpretation*: Interpreted unit origin focusing mainly on origin of primary features and stratigraphic relationships; secondary features may also be discussed as they relate to the unit (i.e., fracture systems related to contraction, compositional information relating to surface alteration, etc.); and model crater absolute age

- (optional). As maps are meant to be enduring products, the interpretations should be inclusive of all reasonably possible alternatives, and wording should reflect the degree of uncertainty (e.g., ‘lava flows’ vs. ‘possible lava flows’ vs. ‘uncertain; may be lava flows, pyroclastic or impact-related deposits, or tabular sedimentary deposits’).
- 8) Unit stratigraphic relations table: For each unit, show total areal extent in map area and relative-age relations (younger, older, similar in age, or younger and older) for every adjacent unit. Where crater density data are available, show helpful crater density values, including standard deviations. Additional columns can be used for assigned chronologic units and model crater absolute ages. Use footnotes to explain abbreviations used and other important details.
 - 9) Feature table(s): Additional tables can be added as needed to describe the characteristics, relationships, and interpretation of other mapped features, such as tectonic structures, volcanic features, erosional and modificational features, surficial materials, and impact craters.
 - 10) Additional tables: Other useful map information can often be summarized in a table for easier reference and comparisons, such as quantitative aspects of map units, their appearance in specific image data sets, etc.
 - 11) Figures: Figures typically will not be included in the pamphlet. See digital data and map sheet components sections for formatting and possible placement.
 - 12) Digital supplement table: All materials appearing in a digital supplement should be listed in a summarized fashion, such as data and mapping layers, measurements and statistics, and figures.

c. Digital data products. Authors are encouraged to make use of digital repositories for useful ancillary data products and figures. When in GIS form, the products are more accessible to researchers via digital tools and methods. Map authors should follow all guidelines, so that modifications using the original digital files by the [USGS Production Cartographer](#) and perhaps other specialists will be minimal in order to meet publication standards.

- 1) Supplemental figures: These may include, for example, a few reduced-scale images of the map region showing key data sets, distributions of key features, contact relationships, and geologic cross sections. However, additional, digital-only figures can be used generously to show unit characteristics, superposition relations, crater size-frequency distributions, and secondary features as desired. Images, image mosaics, and thematic maps should include in the caption or on the figure as appropriate the data source, type, and resolution (e.g., ‘THEMIS daytime infrared mosaic at 100 m/pixel’), solar/incoming energy incidence angle and azimuth, north direction, scale bar (or image width), and latitude/longitude grid. Figures should be prepared at intended publication size with consistent label font types and sizes.
- 2) GIS layers: For GIS maps, authors can construct raster and vector data layers that are georegistered to map bases as digital-only supplements. These can be used to effectively show ancillary data sets and detailed feature mapping.
- 3) GIS maps: USGS GIS specialists will convert map files and supplemental figures and GIS layers as needed to conform to USGS geodatabase and FGDC metadata standards. GIS data supplements will be served via the web.

- 4) On-line map: The map, text, and supplemental figures will be converted to PDF format and made available for download via a USGS server and web page by the USGS PSC. GIS products, if available, will also be included for download.

5. REFERENCES

- Banerdt, W.B., 2000, Surface drainage patterns on Mars from MOLA topography: Eos, Transactions of the American Geophysical Union, fall meeting supplement, v. 81, no. 48, Abstract #P52C-04.
- Grant, J.A., 1987, The geomorphic evolution of eastern Margaritifer Sinus, Mars, *in* Advances in planetary geology: Washington, D.C., National Aeronautics and Space Administration Technical Memorandum 89871, p. 1–268.
- Hackman, R.J., 1962, Geologic map and sections of the Kepler region of the Moon: U.S. Geological Survey Miscellaneous Geologic Investigations I-355 (LAC-57), scale 1:1,000,000.
- Hansen, V.L., 2000, Geologic mapping of tectonic planets: Earth and Planetary Science Letters, v. 176, p. 527-542.
- Hare, T.M., Kirk, R.L., Skinner, J.A., Jr., and Tanaka, K.L., 2009, Chapter 60: Extraterrestrial GIS, *in* Madden, Marguerite, ed., Manual of Geographic Information Systems: Bethesda, The American Society for Photogrammetry and Remote Sensing, p. 1199-1219.
- Howard, A.D., Kochel, R.C., and Holt, H.E., eds., 1988, Sapping features of the Colorado Plateau—A comparative planetary geology field guide: Washington, D.C., National Aeronautics and Space Administration Special Publication, NASA SP-491, 108 p.
- Price, K.H., 1998, Geologic map of the Dao, Harmakhis, and Reull Valles region of Mars: U.S. Geological Survey Geologic Investigations Map I-2557, scale 1:1,000,000.
- Shevchenko, V., El-Baz, F., Gaddis, L., and 5 others, 2009, The IAU/WGSPN Lunar Task Group and the status of lunar nomenclature [abs.], *in* Lunar and Planetary Science Conference XV: Houston, Tex., Lunar and Planetary Science Institute, Abstract #2016, [CD-ROM].
- Skinner, J.A., Jr., and Tanaka, K.L., 2003, How should planetary map units be defined? [abs.], *in* Lunar and Planetary Science Conference XXXIV: Houston, Tex., Lunar and Planetary Science Institute, Abstract #2100, [CD-ROM].
- Tanaka, K.L., Moore, H.J., Schaber, G.G., and 9 others, 1994, The Venus geologic mappers' handbook: U.S. Geological Survey Open-File Report 94-438, 66 pp.
- Tanaka, K.L., Skinner, J.A., Jr., and Hare, T.M., 2005, Geologic map of the northern plains of Mars: U.S. Geological Survey Science Investigations Map 2888, scale 1:15,000,000.
- Tanaka, K.L., Anderson, R., Dohm, J.M., and 5 others, in press, Planetary structural mapping, *in* Watters, T., and Schultz, R., eds., Planetary Tectonics: New York, Cambridge University Press.
- Varnes, D.J., 1974, The logic of geological maps, with reference to their interpretation and use for engineering purposes: U.S. Geological Survey Professional Paper 837, 48 pp.
- Young, D.A., and Hansen, V.L., 2003, Geologic map of the Rusalka Planitia quadrangle (V-25), Venus: U.S. Geological Survey Geologic Investigations Series, I-2783, scale 1:5,000,000 [<http://pubs.usgs.gov/imap/i2783/>].
- Wilhelms, D.E., 1972, Geologic mapping of the second planet: U.S. Geological Survey Interagency Report, Astrogeology, v. 55, 36 pp.

Wilhelms, D.E., 1990, Geologic mapping, in Greeley, R, and Batson, R.M., eds., Planetary Mapping: New York, Cambridge University Press, p. 208-260.

6. USEFUL WEB PAGES

FGDC (Federal Geographic Data Committee) Digital Cartographic Standard for Geologic Map

Symbolization: http://ngmdb.usgs.gov/fgdc_gds/geolsymstd.php

IAU Gazetteer of Planetary Nomenclature home page: <http://planetarynames.wr.usgs.gov/>

IAU Gazetteer of Planetary Nomenclature descriptor terms:

<http://planetarynames.wr.usgs.gov/jsp/append5.jsp>

IAU Gazetteer of Planetary Nomenclature feature name request form:

<http://planetarynames.wr.usgs.gov/jsp/request.jsp>

NASA MEPAG calendar: <http://mepag.jpl.nasa.gov/calendar/index.html>

NASA research opportunities: <http://nspires.nasaprs.com>

USGS Planetary Geologic Mapping: <http://astrogeology.usgs.gov/Projects/PlanetaryMapping/>

USGS Planetary Interactive GIS on-the-Web Analyzable Database (PIGWAD):

<http://webgis.wr.usgs.gov/>

USGS Map-a-Planet: <http://www.mapaplanet.org/>

USGS PSC author submission checklist for planetary maps:

http://astrogeology.usgs.gov/Projects/PlanetaryMapping/guidelines/PSC_author_checklist_7-20-09.pdf

USGS Astrogeology manuscripts to PSC submission process:

http://astrogeology.usgs.gov/Projects/PlanetaryMapping/guidelines/AstroSubmitProcess_june2009.pdf

USGS tips and information for preparation of astrogeology maps:

<http://astrogeology.usgs.gov/Projects/PlanetaryMapping/guidelines/preparationTips.pdf>

USGS instructions on building polygons in Illustrator:

http://astrogeology.usgs.gov/Projects/PlanetaryMapping/guidelines/layersexample_small.pdf

7. PLANETARY GEOLOGIC MAPPING SUPPORT PERSONNEL

Position/Function	Name	Email	Institution
Map Coordinator	Ken Tanaka	ktanaka@usgs.gov	USGS ASC
GIS Data Specialist	Trent Hare	thare@usgs.gov	USGS ASC
GIS Project Specialist	Jim Skinner	jskinner@usgs.gov	USGS ASC
Map base Specialist	Bob Sucharski	bsucharski@usgs.gov	USGS ASC
Nomenclature Specialist	Jen Blue	jblue@usgs.gov	USGS ASC
PGM Administrative Specialist	Jen Blue	jblue@usgs.gov	USGS ASC
Regional Planetary Image Facility Director	Justin Hagerty	jhagerty@usgs.gov	USGS ASC
Regional Planetary Image Facility Manager	David Portree	dportree@usgs.gov	USGS ASC
Digital Map Editor	Jan Zigler	jzigler@usgs.gov	USGS PSC
Production Cartographer	Darlene Ryan	dryan@usgs.gov	USGS PSC
Map Submission Editor	Carolyn Donlin	cdonlin@usgs.gov	USGS PSC
GEMS Chair	Leslie Bleamaster	lbleamas@psi.edu	NASA PGG
Discipline Scientist	Michael Kelley	Michael.S.Kelley@nasa.gov	NASA PGG

8. ABBREVIATIONS

ASC	Astrogeology Science Center (part of USGS)
CMU	Correlation of Map Units
DMU	Description of Map Units
FGDC	Federal Geographic Data Committee
GEMS	Geologic Mapping Subcommittee (of PCGMWG)
GIS	Geographic Information System
GPO	Government Printing Office
IAU	International Astronomical Union
MC	Map Coordinator
NASA	National Aeronautics and Space Administration
PCGMWG	Planetary Cartography and Geologic Mapping Working Group (part of PGG)
PEN	Planetary Exploration Newsletter
PGG	Planetary Geology and Geophysics Program
PGM	Planetary Geologic Mapping
PIGWAD	Planetary Interactive GIS on-the-Web Analytical Database
PSC	Publications Services Center
SMU	Sequence of Map Units
USGS	U.S. Geological Survey

Figure 1 - GIS MAPPING TEMPLATE PREPARATION

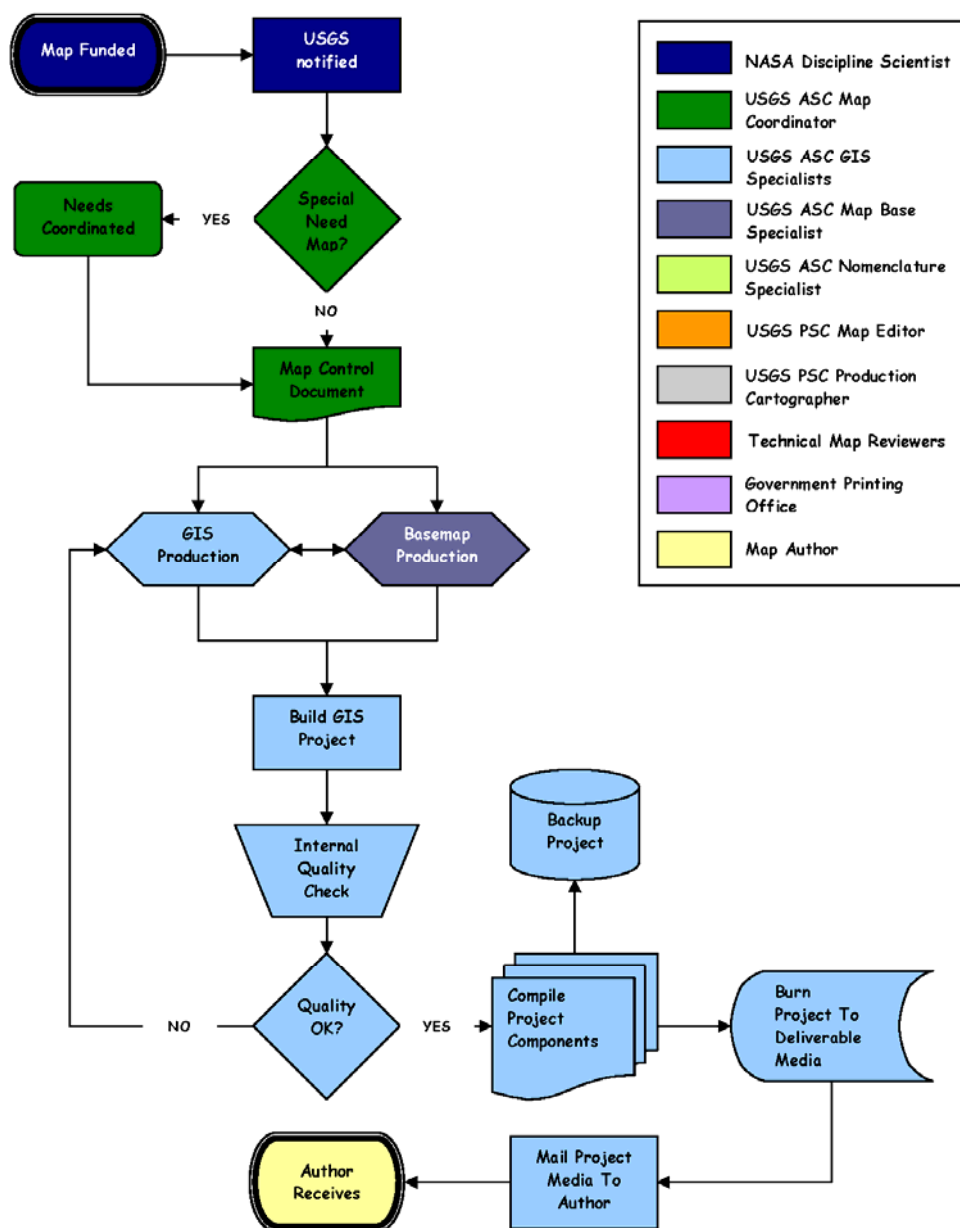


Figure 2 - SUBMISSION AND TECHNICAL REVIEW

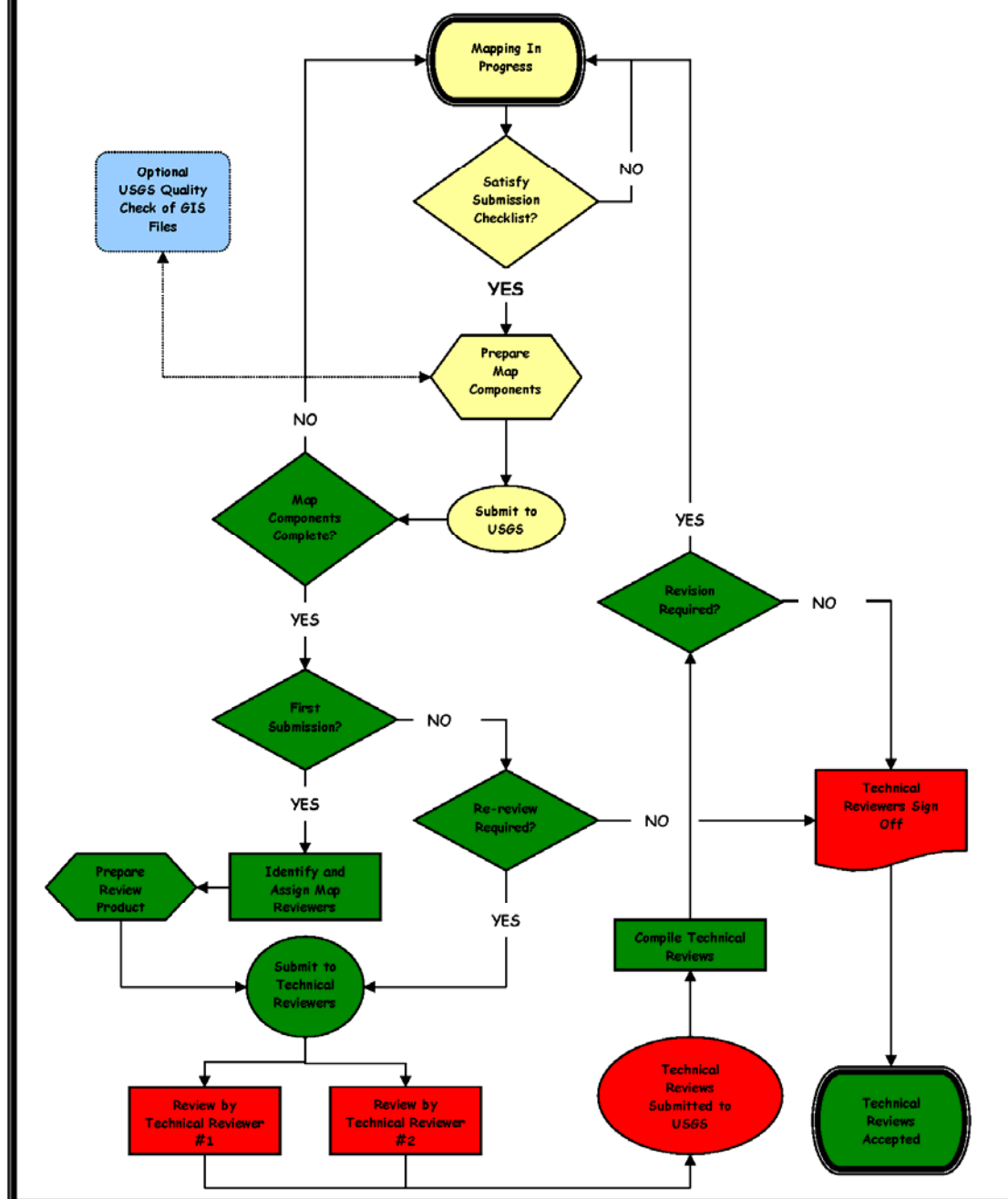


Figure 3 – USGS REVIEW AND PRODUCTION

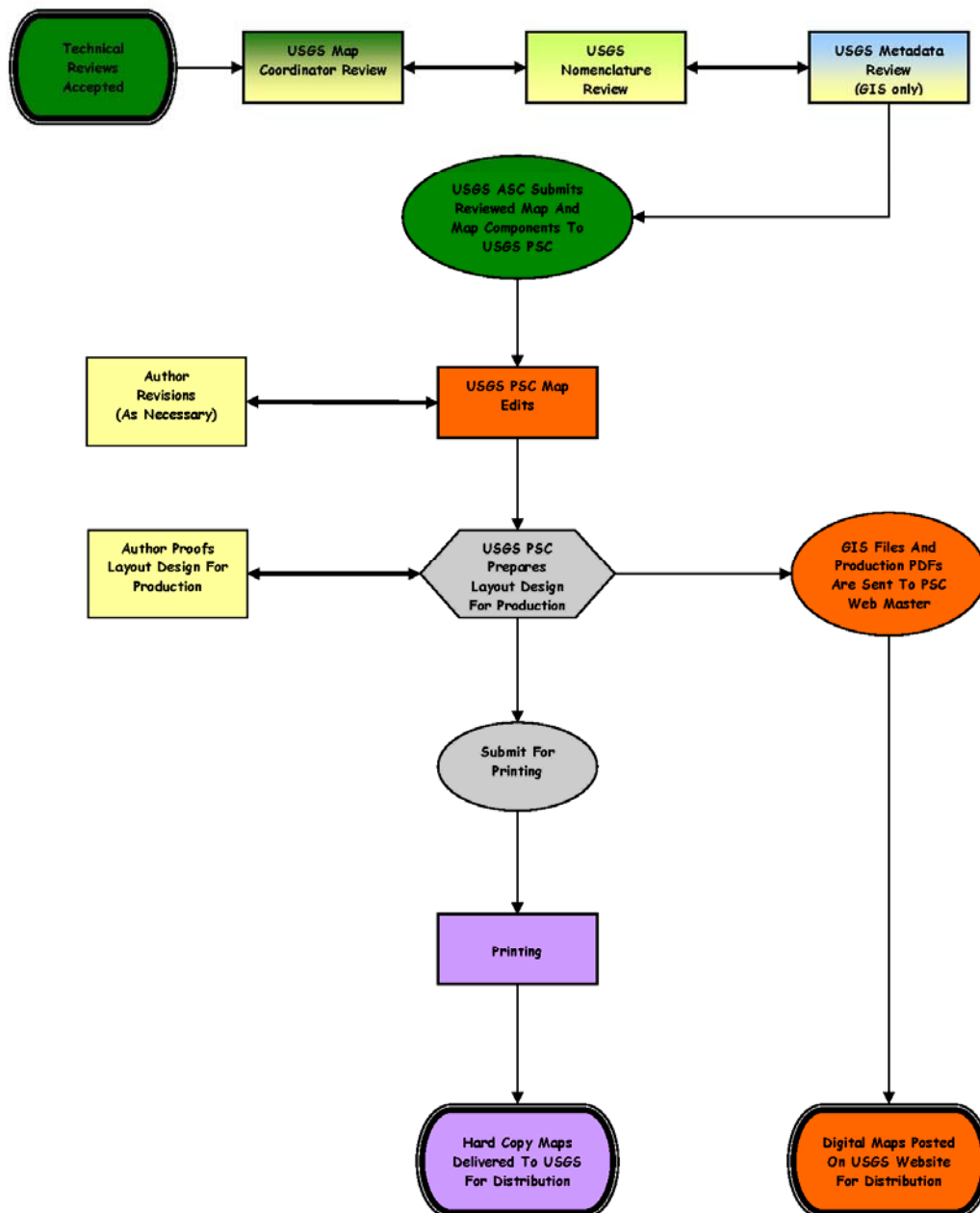


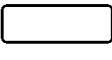
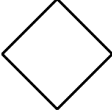
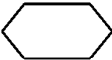
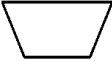



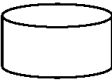
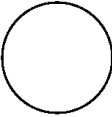


Figure 4 - FLOWCHART SYMBOL DEFINITIONS

Symbol	Symbol Name	Symbol Description and Example Activity
	Terminator	Terminators show the start and stop points in a process flow. <i>A proposed map is accepted for funding.</i>
	Process	A process or action step, perhaps comprised of multiple segmented actions. <i>Layout and proofing of final map.</i>
	Alternate Process	A process or action step that is an alternate (or option) to normal process flow. <i>Preparation of non-standard map base.</i>
	Decision	Indicates a critical question or branch in the process flow. <i>Does the submitted map adhere to submission requirements?</i>
	Preparation	Any step that is substantially comprised of preparation and/or collation of digital and/or hard copy product. <i>Creation of map base.</i>
	Manual Operation	Any step that is substantially comprised of manual (non-automated) input. <i>Map reviews.</i>
	Document	Any process flow step that results in the creation of a critical document. <i>Map Control Document.</i>
	Multi-document	Any process flow step that results in the creation of a critical package of documents. <i>Prepare review package.</i>
	Copy to digital media	Any process flow step that results in the creation of (transitory) digital copy. <i>Copy to DVD for review.</i>
	Back-up	Any process flow step that results in the creation of permanent digital copy. <i>Copy to map base to USGS hard-drive.</i>
	Shipping/Delivery	Denotes process step comprised of packaging, shipping, or delivery. <i>Submit map project to USGS.</i>

Form 9-1325 (revised, August 2006) USGS		INFORMATION PRODUCT REVIEW AND APPROVAL SHEET				SCIENCE CENTER		INFORMATION PRODUCT TRACKING NO.	
AUTHOR(S): (last name first; show first name and (or) initials as shown in manuscript) TEMPLATE! SAVE AS: your document filename_RAS in X: Publications/From Authors folder (write access granted)						Yucca Mountain Project Branch		IP-	
TITLE:						SCIENCE CENTER CONTACT: (name, address, telephone, fax, email) Pamela B. Daddow U.S. Geological Survey Box 25046 MS 421 DFC Building 53 Denver, Colorado 80225 303-236-5050, ext. 249 Fax 303-236-5047 pbdaddow@usgs.gov			
FORM OF PUBLICATION <div style="display: flex; justify-content: space-between;"> <div style="width: 45%;"> <i>USGS series</i> <input type="checkbox"/> Administrative Report <input type="checkbox"/> Circular <input type="checkbox"/> Data Series <input type="checkbox"/> Fact Sheet <input type="checkbox"/> General Information Product <input type="checkbox"/> Open-File Report <input type="checkbox"/> Professional Paper <input type="checkbox"/> Scientific Investigations Map <input type="checkbox"/> Scientific Investigations Report <input type="checkbox"/> Techniques and Methods </div> <div style="width: 45%;"> <input type="checkbox"/> Outside information product <input type="checkbox"/> Edit requested <input type="checkbox"/> No edit requested <input type="checkbox"/> Abstract PUBLISHER, JOURNAL, OR MEETING: </div> </div>						<i>Format</i> <input type="checkbox"/> Print <input type="checkbox"/> CD-ROM <input type="checkbox"/> WWW <input type="checkbox"/> Video <input type="checkbox"/> Print on Demand <input type="checkbox"/> Other Check all of above that apply		TOTAL PAGES (including title page and all page-size figures and tables) _____	
IF PART OF A MULTICHAPTER USGS PUBLICATION: Total number of chapters <input type="checkbox"/> To be published <input type="checkbox"/> Together <input type="checkbox"/> Separately						DEADLINE:		ARE GEOLOGIC NAMES USED? IF YES, REVIEW REQUIRED. Yes <input type="checkbox"/> No <input type="checkbox"/>	
REMARKS: (with initials, add additional pages if needed)						SUPERSEDES OPEN-FILE REPORT? Yes <input type="checkbox"/> No <input type="checkbox"/> Yes, number: _____			
PUBLICATION CONTENTS <input type="checkbox"/> New interpretive <input type="checkbox"/> Previously approved interpretive <input type="checkbox"/> Noninterpretive									

NAME, TITLE, AFFILIATION	DATE IN	DATE OUT (indicate hours spent)	CHECK PROCESSING STEP WITH "X"										SIGNATURE (or attach e-mail)
			Author Submission	Supervisor Approval	Peer Review	Technical Specialist Review	Office of Communications Review	Science Center Approval	Editorial Review	PSC Approval	Bureau Approval		

CONTINUE ON ADDITIONAL FORMS IF NECESSARY

Figure 5: USGS Information Product Review and Approval Sheet.